DISSERTATION

GEOGRAPHIC STRUCTURE AND DYNAMICS IN MOUNTAIN PLOVER

Submitted by

Michael B. Wunder

Graduate Degree Program in Ecology

In partial fulfillment of the requirements

For the Degree of Doctor of Philosophy

Colorado State University

Fort Collins, CO

Spring 2007

Reproduced with permission of the copyright owner. Further reproduction prohibited without permission.

UMI Number: 3266341

INFORMATION TO USERS

The quality of this reproduction is dependent upon the quality of the copy submitted. Broken or indistinct print, colored or poor quality illustrations and photographs, print bleed-through, substandard margins, and improper alignment can adversely affect reproduction.

In the unlikely event that the author did not send a complete manuscript and there are missing pages, these will be noted. Also, if unauthorized copyright material had to be removed, a note will indicate the deletion.

UMI®

UMI Microform 3266341

Copyright 2007 by ProQuest Information and Learning Company.

All rights reserved. This microform edition is protected against unauthorized copying under Title 17, United States Code.

ProQuest Information and Learning Company
300 North Zeeb Road
P.O. Box 1346
Ann Arbor, MI 48106-1346

Reproduced with permission of the copyright owner. Further reproduction prohibited without permission.

COLORADO STATE UNIVERSITY

April 2, 2007

WE HEREBY RECOMMEND THAT THE DISSERTATION PREPARED UNDER OUR SUPERVISION BY MICHAEL B. WUNDER ENTITLED "GEOGRAPHIC STRUCTURE AND DYNAMICS IN MOUNTAIN PLOVER" BE ACCEPTED AS FULFILLING IN PART REQUIREMENTS FOR THE DEGREE OF DOCTOR OF PHILOSOPHY.

Committee on Graduate Work

Merav Ben-David

Fritz Knopf

Colleen Webb

Advisor, Barry Noon

Director, William Lauenroth/Ingrid Burke

Reproduced with permission of the copyright owner. Further reproduction prohibited without permission.

ABSTRACT OF DISSERTATION

GEOGRAPHIC STRUCTURE AND DYNAMICS IN MOUNTAIN PLOVER

The mountain plover population is thought to have declined by sixty percent over the past 30 years. Most mountain plovers spend the winter in a highly agricultural landscape in Imperial County, California where the habitat dynamics are completely determined by human policy. To better understand potential impacts of land use decisions in Imperial County, I studied range-wide spatio-temporal links in the demography of mountain plover. I used color bands and stable isotope concentrations in feathers to describe the provenance of plovers wintering in California. Because the use of stable isotopes for this purpose is relatively new, the efficacy of the tool is not well understood. I used feathers of known origin to study some fundamental assumptions of the approach and proceeded to derive a modeling framework to better reflect the state of knowledge about stable isotope ecology. The geographic resolution associated with assigning an individual to a location is relatively coarse, but informative.

My work is presented in four chapters, each intended as a stand-alone contribution. Chapter one tests the use of stable isotopes for studying the breeding provenance of wintering mountain plovers based on methods described in the literature. The inferential and sampling frameworks in the literature were inconsistent and I suggest a discrete assignment test framework instead. Chapter two investigates the influence of

Reproduced with permission of the copyright owner. Further reproduction prohibited without permission.

known sources of error on the certainty of geographic assignments with the approach described in chapter one. Chapter three departs from the assignment test approach and presents a way to directly model sampling effects over a known process based on the physical chemistry of stable hydrogen isotopes in precipitation. I use this model to build and explore probability surfaces that describe the probability of origin for birds from stable hydrogen isotopes in feathers. Chapter four tests the use of these probability surfaces using recaptured plovers and illustrates the application of these surfaces to the problem of mountain plover provenance. In this last chapter, I present evidence for climate-related shifts in geographic provenance of recruitment into the population of mountain plovers.

Michael B. Wunder
Graduate Degree Program in Ecology
Colorado State University
Fort Collins, CO 80523
Spring 2007

Reproduced with permission of the copyright owner. Further reproduction prohibited without permission.

TABLE OF CONTENTS

Reproduced with permission of the copyright owner. Further reproduction prohibited without permission.

ACKNOWLEDGEMENTS

Although the pursuit of a PhD is a personal endeavor, the work necessary to obtain one it is rarely carried out in isolation. I was fortunate to have worked with so many talented and dedicated individuals over the course of this project. I want to thank my committee for treating me as a colleague rather than as a student, for allowing me to wander toward and away from my own mistakes and for not hiding sundry dead ends along the way. I am grateful to Fritz Knopf for providing me with the opportunity to shape this project and for taking a chance on an aging field ecologist. I am grateful to Barry Noon for continually reminding me that our work and influence does not stop at the edge of campus. I am grateful to Merav Ben-David for encouraging me to consider applied problems from a perspective rooted in first principles and I am grateful to Colleen Webb for showing me how to solve such problems while also maintaining a skeptical optimism toward progress in our discipline.

I was fortunate to find productive collaboration and healthy discussion from Martin Margulies, Vicky Dreitz, Steve Dinsmore, Regan Plumb, and Scott Schneider. Aaron Brees, Carla Hanson, Victor Sepulveda, and Chris Mettenbrink were dedicated to this species and this project; I thoroughly enjoyed our time in the field. Ryan Norris has become an especially admirable colleague. Without hesitation, he very generously provided data and was willing to explore the potential ramifications of a reanalysis of those data knowing full well that the results might overturn conclusions he had already published. I appreciate that he regards the potential for discovery above all else. The stable isotope lab at USGS in Denver was incredibly supportive of this project. Bob Rye,

Reproduced with permission of the copyright owner. Further reproduction prohibited without permission.

Gary Landis, Craig Johnson, Craig Stricker, Cayce Gulbranson, and Carl Bern were very patient with a newcomer to the field of stable isotope ecology. I am most grateful to Cyndi Kester for going well beyond these patient explanations; in addition to pioneering the implementation of many of the methods used in this study, she shared my interest in really trying to understand both the potential and the limitations of this new tool.

I am especially grateful to my parents Bruce and Gayle for creating an environment that taught me to value the worth of education and to maintain a persistent curiosity toward the world around me. Both worked as well-respected educators, but my respect for the education they provided me cannot be surpassed. I love them both. I am fortunate to have two children of my own now and I am continually struck by how grounding it is to simultaneously see both the past and the future in each of them. I could not have, and almost certainly would not have done this had it not been for my wife Emily. She has been a model of grace and patience. I thank her for stargazing with me in Horse Gulch and for everything that followed. I dedicate this to her and to our children Silas and Helen.

Reproduced with permission of the copyright owner. Further reproduction prohibited without permission.

CHAPTER ONE

A TEST OF GEOGRAPHIC ASSIGNMENT USING ISOTOPE TRACERS IN FEATHERS OF KNOWN ORIGIN

Reproduced with permission of the copyright owner. Further reproduction prohibited without permission.

ABSTRACT

I used feathers of known origin collected from across the breeding range of a migratory shorebird to test the use of isotope tracers for assigning breeding origins. I analyzed δD, δ^{13}C, δ^{15}N in feathers from 75 mountain plover (*Charadrius montanus*) chicks sampled in 2001 and from 119 chicks sampled in 2002. I estimated parameters for continuous-response inverse regression models and for discrete-response Bayesian probability models from data for each year independently. I evaluated model predictions with both the training data and by using the alternate year as an independent test dataset. My results provide weak support for modeling latitude and isotope values as monotonic functions of one another, especially when data are pooled over known sources of variation such as sample year or location. I was unable to make even qualitative statements, such as north vs. south, about the likely origin of birds using both δD and δ^{13}C in inverse regression models; results were no better than random assignment. Probability models provided better results and a more natural framework for the problem. Correct assignment rates were highest when considering all three isotopes in the probability framework, but the use of even a single isotope was better than random assignment. The method appears relatively robust to temporal effects and is most sensitive to the isotope discrimination gradients over which samples are taken. I offer that the problem of using isotope tracers to infer geographic origin is best framed as one of assignment, rather than prediction.

Keywords: assignment test, feathers, migration, stable isotopes

Reproduced with permission of the copyright owner. Further reproduction prohibited without permission.

INTRODUCTION

In the study of seasonally migratory animals, strong conclusions from site-specific investigations are not possible without also considering activities over the complete annual biogeography of the species (Gill et al. 2001). For example, assuming uniform wintering histories for individuals in a study of migrant bird breeding biology overlooks a potentially important mechanistic source of variation; events during winter can influence events during the subsequent breeding season (Marra et al. 1998, Norris et al. 2004). Such improved understandings of the links between seasonal distributions of migratory animals have obvious conservation implications. This is particularly true for rare or sparsely distributed species that are vulnerable to stochastic events that can occur at any point across their biogeography.

Traditional methods for studying continental-scale migrations of small or medium-sized birds have been limited, expensive and marginally helpful at best. Off-site band returns for non-game birds are notoriously scarce (Wassenaar and Hobson 2001). UHF radio telemetry is logistically impractical over the scales of most migratory routes and satellite telemetry is not yet possible for any but the largest animals. Recently, advances in the use of molecular and chemical markers to study questions of migration have been gaining momentum (Webster et al. 2002).

Naturally-occurring ratios of stable isotopes of some elements vary over ecologically convenient scales. Ratios of nitrogen have been used to trace anthropogenic inputs to birds from the environment (Hobson 1999, Hebert and Wassenaar 2001) and also to determine dietary status (Hobson et al. 1993). Carbon isotope ratios vary most

Reproduced with permission of the copyright owner. Further reproduction prohibited without permission.

strongly with photosynthetic pathway (Smith and Epstein 1971), but also with latitude and altitude (Körner et al. 1991). Hydrogen ratios vary with precipitation and geomorphology (Meehan et al. 2004). In general, these differences in isotope ratios are transferred through the food web such that biogeographic patterns are reflected in animal tissues, but see Gannes et al. (1997), Hobson et al. (1999), and McKechnie et al. (2004) for important associated considerations.

A number of recent studies have exploited patterns in naturally-occurring isotope ratios to link winter and summer ranges of migratory birds. Some have suggested apparent utility of using only stable-hydrogen values (δD) in feathers coupled with models interpolating long-term averages of spatially sparse precipitation values (e.g. Hobson and Wassenaar 1997, Meehan et al. 2001, Kelly et al. 2002, Smith et al. 2003), but the use of more than one element seems to offer more promise. For example, Lott et al. (2003) used sulfur isotope values (δ^{34}S) to censor their data such that marine effects on δD trends were removed from analysis. Using a combination of hydrogen and carbon isotopes has yielded promising results (Wassenaar and Hobson 2000, Hobson and Wassenaar 2001, Rubenstein et al. 2002). Chamberlain et al. (2000) suggest that a combination of carbon and nitrogen isotopes can discern geographically distinct subspecies of willow warblers (*Phylloscopus trochilus*), although few of their data could be uniquely assigned to a particular area (see Fig. 2 of that study). Finally, at least three studies have shown the utility of using isotopes of three elements, but each study examined a different set of three (Chamberlain et al. 1997, Caccamise et al. 2000, Pain et al. 2004).

Reproduced with permission of the copyright owner. Further reproduction prohibited without permission.

In general, there have been three common feather sampling scenarios, each addressing a slightly different aspect of the question of geographic links in migration. First, feathers grown on the breeding grounds in the year prior to sampling are sampled on the breeding grounds. Philopatry is often the focus in these cases (e.g. Graves et al. 2002, Hobson et al. 2004) and often only territorial males are sampled in attempts to better address the question. Second, and most commonly, feathers grown on the breeding grounds in the year of sampling are sampled away from breeding areas either during migration or on the wintering grounds. Inference from this strategy often relies on spatially interpolated maps of long-term average δD in precipitation, further assuming that discrimination against ^{2}H in feathers is constant over individual birds, species, habitats, locations and time (e.g. Hobson and Wassenaar 1997). Third, feathers grown in winter are sampled on the breeding grounds. Studies that sample via the third scenario generally address questions of population mixing or habitat quality differences during winter, assuming distinct wintering areas or habitats are isotopically recognizable (e.g. Evans et al. 2003). Most studies sampled feathers of unknown origin. Accordingly, the vast majority of conclusions have been based on largely untested assumptions about the degree of natural variation in molt strategy and isotopic discrimination factors among individuals, species, habitats, locations, seasons, and years. Direct tests of such key assumptions would clearly benefit not only studies of avian migration, but also the more general range of applications that interpret naturally occurring stable isotopes to infer dispersal, migration, and origins of individual animals of many varieties.

The intent of this study was to test the use of isotope values (δD, δ^{13}C, δ^{15}N) in feathers to make predictions about bird origin. By sampling feathers from precocial

Reproduced with permission of the copyright owner. Further reproduction prohibited without permission.

mountain plover (*Charadrius montanus*) chicks from across the breeding range in two consecutive breeding seasons, I generated two independent datasets comprised entirely of known origin samples. Using regression models, I characterized the mean variation in isotope values over the sampled latitude range. Using two different methods for inverting these conditional data, I generated models to assign specific geographic origins. I used one year of data to generate, or train the models. Data from the alternate year was used to test model performance. I discuss the roles of appropriate sampling and model frameworks as they relate to limits in the use of isotope ratios to predict or assign geographic origin to birds of unknown origin.

MATERIALS AND METHODS

Mountain plovers

Mountain plover chicks forage independently for invertebrates within the first hours after hatching (Knopf 1996). At hatching, chicks are covered in natal down. Contour feathers and flight feathers in sheath begin to show by about 7 days of age (MBW personal observation). Because plover chicks prey on terrestrial invertebrates and because they cannot fly, isotope ratios in new feathers are likely related to those of the environment within an area of approximately 56 ha, the mean home range size for plovers with broods (Knopf and Rupert 1996). It is possible that chicks use some tissue reserves inherited from parental birds for the development of feathers. However, because this is an energetically demanding period during which all tissues, including feathers, are growing, it is more likely that the resources necessary for such development are primarily

Reproduced with permission of the copyright owner. Further reproduction prohibited without permission.

provided by food intake (Schekkerman and Visser 2001). I therefore assume that mountain plover chicks provided feathers exclusively of known geographic origin.

Feather sampling

I sampled body feathers from 75 mountain plover chicks caught by hand between 12 June and 18 August 2001 at six locations across nine degrees of latitude within the breeding range. Between 10 June and 6 August 2002, I sampled 119 chicks from eight locations across six degrees of latitude within the breeding range. The three southernmost locations were also sampled in 2001 (Fig. 1). Feathers were stored in individually-marked bags and frozen until analyses.

Isotopic Analysis

I report stable isotope ratios as relative values in parts per mil (‰) using the standard δ notation: $\delta_{samp} = \left({R_{samp}}/{R_{std}} - 1 \right) \times 1000$ where δ_{samp} is the reported value of isotope ratios of the sample relative to a standard, and R_{samp} and R_{std} are the isotope ratios of the sample and the standard, respectively.

After thawing, feathers were washed of surface oils with a 2:1 chloroform/methanol solution and allowed to air dry overnight under a fume hood. Approximately 1.7mg of feather tissue was loaded into pressed tin capsules for $\delta^{13}C$ and $\delta^{15}N$. If a feather was still partially in sheath, only the fully-developed vanes were used. Samples were analyzed for $\delta^{13}C$ and $\delta^{15}N$ by continuous flow methods using an elemental analyzer coupled to either a Micromass Optima mass spectrometer or a

Reproduced with permission of the copyright owner. Further reproduction prohibited without permission.

Finnigan Delta Plus XL mass spectrometer (Fry et al. 1992). Isotopic compositions of $\delta^{13}C$ and $\delta^{15}N$ are reported relative to PDB and Air, respectively, using internal laboratory standards calibrated against ANU sucrose ($\delta^{13}C$ = -10.4‰), NBS 22 ($\delta^{13}C$ = -29.6‰), USGS 25 ($\delta^{15}N$ = -30.4‰), and USGS 26 ($\delta^{15}N$ = 53.7‰). Analytical error for C and N was ± 0.2 ‰.

For hydrogen isotope (δD) analysis, approximately 0.5mg of tissue was loaded into pressed silver capsules. Samples were then analyzed by continuous flow isotope ratio mass spectrometry using a Finnigan TC/EA coupled to a Finnigan Delta Plus XL mass spectrometer (Wassenaar and Hobson, 2003). Hydrogen isotopic compositions are reported relative to Vienna Standard Mean Ocean Water (VSMOW) using internal laboratory standards calibrated against IAEA-CH-7 (δD = -100‰). Non-exchangeable hydrogen isotopic compositions were determined by comparative equilibration techniques described by Wassenaar and Hobson (2003). Analytical error of non-exchangeable hydrogen isotope values was ± 4‰.

Data Analysis

I observed inter-annual differences in all three isotopes from one site that was sampled in both years (95% CI for δD in 2001, -51.73:-45.55, and -32.31:-26.48 in 2002; 95% CI for $\delta^{13}C$ in 2001, -19.66:-19.13, and -18.48:-18.10 in 2002; 95% CI for $\delta^{15}N$ in 2001, 9.71:10.29 and 10.50:11.03 in 2002). I evaluated general latitudinal patterns in the isotopes for each year using least squares regression to model each isotope value in turn as a function of latitude. I parameterized both continuous- and discrete-response models for each year to predict geography of origin from isotope ratios in

Reproduced with permission of the copyright owner. Further reproduction prohibited without permission.

feathers. I then used the independent datasets to evaluate model predictions. That is, I used the 2002 data to evaluate predictions from models generated with 2001 data and vice versa.

I first wrote the inverse regression model reported by Rubenstein et al. (2002). This was $y_i = \hat{\alpha} + \hat{\beta}_1 \delta \mathrm{D}_i + \hat{\beta}_2 \delta^{13}\mathrm{C}_i + \varepsilon_i, i = 1,...,n$, where y_i are the observed latitudes, $\hat{\alpha}$ is the estimated constant intercept, $\hat{\beta}_x$ is the estimated coefficient for the respective isotope ratios and $\varepsilon_i \sim N(0,\sigma^2)$. As with Rubenstein et al. (2002), I assumed that the data were independent random samples and estimated model parameters with least squares. However, because multiple birds were sampled at each location, the data did not represent independent random samples. Additionally, writing the model as above clearly illustrates that residual variance in the data must occur in the *y*-direction. In the case of these models, the overwhelming source of variance in the *y*-direction derived from the difference in latitudes of the sites we sampled. To address these issues, I added sampling location as a random effect. This modified the model as follows

$y_{ij} = \hat{\alpha} + \hat{\beta}_1 \delta \mathrm{D}_{ij} + \hat{\beta}_2 \delta^{13}\mathrm{C}_{ij} + u_i + \varepsilon_{ij}, i = 1,...,g, j = 1,...,n$ where y_{ij} are the observed latitudes, g is the number of sample locations, n is the number of individual birds, $\hat{\alpha}$ and $\hat{\beta}_x$ are as in the previous model, $u_i \sim N(0,\sigma_1^2)$ and $\varepsilon_{ij} \sim N(0,\sigma^2)$. This model partitioned the variance into within- and among-location components. I estimated parameters for the mixed effects model using Residual Maximum Likelihood (REML).

I evaluated the relative strength of evidence in the data for the fixed and mixed effects regression models by comparing AICc statistics and relative evidence ratios ($e^{0.5\Delta\mathrm{AICc}}$; Burnham and Anderson 2002). I validated these inverse regression models by

Reproduced with permission of the copyright owner. Further reproduction prohibited without permission.

examining predicted values and prediction intervals for both the model generating data and the independent datasets and by considering the associated model assumptions.

Because I was interested in the probability that an individual feather was from a particular geographic location given measured ratios of isotopes in the feather, I also explored a discrete-response framework. For this, I used Bayes Rule to invert the conditional probabilities of all three measured isotope ratios in feathers given sampling location. I wrote $P(A_i \mid B) = \frac{P(B \mid A_i)P(A_i)}{\sum_i P(B \mid A_i)P(A_i)}$ where $P(A_i \mid B)$ is the (posterior) probability distribution of a feather originating in geographic location *i*, given the observed δD, δ^{13}C, δ^{15}N. $P(B \mid A_i)$ is the (sampling) probability distribution of observing the isotope values, given the geographic locations *i*, and $P(A_i)$ is the (prior) probability distribution of a feather originating in geographic location *i*, given assumptions or knowledge prior to observing any isotope values.

I assumed the feathers I sampled were of known origin and sample data are fixed in this framework, so the distribution of sample sizes across the locations provided a reasonable *a priori* approximation of the prior probabilities over the locations. Therefore, I set the prior probability density proportional to the per location sample sizes. Depending on the number of isotopes considered, I assumed either normal, bivariate normal or multivariate normal distributions using the within-location variance-covariance matrices for the sampling distributions. I estimated parameters for the sampling distribution functions from the data using maximum likelihood.

If the number of sites, S, is finite, then $P(A_i \mid B)$ over $i = 1,\ldots,S$ can be interpreted as a set of competing hypotheses about the geographic origin of a bird, given the

Reproduced with permission of the copyright owner. Further reproduction prohibited without permission.

measured isotope values. Thus, in all cases, individual birds were assigned to the population x for which $P(A_x \mid B)$ was maximal. I applied this probability approach at two levels of spatial resolution – U.S. state (pooling data across sampling locations within a state), and individual sampling location (pooling individuals within sampling sites). I included all samples for the state-level analyses, but excluded locations with ≤ 5 samples from the location-level analyses. Thus, for the 2001 data, I used feathers from five locations in three states in the location-level analysis. For 2002 location-level resolution, I used feathers from four sites in two states. In all cases, I evaluated assignments with leave-one-out cross-validation and by assigning 2001 data with posteriors from the 2002 data and vice versa.

RESULTS

Latitudinal patterns of isotope ratios

Hydrogen isotope values in feathers tended to show an inverse relationship with latitude across my study area but with overlap among the latitudes (Fig.2). The δD regression coefficients ranged from -5.3 to -3.9 (95% CI) and from -6.4 to -3.2 (95% CI) for 2001 and 2002 respectively. Between-location variation accounted for 80.9% of the total variance in δD for the 2001 data, whereas 45.7% of the total in 2002 was accounted for by between-location variation. Accordingly, the regression of δD on latitude explained more of the variation in the 2001 data (Adjusted $R^2 = 0.71$) than in that for 2002 (Adjusted $R^2 = 0.23$).

Carbon isotope values also tended to decrease with latitude, although less strongly (95% CI for $\delta^{13}C$ regression coefficient, 2001 data: -0.33 to -0.03, 2002 data: -0.81 to -

Reproduced with permission of the copyright owner. Further reproduction prohibited without permission.

0.24). Most of the total variation in $\delta^{13}C$ was attributed to between-location variation in both years (78.8% in 2001, 87.1% in 2002), but the values did not vary systematically with latitude (Adjusted $R^2 = 0.06$ and 0.10 for 2001 and 2002 respectively).

Nitrogen isotope values were not associated with latitude in 2001 (95% CI for $\delta^{15}N$ regression coefficient: -0.17 to 0.03, Adjusted $R^2 = 0.01$), but were in 2002 (95% CI for $\delta^{15}N$ regression coefficient: -0.95 to -0.57, Adjusted $R^2 = 0.35$). In both years, most of the total variation was between locations (83.3% in 2001, 66.4% in 2002).

Continuous-response prediction of latitudinal origin

Fixed-effect inverse regression models for latitude using hydrogen and carbon isotope values as explanatory variables appeared to describe the data reasonably well in 2001 (Adjusted R^2=0.76, p<0.0001, $\sqrt{MSE}$ =1.75), and less so in 2002 over a reduced latitudinal range (Adjusted R^2=0.24, p<0.0001, $\sqrt{MSE}$ =1.08). However, the models produced poor predictions for both the generating and the independent datasets (Fig. 3). Prediction intervals were similar in magnitude to the entire sampling ranges; the intervals for individual predictions of latitude ranged 7 degrees and 4.3 degrees for the 2001 and 2002 data respectively.

The fixed effects inverse regression models for both years yielded substantial non-random structure in the residuals violating the assumption $\varepsilon_i \sim N(0,\sigma^2)$ (Fig 4a). Most of this structure was attributed to residuals associated with δD (Fig. 4b). This is an artifact of the sampling structure that was likely amplified for δD because the within-location variance of δD was substantial, yet most of the overall variation was still among locations. Partitioning the variance into within- and among-location components removed

Reproduced with permission of the copyright owner. Further reproduction prohibited without permission.

the structure in the residuals, satisfied the assumption, and resulted in much smaller AICc scores (Fig 4b, Table 1).

The most parsimonious model for latitude in both years included only a fixed intercept and location as a random effect. Evidence ratios were overwhelmingly in favor of this intercept-only mixed model over models that included isotope ratios as predictors (Table 1). Removing the intercept-only model from the candidate set did not reduce the disparity between the fixed and mixed effects models. Evidence ratios favor the model that includes location as a random effect and isotope values as fixed effects by 6.5×10^{91} to 1 and 3.4×10^{108} to 1 over the model that includes only the isotopes for 2001 and 2002 respectively.

Discrete-response prediction of geographic origin

The probability models correctly assigned 73% - 93% of the observations in a leave-one-out cross-validation of the 2001 data. Correct assignment rates increased with the number of isotopes used. Cross-validation of the 2002 data was similar (Table 2). For comparison, random assignment rates for tests based on 2001 data were 33% to the correct state and 20% to the correct location. Random assignment rates for 2002-based tests were 50% to state and 25% to location.

State-level assignment rates of 2002 data using posteriors estimated from 2001 data were similar to those from cross-validation and were an improvement from random rates. State-level assignment rates of 2001 data using posteriors from 2002 data were also improvements from random for all isotope combinations considered, but only the use of all three isotopes provided better than a marginal improvement (Table 2). Recalling that

Reproduced with permission of the copyright owner. Further reproduction prohibited without permission.

only two states were sampled in 2002 and three in 2001, 23% of the 2001 data were necessarily misclassified. When considering only the remaining 77% of the data that were from the two states also sampled in 2002, correct assignment rates were 73%, 66%, and 84% for posteriors from hydrogen, hydrogen + carbon, and hydrogen + carbon + nitrogen, respectively.

Location-level assignment using only hydrogen from 2001 to assign 2002 data yielded a slight improvement over random assignment. When considering only those locations that were sampled in both years, the rate increased slightly to 29%. Correct assignment rate more than doubled when using all three isotopes (Table 2). That rate increased to 69% when considering only locations sampled in both years. Similarly, tests based on only hydrogen values in 2002 assigned 26% of the 2001 data to the correct location. That compared with a 25% random assignment rate. This improved to 38% if we considered only data from locations that were sampled in both years. The assignment rate again doubled when using all three isotopes from 2002 to assign 2001, and increased to 81% if considering only locations sampled in both years.

DISCUSSION

Latitudinal patterns of variation in isotope values

Isotope values in feathers of mountain plover chicks varied with geography, but not always systematically so. As expected, mean hydrogen values varied systematically to different degrees over ranges of both six and nine degrees of latitude. This supports most other North American studies that have used hydrogen values in feathers to describe

Reproduced with permission of the copyright owner. Further reproduction prohibited without permission.

geographic origins of birds (Chamberlain et al. 1997, Hobson and Wassenaar 1997, Meehan et al. 2001, Kelly et al. 2002).

Carbon values were not well predicted by latitude in either year. In contrast to many studies of migrating birds using stable isotopes, both C3 and C4 plants occur in habitats used by plover chicks. For example, in Colorado plovers use a combination of habitats including native prairie dominated by C4 grasses and dryland crops of C3 plants, especially winter wheat (Knopf and Rupert 1999). Regional trends in carbon values that have been reported by others (Körner et al. 1991, Rubenstein et al. 2002) are likely swamped by local effects from C3-C4 mixtures at similar latitudes across the western Great Plains of North America (Fig. 2). Wassenaar and Hobson (2000) reported similar results for central North America in red-winged blackbirds (*Agelaius phoeniceus*) that used both C3 and C4 habitats. Graves et al. (2002) demonstrated that local geographic and demographic effects are stronger sources of variation in $\delta^{13}C$ than more regional or continental effects. Our data support the assertion that variation of $\delta^{13}C$ in bird feathers from across a continental geography derives predominantly from local sources, rather than regional phenomena.

Surprisingly, nitrogen values appeared to vary systematically with latitude in 2002 (Fig. 2). In fact, the adjusted R^2 for the nitrogen model was greater than that for hydrogen in the same year, improbably suggesting that latitude explained more variation in nitrogen than in hydrogen. I do not believe the pattern has any phenomenological merit and offer instead that this finding was spurious; it exposes how *ad-hoc* regression approaches to modeling data that are not independent random samples can be misleading. The 2001 data for nitrogen were not remotely related to latitude, as expected.

Reproduced with permission of the copyright owner. Further reproduction prohibited without permission.

Predicting latitudes with continuous models

Predictions from the inverse regression models were not useful for assigning latitudinal origins. The model based on the 2001 data generated large location-specific prediction intervals. For example, when predicting the model-generating data, known Colorado birds from the two southernmost sites (latitude 38.5°-39.2°N) were predicted as having originated somewhere between 32° and 47°N (Fig. 3a). This range includes the full extent of the breeding range for mountain plover (Fig. 1). When using the same 2001-based model to predict the independent data from 2002 for those same two southernmost sites, the predicted range was even larger, spanning from Mexico (28°N) north to Montana (45°N). The predictions from the 2002-based model were similarly vague, failing to distinguish northern birds from southern birds in either the model-generating data or in the independent 2001 data (Fig. 3b, d). This precludes even qualitative statements about the likelihood of a bird originating from any particular portion of the overall breeding range.

Kelly et al. (2002) reported that an inverse regression model using only δD for range-wide Wilson's warbler (*Wilsonia pusilla*) samples yielded similarly poor results. For most values of δD, prediction intervals that incorporated model uncertainty included the entire breeding range of the warblers, despite the fact that the data in that study more closely represented independent random samples. Rubenstein et al. (2002) used inverse regression with both δD and δ^{13}C to predict latitude and longitude of origin for samples of black-throated blue warblers (*Dendroica caerulescens*) and reported better precision in their predictions. However, that study reported but did not consider or propagate any

Reproduced with permission of the copyright owner. Further reproduction prohibited without permission.

uncertainty in the model predictions. Reported values of $\sqrt{MSE} = 3.18$ for latitude and $\sqrt{MSE} = 6.40$ for longitude yield prediction intervals for an individual bird that span ~13°of latitude and ~26°of longitude, or slightly larger than geographic range over which birds were sampled. If variance among individuals within each of the ten locations is also considered, the overall uncertainty range of isotope values would widen even further, effectively precluding assignments of origin. Such results align better with those of Kelly et al. (2002) and results reported here.

Both Kelly et al. (2002) and Rubenstein et al. (2002) pooled samples over many years, used feathers of uncertain origin, and measured isotope values for combined exchangeable and non-exchangeable hydrogen. This study attempted to control for those three sources of potential variation, yet inverse regressions, albeit over a more restricted range of latitudes, yielded similarly poor results. Thus, the inverse regression framework is inappropriate for the problem of assigning geographic origins. The problems with regression are most easily seen in the comparisons between the fixed and mixed effects models.

The difference in AICc scores between the fixed and mixed effects models (Table 1) demonstrates the importance of incorporating the spatially hierarchical structure of the data. Pooling data across years revealed a substantial cost associated with ignoring the temporal structure in the data as well. I fit the temporally pooled data to the same models for latitude as for each year separately. The difference in AICc between the fixed and mixed effects models for the temporally-pooled data (ΔAICc = 1034 , evidence ratio = 4.1×10^{224}) was about twice as large as for the year-specific comparisons. This disparity relative to that for the year-specific models represents the compounded costs of ignoring

Reproduced with permission of the copyright owner. Further reproduction prohibited without permission.

both temporal and spatial structure in the data. It suggests that the cost of pooling over annual fluctuations in isotope values is on the same order as that for ignoring spatial dependencies, and both are large. This finding further implies potential challenges associated with prediction methods that rely on the use of spatially-smoothed models of temporally-averaged (pooled) δD in precipitation.

The disparity between the fixed and mixed effects models for all datasets was substantial, but not surprising. Birds from a given sample location shared the same (or nearly so) latitude such that the values of the response variable for all data were clustered into a small set of discrete groups (Fig. 2). The mixed effects model used some of the degrees of freedom to adjust the intercept for each location-specific group of data, whereas the fixed effect model was forced to interpolate between the clusters. This means that the fixed effect model predicted the pattern in general, but not in particular, whereas the reverse was true for the mixed effects model. This likely stems from the mismatch between sample and model structures that resulted in assumption violations. Unfortunately, the mixed effects model that satisfies the assumption for the residuals requires *a priori* information about sample origin, precisely the information we hope to learn from the model.

The discrete-response framework

The use of discrete-response models is not new to assignment problems using stable isotopes. Rocque (2003) used a Bayesian approach that jointly incorporated both continuous (isotopes and skeletal measurements) and discrete (microsatellite) marker types. Royle and Rubenstein (2004) used a likelihood approach that they extended to a

Reproduced with permission of the copyright owner. Further reproduction prohibited without permission.

Bayesian approach incorporating estimated relative abundance. Caccamise et al. (2000) and Wassenaar and Hobson (2000) each used linear discriminant analysis, which is similar to the likelihood approach described in Royle and Rubenstein (2004).

In general, the probability approach in this study did better than random assignment, and therefore also better than the inverse regressions. The probability approach performed better with increasing number of isotope markers. In all but one case, using posteriors generated from all three isotopes resulted in the highest proportion of correct assignments (Table 2). The approach provided promising results from cross-validation with the training data, regardless of the spatial resolution of assignment. The tests with independent data, however, were much more sensitive to the relative geographic representations of the datasets. Specifically, the geographic range sampled in 2002 was more restricted than that of 2001. Consequently, assignment rates were similar for independent and training data only in the case where the range of training data was greater than that of the independent data.

My results were most similar to those of Caccamise et al. (2000), a study that also used three isotope values from newly growing (known origin) feathers collected in a single year. The sample groupings were stratified across clear discrimination gradients in the isotopes considered (carbon, nitrogen and sulfur) and the authors reported a 92% correct assignment rate. Wassenaar and Hobson (2000) correctly classified 80% of their data among 11 locations that spanned discrimination gradients in both isotope values considered (carbon and hydrogen), despite the facts that the feathers were collected and pooled over a 17-year period and were of ultimately uncertain origin. Royle and Rubenstein (2004) pooled feathers of uncertain origin collected over ten years into three

Reproduced with permission of the copyright owner. Further reproduction prohibited without permission.

vast geographic categories, each represented by three collection sites. Using the same two isotopes (carbon and hydrogen), 62% of the observations were assigned to the correct region. The relative results from the latter two studies perhaps seem counter-intuitive, given the need for greater discrimination among 11 categories as compared with three. The primary difference between the two studies is that the latter did not span strong discrimination gradients in the isotopes, and it may have also suffered from geographic misrepresentation in the samples, given that many birds sampled from each of a few sites were used to represent much wider geographies.

Probability models do not make assumptions about structural (mechanistic) relationships between isotope values and sample locations. It is a simple matter to directly estimate and apply posteriors empirically from isotope data. This is simultaneously beneficial and limiting. On the one hand, I do not require mechanistic assumptions about the relationship between isotope values and locations. However, for precisely the same reason, the models are difficult to "train". In particular, the precision of these assignment methods is limited by the extent of geographic sampling. Sample design can have a tremendous effect on the resulting inferences, as evidenced by the test results with the independent datasets in this study.

In parametric applications such as in this study, the representation and stratification of locations sampled as well as the absolute number and relative proportions of birds sampled from each location are clear sources of bias in the probability estimations. Take for example the variability in the per-location sample sizes and associated ranges of observed values of δD presented here. All feathers in this study were grown locally where collected, yet δD values for a single location in a single year ranged

Reproduced with permission of the copyright owner. Further reproduction prohibited without permission.

from 7‰ to nearly 60‰ (Fig. 2), suggesting vastly different precisions in the origin assignment probabilities. Interestingly, no obvious outliers were responsible for the widest single-location distributions of δD (Fig. 2), which forces me to question the notion of a characteristic range of δD values for any single location. Although it was not the focus of this paper, this finding has clearly significant implications about the utility of predictive contour maps of δD in feathers or precipitation. Indeed, had I used precipitation-based maps to assign origin based on feathers spanning 60‰ in δD values, I would have predicted that the feathers derived from most of North America, not a single discrete location as was the actual case. I will address this finding more thoroughly elsewhere.

Conclusions

That every animal is "isotopically marked" and therefore intrinsically provides biogeographic information remains a compelling notion. And indeed, many questions concerning migration or dispersal via isotopes are presently approachable with appropriate study designs. This is particularly true for those that are less concerned with geography than with habitat-specific differences over which distinct discrimination patterns occur. There is a swiftly growing collection of case-specific evidence suggesting general isotopic patterns in feathers across vast geographies. However, very few of these studies have tested the idea with tissue of known-origin. Thus, the question of how to appropriately structure the spatial interpolation remains largely unanswered. Increasing knowledge of particular physiological mechanisms in stable isotope biogeochemistry will likely continue to guide efforts to address that question. In the meantime, the *ad-hoc* use

Reproduced with permission of the copyright owner. Further reproduction prohibited without permission.

of assumptive regression models for inferring geographic origin will only continue to mislead. Probability-based models provide a more flexible framework that can be structurally expanded to incorporate mechanistic models as appropriate or available. As pointed out by Webster et al (2002), the refinement of assignment tests is an active area of research in population genetics. Assignment problems using isotopes are directly analogous to those using molecular markers. Continuing to adapt and expand modeling approaches developed for other disciplines to problems using isotopes seems another obvious direction for future effort and collaboration.

Reproduced with permission of the copyright owner. Further reproduction prohibited without permission.

REFERENCES

Burnham KP, Anderson DR. 2002. Model selection and multi-model inference: a practical information-theoretic approach, 2nd edition. Springer, Berlin Heidelberg New York

Caccamise DF, Reed LM, Castellie PM, Wainwright S, Nichols TC. 2000. Distinguishing migratory and resident Canada Geese using stable isotope analysis. Journal of Wildlife Manage **64**:1084-1091

Chamberlain CP, Blum JD, Holmes RT, Feng X, Sherry TW, Graves GR. 1997. The use of isotope tracers for identifying populations of migratory birds. Oecologia **109**:132-141

Chamberlain CP, Bensch S, Feng X, Akesson S, Andersson T. 2001. Stable isotopes examined across a migratory divide in Scandinavian willow warblers (*Phylloscopus trochilus trochilus* and *Phylloscopus trochilus acredula*) reflect their African winter quarters. Proceedings of the Royal Society of London, series B **267**:43-48

Evans KL, Waldron S, Bradbury RB. 2003. Segregation in the African wintering ranges of English and Swiss swallow *Hirundo rustica* populations: a stable isotope study. Bird Study **50**:294-299

Fry B, Brand W, Mersch FJ, Tholke K, Garritt R. 1992. Automated analysis system for coupled δ^{13}C and δ^{15}N measurements. Analytical Chemistry **64**:288-291

Reproduced with permission of the copyright owner. Further reproduction prohibited without permission.

Gannes LZ, O'Brien DM, Martinez del Rio C. 1997. Stable isotopes in animal ecology: assumptions, caveats, and a call for more laboratory experiments. Ecology **78**:1271-1276

Gill JA, Norris K, Potts PM, Gunnarsson TG, Atkinson PW, Sutherland WJ. 2001. The buffer effect and large-scale population regulation in migratory birds. Nature **412**:436-438

Graves GR, Romanek CS, Navarro AR. 2002. Stable isotope signature of philopatry and dispersal in a migratory songbird. Proceedings of the National Academy of Science USA **99**:8096-8100

Hebert CE, Wassenaar LI. 2001. Stable nitrogen isotopes in waterfowl feathers reflect agricultural land use in western Canada. Environmental Science and Technology **35**:3482-3487

Hobson KA. 1999. Stable-carbon and nitrogen ratios of songbird feathers grown in two terrestrial biomes: implications for evaluating trophic relationships and breeding origins. Condor **101**:799-805

Hobson KA, Alisauskas RT, Clark RG. 1993. Stable-nitrogen isotope enrichment in avian tissues due to fasting and nutritional stress: implications for isotopic analysis of diet. Condor **97**:752-762

Hobson KA, Wassenaar LI. 1997. Linking breeding and wintering grounds of neotropical migrant songbirds using stable hydrogen isotopic analysis of feathers. Oecologia **109**:142-148

Reproduced with permission of the copyright owner. Further reproduction prohibited without permission.

Hobson KA, Atwell L, Wassenaar LI. 1999. Influence of drinking water and diet on the stable-hydrogen isotope ratios of animal tissues. Proceedings of the National Academy of Science USA **96**:8003-8006

Hobson KA, McFarland KP, Wassenaar LI, Rimmer CC, Goetz JE. 2001. Linking breeding and wintering grounds of Bicknell's thrushes using stable isotope analysis of feathers. Auk **118**:16-23

Hobson KA, Wassenaar LI. 2001. A stable isotope approach to delineating population structure in migratory wildlife in North America: an example using the loggerhead shrike. Ecological Applications **11**:1545-1553

Hobson KA, Wassenaar LI, Bayne E. 2004. Using isotopic variance to detect long-distance dispersal and philopatry in birds: an example with ovenbirds and American redstarts. Condor **106**:732-743

Kelly JF, Atudorei V, Sharp ZD, Finch DM. 2002. Insights into Wilson's warbler migration from analyses of hydrogen stable-isotope ratios. Oecologia **130**:216-221

Knopf FL. 1996. Mountain Plover (*Charadrius montanus*). *In* A. Poole and F. Gill [eds] The Birds of North America, No. 211. The Academy of Natural Sciences, Philadephia, PA, and The American Ornitholigsts' Union, Washington, D.C.

Knopf FL, Rupert JR. 1996. Productivity and movements of Mountain Plovers breeding in Colorado. Wilson Bulletin **108**:28-35

Knopf FL, Rupert JR. 1999. Use of cultivated fields by breeding Mountain Plovers in Colorado. In: Vickery PD, Herkert JR (eds) Studies in avian biology, No. 19, Cooper Ornithological Society and Allen Press, Kansas, pp 81-86

Reproduced with permission of the copyright owner. Further reproduction prohibited without permission.

Körner C, Farquhar GD, Wong SC. 1991. Carbon isotope discrimination by plants follows latitudinal and altitudinal trends. Oecologia **74**:623-632

Marra PP, Hobson KA, Holmes RT. 1998. Linking winter and summer events in a migratory bird by using stable-carbon isotopes. Science **267**:1340-1343

McKechnie AE, Wolf BO, Martinez del Rio C. 2004. Deuterium stable isotope ratios as tracers of water resource use: an experimental test with rock doves. Oecologia **140**:191-200

Meehan TD, Lott CA, Sharp ZD, Smith RB, Rosenfield RN, Stewart AC, Murphy RK. 2001. Using hydrogen isotope geochemistry to estimate the natal latitudes of immature Cooper's Hawks migrating through the Florida Keys. Condor **103**:11-20

Meehan TD, Rosenfield RN, Atudorei VN, Bielefeldt J, Rosenfield LJ, Stewart AC, Stout WE, Bozek MA. 2003. Variation in hydrogen stable-isotope ratios between adult and nestling Cooper's Hawks. Condor **105**:567-572

Meehan TD, Giermakowski JT, Cryan PM. 2004. GIS-based model of stable hydrogen isotope ratios in North American precipitation for use in animal movement studies. Isotopes in Environmental Health Studies **40**:291-300

Norris DR, Marra PP, Kyser TK, Sherry TW, Ratcliffe LM. 2004. Tropical winter habitat limits reproductive success on the temperate breeding grounds in a migratory bird. Proceeding of the Royal Society of London, Series B **271**:59-64

Pain DJ, Green RE, Gießing B, Kozulin A, Poluda A, Ottosson U, Flade M, Hilton GM. 2004. Using stable isotopes to investigate migratory connectivity of the globally threatened aquatic warbler *Acrocephalus paludicola*. Oecologia **138**:168-174

Reproduced with permission of the copyright owner. Further reproduction prohibited without permission.

Rocque DA. 2003. Intrinsic markers in avian populations: explorations in stable isotopes, contaminants, and genetics. PhD Diss University of Alaska, Fairbanks

Royle JA, Rubenstein DR. 2004. The role of species abundance in determining the breeding origins of migratory birds using stable isotopes. Ecological Applications **14**:1780-1788

Rubenstein DR, Chamberlain CP, Holmes RT, Ayers MP, Waldbauer JR, Graves GR, Tuross NC. 2002. Linking breeding and wintering ranges of a migratory songbird using stable isotopes. Science **295**:1062-1065

Schekkerman H, Visser GH. 2001. Prefledging energy requirements in shorebirds: energetic implications of self-feeding precocial development. Auk **118**:944-957

Smith BN, Epstein S. 1971. Two categories of $^{13}C/^{12}C$ ratios for higher plants. Plant Physiology **47**:380-384

Smith RB, Meehan TD, Wolf BO. 2003. Assessing migration patterns of sharp-shinned hawks *Accipiter striatus* using stable-isotope and band encounter analysis. Journal of Avian Biology **34**:387-392

Wassenaar LI, Hobson KA. 2000. Stable carbon and hydrogen isotope ratios reveal breeding origins of red-winged blackbirds. Ecological Applications **10**:911-916

Wassenaar LI, Hobson KA. 2001. A stable isotope approach to delineate geographical catchment areas of avian migration monitoring stations in North America. Environmental Science and Technology **35**:1845-1850

Wassenaar LI, Hobson KA. 2003. Comparative equilibration and online technique for determination of non-exchangeable hydrogen of keratins for animal migration studies. Isotopes in Environmental Health Studies **39**:211-217

Reproduced with permission of the copyright owner. Further reproduction prohibited without permission.

Webster MS, Marra PP, Haig SM, Bensch S, Holmes RT. 2002. Links between worlds: unraveling migratory connectivity. Trends in Ecology and Evolution **17**:76-83

Reproduced with permission of the copyright owner. Further reproduction prohibited without permission.

Figure 1. Map of mountain plover breeding range. Dots mark sample locations for 2001. Triangles mark sample locations for 2002. Diamonds mark locations sampled in both 2001 and 2002.

Figure 2. Data for δD, δ^{13}C and δ^{15}N from mountain plover chick feathers collected in 2001 (top row) and 2002 (bottom row). δD is for non-exchangeable hydrogen only and is reported relative to VSMOW. δ^{13}C is reported relative to PDB. δ^{15}N is reported relative to Air. Note the between-year difference in ranges of latitude sampled.

Figure 3. Observed versus predicted latitudes of origin using inverse regression model framework. δD and δ^{13}C in mountain plover chick feathers were used as independent variables to model latitude of origin. δ^{13}C is reported relative to PDB, and δD is reported relative to VSMOW. Error bars extend to the 95% prediction limits. Diagonal lines show 1:1 observed:predicted ratio. a) 2001 predictions for model-generating data. b) 2002 predictions for model-generating data. c) model generated from 2001 data used to predict 2002 observations. d) model generated from 2002 data used to predict 2001 observations.

Figure 4. Residuals from inverse regression model of latitude using δD and δ^{13}C as explanatory variables. δ^{13}C is reported relative to PDB, and δD is reported relative to VSMOW. Horizontal bars at zero are for reference and do not indicate mean of the residuals. Left column is 2001 data, right column is 2002 data. a) residuals of predicted latitude for model-generating data. b) residuals of δD from model with δD and δ^{13}C as explanatory variables (top row) and with location added as a random effect (bottom row).

Reproduced with permission of the copyright owner. Further reproduction prohibited without permission.

Figure1

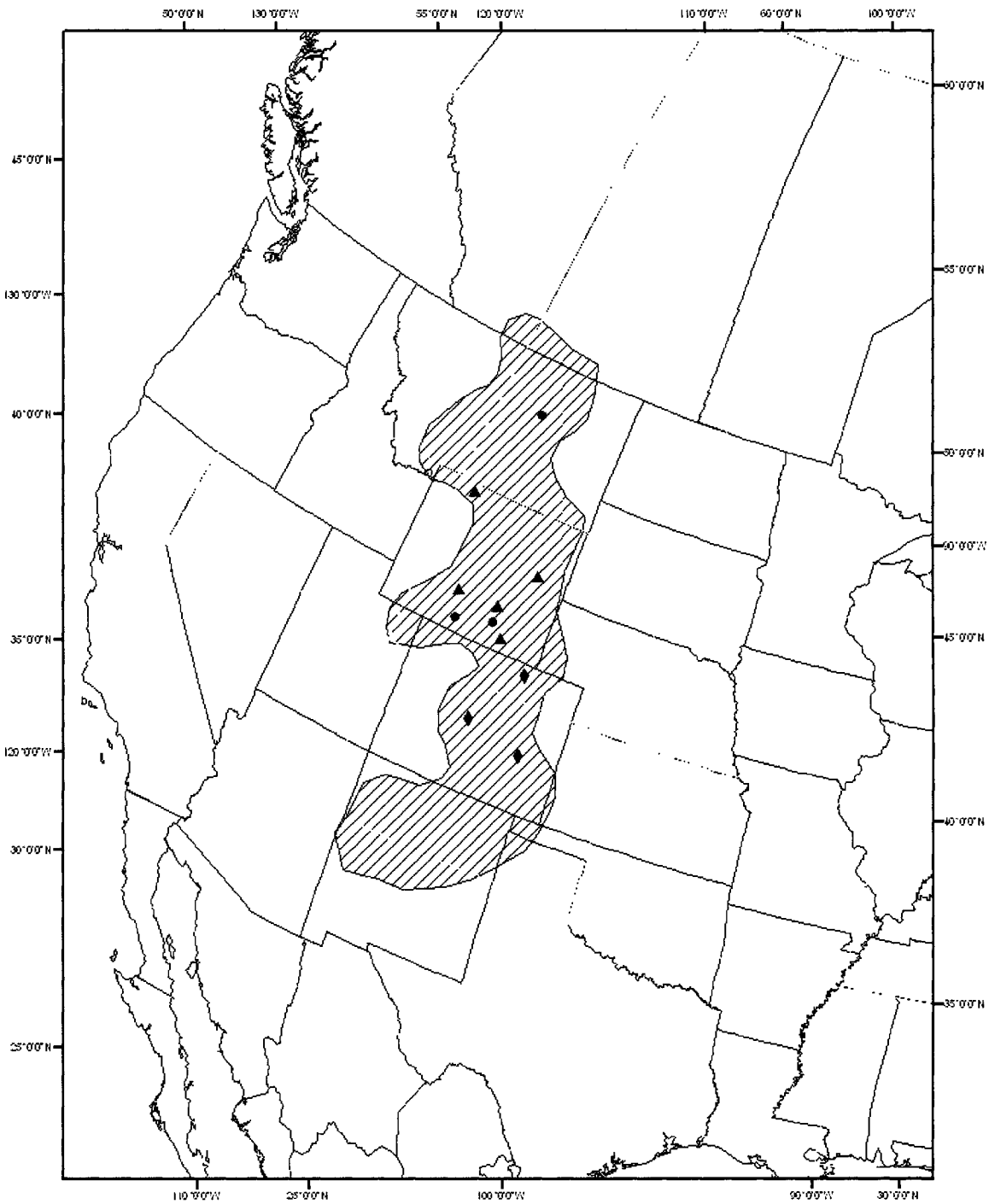

Reproduced with permission of the copyright owner. Further reproduction prohibited without permission.

Figure 2

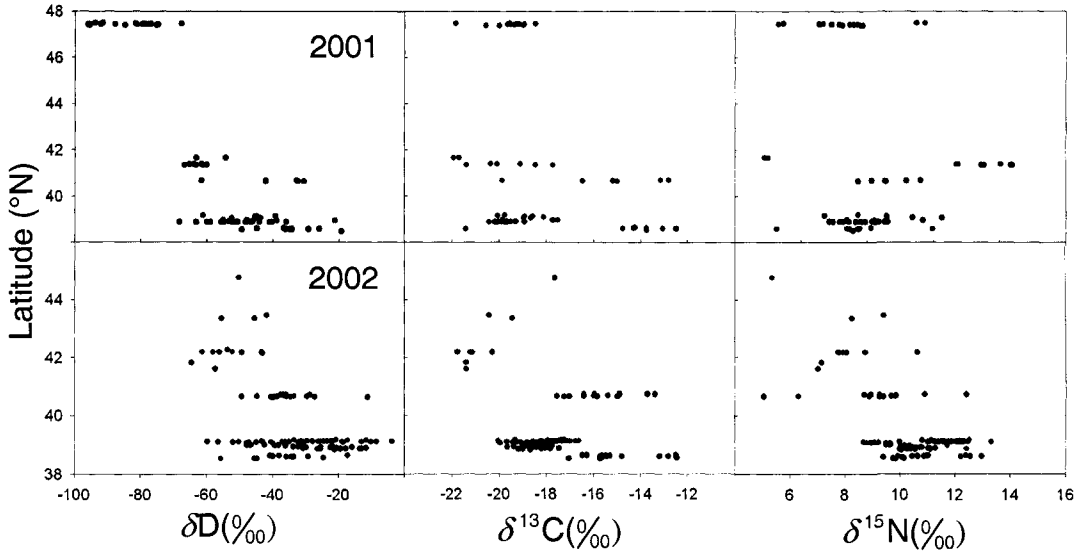

Reproduced with permission of the copyright owner. Further reproduction prohibited without permission.

Figure 3

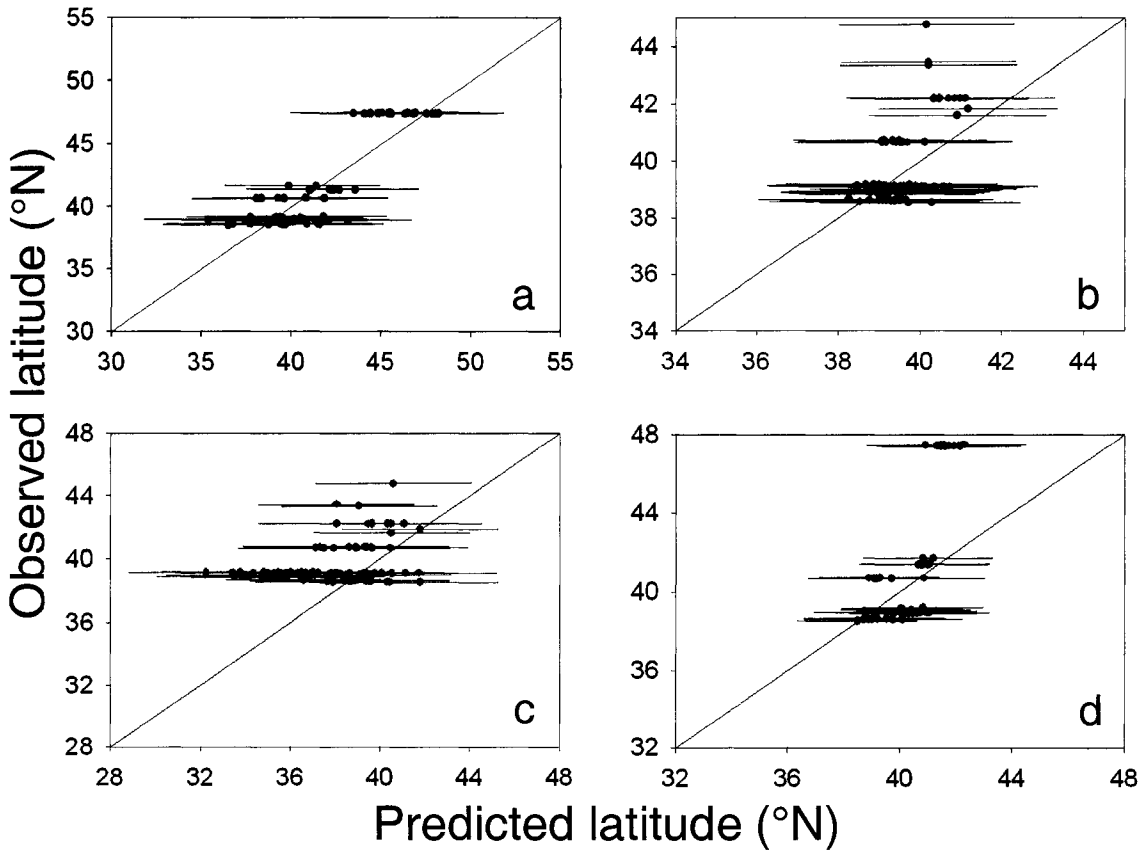

Reproduced with permission of the copyright owner. Further reproduction prohibited without permission.

Figure 4

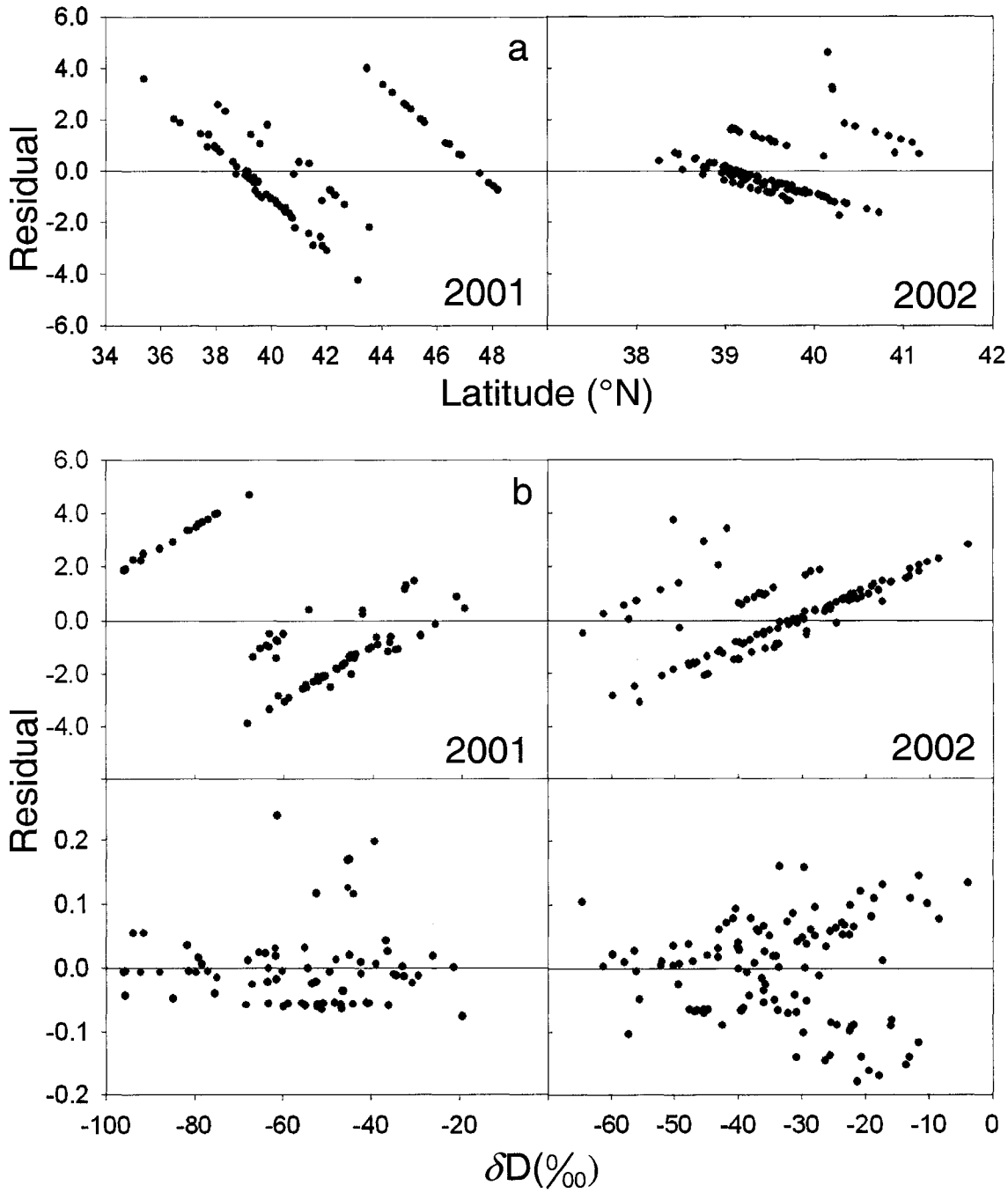

Reproduced with permission of the copyright owner. Further reproduction prohibited without permission.

Table 1. Differences in AICc scores and evidence ratios (E.R.) for inverse regression models of latitude. Mixed models included sample location as a random effect in addition to the fixed effects of either just an intercept or an intercept plus hydrogen (H) and carbon (C) isotope values.

Model	2001 data		2002 data	
	ΔAICc	E.R.	ΔAICc	E.R.
Intercept only, mixed	0[a]	1	0[a]	1
H + C, mixed	20.0	22 026	26.6	597 195
H+ C, fixed	442.8	1.4×10^{96}	526.4	2.0×10^{114}

[a] AICc score for the top model was -136.1 and -184.5 for 2001 and 2002 respectively

Reproduced with permission of the copyright owner. Further reproduction prohibited without permission.

Table 2. Assignment rates from Bayes Rule inversions. Leftmost column lists isotopes used to generate probability density functions. Second and third columns from the left show results from leave-one-out cross-validation. Rightmost two columns show assignment results for independent datasets.

Isotopes	2001 CV		2002 CV		2001 – 2002[a]		2002 – 2001[b]	
in pdfs	state	loc	state	loc	state	loc	state	loc
HCN	0.93	0.86	0.95	0.90	0.94	0.64	0.63	0.55
HC	0.88	0.77	0.94	0.86	0.91	0.52	0.51	0.56
H	0.91	0.73	0.92	0.65	0.88	0.25	0.57	0.26

[a] assignment of 2002 data with probability densities estimated from 2001 data

[b] assignment of 2001 data with probability densities estimated from 2002 data

Reproduced with permission of the copyright owner. Further reproduction prohibited without permission.

CHAPTER TWO

IMPROVED ESTIMATES OF CERTAINTY IN STABLE ISOTOPE-BASED GEOGRAPHIC ASSIGNMENTS FOR TRACKING MIGRATORY ANIMALS

Reproduced with permission of the copyright owner. Further reproduction prohibited without permission.

Abstract. The use of stable-hydrogen isotopes (δD) has become a common tool for estimating geographic patterns of movement in migratory animals. This method relies on broad and relatively predictable geographic patterning in δD values of precipitation, but these patterns are not estimated without error. In addition, δD measurements are relatively imprecise, particularly for organic tissue. Most models for estimating geographic locations have ignored these sources of error. Common modeling approaches include regression, range-matching and likelihood-based assignment tests (including discriminant analysis). Here, I show the benefits of a simple stochastic extension to likelihood-based assignment tests that incorporates two estimable sources of error and describe the resulting influence on the certainty of assigning breeding origins for wintering American redstarts (*Setophaga ruticilla*), a small Nearctic-Neotropical migratory bird. Through simulation, I incorporated both interpolation error associated with models of δD in precipitation and analytical error associated with the measurement of δD in tissue samples. In general, assignments that did not include these sources of error fell within the ranges of the stochastic results but the difference in proportion of birds assigned to any one breeding region varied by as much as 54%. To explore how the distribution of assignments generated from error models influenced the application of these results, I developed a simple model of winter habitat loss. I removed the proportion of redstarts wintering at a particular site from the global population and then used the isotope-based assignments to predict the resulting population declines for each breeding region. This gave distributions of change in population sizes, some of which included no change or even a population increase. The sources of error I modeled may challenge the degree of certainty in the use of stable isotope-based data on connectivity to predict

Reproduced with permission of the copyright owner. Further reproduction prohibited without permission.

population dynamics of migratory animals. I suggest that stronger inference will result from incorporating these sources of error into future studies that use δD or other stable isotopes to infer the geographic origin of individuals.

Key words: stable-hydrogen isotopes; migratory connectivity; uncertainty; likelihood; assignment; American redstarts

Reproduced with permission of the copyright owner. Further reproduction prohibited without permission.

INTRODUCTION

Stable isotope analysis has become one of the most widely used and cost-effective tools for tracking seasonal movements of migratory animals (Hobson 1999, Webster et al. 2002, Rubenstein and Hobson 2004, Hobson 2005). Atoms of elements that vary naturally in their atomic weight are referred to as stable isotopes; the isotopic composition of any material is expressed as the ratio of the heavy to light isotope, relative to an internationally accepted standard. Geographic variation in stable isotope compositions can arise through various biological, climatic, or geological processes (Kelly 2000, Rubenstein and Hobson 2004, Bowen et al. 2005). Because animals incorporate isotopic signatures from local food webs and because the turnover of elements in certain tissues is not immediate, individuals can be sampled in one season to estimate their geographic origin in a previous season (e.g. Chamberlain et al. 1997, Hobson and Wassenaar 1997).

In spite of its widespread popularity, many of the assumptions underlying the use of stable isotopes to track the long-distance movements of animals are only now being rigorously tested. For example, recent studies analyzing the isotopic compositions of known origin birds have revealed that the spatial accuracy in the use of some elements, such as hydrogen (deuterium:protium; δD), is probably lower than previously assumed, at least for some systems (Wunder et al. 2005 (Chapter one), Rocque et al. 2006, Langin et al. *in press*). Recent studies have also provided evidence that diet-tissue discrimination factors may not be uniform across a species range (Lott and Smith 2006), or among age classes within a population (Meehan et al. 2003).

Reproduced with permission of the copyright owner. Further reproduction prohibited without permission.

Common statistical methods for estimating the origin of individuals using stable isotopes include simple regression (Kelly et al. 2002, Rubenstein et al. 2002), range matching (Boulet et al. 2006), and assignment methods based on likelihoods or probabilities (Royle and Rubenstein 2004, Wunder et al. 2005 (Chapter one), Norris et al. 2006). Range matching and assignment methods have an advantage over regression models in that the specific geographic origin of animals can be directly estimated. Here, I examine how two known sources of variation in δD influence assignment probabilities and the practical application of assignment results. The first source of variation I call *interpolation error.* Many previous studies have relied on expected δD values from precipitation-based models (and have assumed a constant discrimination factor between precipitation and animals). In these cases, because geographic regions are characterized by mean values from a spatially interpolated map, such studies are subject to random process error associated with the interpolation that could translate to variation in assignment probabilities.

The second source of variation I refer to as *analytical (or measurement) error* and is generated during the analysis of samples for stable isotope compositions (typically with continuous flow isotope ratio mass spectrometry [CF-IRMS]). Because it is not possible to count the number of atoms of each isotope in a sample gas and because conditions vary within the laboratory and within the CF-IRMS apparatus, the isotopic values depend on run-time calibration curves. Thus, the output values are actually expected (mean) values and repeated measurements for the same sample are rarely the same. Analytical error occurs in all elements but is particularly large for δD values because the hydrogen isotopes are relatively volatile; this can be especially problematic in measuring organic

Reproduced with permission of the copyright owner. Further reproduction prohibited without permission.

tissues as some of the hydrogen in organic tissues freely exchanges with ambient water vapor. Typical analytical error values reported for δD range from 1-5‰ (SD) and may therefore contribute significant uncertainty, especially when considering regions or populations with mean values that differ by an amount within this scale (e.g. 4-20‰).

In this paper, I explore how these two sources of error affect analysis of δD data and conclusions about migratory connectivity in American redstarts (*Setophaga ruticilla*), a long-distance migratory songbird that winters in the Caribbean and Central America and breeds in North America. Norris et al. (2006) analyzed δD values in feathers of birds sampled throughout the wintering range. Because redstarts molt on or near the breeding grounds, δD values from wintering birds were used to estimate breeding origin. The breeding range was divided into five breeding regions and a likelihood-based assignment test was used to determine a birds' most likely breeding origin (described in more detail in the methods). My two goals are to (1) examine the degree to which assignment probabilities change when both interpolation and measurement error are incorporated into the assignment test, and (2) use these sources of error to generate a distribution of possible assignments for a given individual bird instead of using a single 'most likely' value. To demonstrate the utility and implications of the second goal, I apply these assignment distributions to a simple model of habitat loss allowing me to generate a range of expected values for population declines.

METHODS

The dataset and presentation of results

Reproduced with permission of the copyright owner. Further reproduction prohibited without permission.

I examined how two potential sources of error could influence the assignment of birds using a stable isotope dataset from Norris et al. (2006) on American redstarts. To describe patterns of connectivity between the wintering and breeding grounds, they analyzed δD values from 188 birds captured at 12 sites across the tropical wintering range. Because feathers were molted on or near the breeding grounds, δD values from wintering birds were used to estimate (assign) breeding origin. *A priori*, the redstart breeding range was divided into five regions and a mean and standard deviation of δD for each region was calculated using values from a precipitation-based interpolation model developed by Bowen and Revenaugh (2003). For each individual sampled on the wintering grounds Norris et al. (2006) then calculated probabilities of growing feathers in each of the five breeding regions based on a normal likelihood function. In addition to regional δD values extrapolated from precipitation maps, Norris et al. (2006) used Bayes Rule to incorporate a prior probability of breeding abundance using estimates from interpolated Breeding Bird Survey data (Sauer et al. 2004). The breeding region with the highest posterior probability was considered to be the region where the individual bred the previous season (referred to here as the 'assignment'). For purposes here, I used a flat (uniform) prior probability both for the original dataset from Norris et al. (2006) and for our simulation models because I was interested in the influence of random error due solely to δD. However, my use of a flat prior does not mean that I think relative breeding abundance does not provide useful information for calculating probabilities of origin; I encourage the use of all types of prior information in the development and refinement of models used for migratory connectivity studies.

Reproduced with permission of the copyright owner. Further reproduction prohibited without permission.

Using the δD dataset on American redstarts, I modeled (1) the effects of interpolation error derived from precipitation-based maps of expected δD values, (2) the effects of analytical error derived from measurements of δD, and (3) the effects from both sources of error combined. For each of these scenarios, I quantified the range of probable outcomes (i.e. distribution of assignments to each of the five breeding regions derived from simulations) and compared this to the original outcome (i.e. the single assignment to the most likely breeding origin). To compare these two results, I present assignments as either pooled within each of the 12 wintering sites or pooled over the entire dataset (all wintering sites). Lastly, to explore how these potential sources of uncertainty could influence the interpretation and application of results, I developed a model simulating habitat loss on the wintering grounds. This model allowed me to compare how a range of possible assignments to breeding regions can be used to describe the degree of certainty in detecting changes in population abundance on the breeding grounds. Below, I describe the sources of error and the habitat loss model in more detail.

Interpolation error

To estimate the mean and standard deviation of δD values for each breeding region, Norris et al. (2006) used rescaled δD values from a spatial interpolation model of growing-season precipitation with a 20' grid map resolution (Bowen and Revenaugh 2003). However, because of the limited spatial distribution of survey stations in North America, the precision of the δD estimate for each grid point in that model depends on the proximity to a station where measurements were made and on the degree to which measured values vary among data stations (Fig. 1). In turn, the distribution of δD values

Reproduced with permission of the copyright owner. Further reproduction prohibited without permission.

used to describe any pre-defined region depends on the number of stations and variance among stations encompassed by the region. To quantify the degree of certainty in the modeled δD values, Bowen and Ravenaugh (2003) jackknifed the data that were used to generate maps for mean annual δD in precipitation (called the 'MAD grid'). Briefly, they simulated ~5000 sets of model parameters, randomly omitting data from one of the original data stations each time. Using these parameters sets and their joint probability distributions, they computed weighted standard deviations for each grid point (called the 'SD grid').

I used both the MAD and SD grids to quantify the effect of interpolation error on the individual-level assignment of wintering birds to each of the pre-defined breeding regions. There were 1261 grid points in the NW breeding region, 1388 in the MW region, 1324 in the NE region, 904 in the CE region, and 1224 in the SE region. I simulated 1000 sets of δD values for each grid point in each of the five breeding regions using independent random draws from a normal distribution with mean given by the value in the MAD grid and the standard deviation given by the SD grid. I then rescaled the δD values for precipitation to expected values for keratin using the rescaling for mean annual δD given in Bowen et al. (2005). For each of these 1000 simulated datasets, I replicated the likelihood-based assignment process for each of the 188 wintering birds. This gave me a distribution of 1000 assignments for each bird.

Analytical error

Analysis of δD values in organic tissue typically produces an analytical error between 1 and 5‰. To quantify the effects of this error type on individual-level

Reproduced with permission of the copyright owner. Further reproduction prohibited without permission.

assignments, I estimated the distribution of standard deviations associated with the measurement of δD from continuous-flow isotope ratio mass spectrometry (CF-IRMS) using a year-long series of measurements for two in-house keratin lab standards from the USGS Stable Isotope Laboratory in Denver, Colorado, USA. The standards were two cryogenically ground and homogenized batches of black bear (*Ursus americanus*) hair, one from a bear collected in Louisiana (LA), and the other from a bear collected in Alaska (AK). The accepted δD value for the LA standard (-78.1 ± 3.0‰) was based on 30 analyses conducted in labs in Denver, Flagstaff, and Saskatoon. The accepted δD value (-171.5 ± 3.3‰) for the AK standard was based on 29 analyses conducted as part of the same effort in the same three labs. These values were calibrated to the VSMOW-SLAP scale via the CFS-CHS-BWBII scaling described in Wassenaar and Hobson (2003). Between two and five replicates of each standard were distributed throughout each of 150 auto-run batches for sample calibration purposes over the course of a year at the Denver lab. The auto-run calibrations were simple regressions of expected (accepted) values on the measured values of the standards. These calibration curves were fitted independently for each auto-run. The residuals from these regressions (782 observations, Fig. 2A) provided a distribution of analytical errors.

I then simulated 10,000 datasets by randomly sampling 16 values from the set of 782 residuals (16 is the number of unknown samples generally included in one auto-run at the Denver lab). For each set of 16 random samples, I computed the mean and standard deviation. In order to increase processing speed for the simulations, I fitted a gamma distribution to the set of 10,000 standard deviations (Fig. 2B); I chose a gamma distribution because values in this distribution are, by definition, always positive (as is

Reproduced with permission of the copyright owner. Further reproduction prohibited without permission.

the case with SD values), because of the relative flexibility (shape and scale) of the distribution, and because it allowed the use of a normal-gamma mixture model for the simulations. For each of the 1000 simulations, I drew an independent random sample from a normal distribution centered on the original measured δD value for each of the 188 birds with standard deviation given by an independent random sample from the gamma distribution described above. Each set of 188 samples was then subjected to the same likelihood-based assignment test as the original data, resulting in a distribution of 1000 assignments for each bird.

Simulation model of habitat loss

To explore a practical implication of incorporating these two sources of error, I developed a simple model of habitat loss for the wintering grounds. My goal was to examine how a distribution of possible assignments to the breeding grounds generated for each individual could influence the confidence in predicting regional population declines.

I set the global population of redstarts (n) to 1000, and let n_i be the population size for each breeding region (where $i = 1...5$). I assumed that the size of n_i was proportional to the winter sampling; each n_i was determined by the proportional number of wintering birds assigned to each breeding region from each wintering site; the number of birds wintering at each site was proportional to the number sampled there. The initial breeding region population sizes without modeling any source of error were n_1 (NW) = 122, n_2 (MW) = 229, n_3 (NE) = 410, n_4 (CE) = 138, n_5 (SE) = 101 and the initial numbers of birds wintering at each site were: Bahamas = 90, Belize = 53, Bermuda = 53, Cuba = 69,

Reproduced with permission of the copyright owner. Further reproduction prohibited without permission.

Dominican Republic = 59, eastern Mexico = 144, Florida = 96, Jamaica = 106, Panama = 53, Puerto Rico = 112, Trinidad-Tobago = 80, western Mexico = 85.

Next, I simulated habitat loss at each wintering site in turn and assumed that all birds at the wintering site that lost habitat perished. I then calculated the proportional reduction in n_i's based on the original assignment outcomes and compared this with the range of declines in n_i's based on the distribution of assignment outcomes generated from our models in the 1000 simulations. The proportional reductions in n_i for the simulations were relative to the respective model used. For example, when the habitat for eastern Mexico was lost, the proportional reduction in n_1 in the analytical error model showed the number of birds that wintered in eastern Mexico and that were assigned to the NW region relative to the overall number of birds that were assigned to the NW region for each given simulation in the analytical error model. In other words, the original number of birds assigned to various breeding regions was not the same for every simulation; the percent reduction in population size was therefore calculated on a per-simulation basis.

RESULTS

Effects of interpolation and analytical error on the assignment of birds

Using δD values from the MAD grid and the original δD values from the 188 redstarts (Norris et al. 2006), 23 individuals were assigned to the NW region, 43 to the MW region, 77 to the NE region, 26 to the CE region, and 19 to the SE region (Fig. 3). In general, I found that these outcomes were likely to occur within the range of outcomes from my simulation models that incorporated analytical error, but not always likely to occur from my simulation models that incorporated interpolation error. Figure 3

Reproduced with permission of the copyright owner. Further reproduction prohibited without permission.

summarizes the distribution of assignments from simulation models that incorporated interpolation error, analytical error, and both types of error and compares these distributions to the original assignments without considering these error types. In each of the 1000 simulations, the interpolation error model predicted fewer assignments to the NW region and more assignments to the MW region. The NW region was subject to the largest degree of interpolation error (Fig. 1), and consequently the intersection between the probability distributions used for making assignments to the NW and MW regions (referred to here as the assignment boundary) shifted by the greatest amount (Fig. 4). However, in all cases, analytical error contributed more to the variation in assignments than interpolation error. Variance in assignments due to analytical error also appeared to be more generally consistent with the original assignments because the variation always encompassed the original outcome, even though it was not always centered on the original outcome. The proportion of birds assigned to any one breeding region differed by as much as 54% when both error types were considered simultaneously. However, the average standard deviation in the difference of assignment proportions was 8%, and differences typically ranged to about 20% (Table 1).

The effects of interpolation error on individual assignments depended on the value of δD for individual birds relative to the distribution of δD values of the regions. Interpolation error changed assignments only for those birds whose δD values were near the original assignment boundaries between any two regions. Interestingly, I identified at least one bird near the assignment boundaries between each of the five breeding regions. There were five such birds in the sample of 188 redstarts; the remaining 183 individuals were assigned to the same region in every one of the interpolation error simulations. In

Reproduced with permission of the copyright owner. Further reproduction prohibited without permission.

contrast, analytical error (by definition of how the error was incorporated in the simulation models) affected δD values for each bird rather than the regional assignment boundaries. Thus, on an individual basis, there were far more changes in the region to which an individual was assigned. In the analytical error simulation models, only 11 of the 188 redstarts were assigned to the same region in all 1000 simulations. These 11 birds were individuals that had δD values near the extreme ends of the range; six were always assigned to the NW region (original δD range [-133, -124‰]), and the other five were always assigned to the SE region (original δD range [-46, -32‰]).

Overall, individual level assignments for the analytical error models remained relatively consistent. Including the 11 birds mentioned above, 130 of the 188 birds (72%) were assigned to the same region in >800 of the 1000 simulations. The results for the model that included both types of error mimicked closely those for the analytical-only model; there were also 130 of the 188 birds assigned to the same region in >800 of the 1000 simulations. However, they were not the same 130 individuals identified in the analytical simulation models; six individuals were assigned to the same region >80% of the time in the analytical error simulation model, but <80% of the time in the simulations that modeled both analytical and interpolation errors, and vice versa.

For illustrative purposes, I also show results of the error simulation for a single wintering site, eastern Mexico, because this site had the largest number of birds sampled during winter and was the only site that had at least one bird assigned to each breeding region (Fig. 5). The interpolation error had no effect on the assignments of any individual wintering in eastern Mexico; all 27 redstarts wintering there were assigned to the same region in each of the 1000 simulations. However, the δD value for one of the

Reproduced with permission of the copyright owner. Further reproduction prohibited without permission.

birds wintering in eastern Mexico was near the assignment boundary between the NW and MW regions, which resulted in the interpolation models consistently assigning one less bird to the NW and one more to the MW than in the original outcome. In contrast, incorporating analytical error into the δD values of each bird resulted in assigning 23 of the 27 birds (85%) to >1 region over the 1000 simulations. Four of these 23 birds were alternately assigned to one of three different regions (NW, MW, or NE) over the course of the simulations. Two individuals were assigned to either the NW or MW regions at about a 50:50 split, and another was assigned to the CE and SE regions with a split of about 50:50. Despite this potential for large variation in individual assignments, 24 of the 27 birds (89%) were assigned to the same breeding region in >800 of the 1000 simulations.

Effects of error on predicting population declines

I simulated habitat loss at each of the wintering sites and assumed that all birds at that site perished after the habitat was removed. For illustrative purposes, I again focus on eastern Mexico. Using the original assignments (i.e. without considering any source of error), the population of the NW region (n_1) was reduced by 60%, the MW region (n_2) by 23%, the NE region (n_3) by 1%, the CE region (n_4) by 4%, and the SE region (n_5) by 5%.

The distribution of reduction in n_i's from the interpolation error model encapsulated the original outcome for all but one region (NW; Fig 6). All original outcomes were contained within the distributions for the simulations that included analytical error, as well as the simulations that included both error types. Based on the

Reproduced with permission of the copyright owner. Further reproduction prohibited without permission.

analytical error models, the relative percent reduction in population size ranged about 25% in the case the NW breeding region, 15% for the MW region, and was bimodal for the NE, CE and SE regions. The bimodality of these distributions indicated that some of the birds wintering in eastern Mexico had δD values within the range of analytical error from the assignment boundaries between regions. More importantly, it suggests that there was more than one "most likely" outcome in terms of potential reduction in population size. Specifically, results for the NE and CE regions suggest that a population change of ≥ 0 was reasonably probable.

DISCUSSION

My results illustrate the potential for relatively large amounts of uncertainty in the use of δD to assign individual migratory animals to particular geographic regions (Table 1). Because most studies in this field have been observational (i.e. unreplicated experiments), it is important to gain a clear understanding of how the associated assumptions affect the degree of certainty in the conclusions of such research. Assuming that the single observed outcome represents the average behavior of a random process is profoundly different than assuming that the outcome could be anywhere within the range of likely outcomes from the same process. For example, even though birds were assigned to the same pre-defined breeding region in most of the simulations that included both error types, 178 of the 188 individuals (95%) were alternately assigned to more than one different breeding region. Moreover, 63 birds (34% of all individuals) were alternately assigned to one of three different breeding regions within those simulations. Given the relatively broad geographic ranges of the pre-defined breeding regions, this was

Reproduced with permission of the copyright owner. Further reproduction prohibited without permission.

somewhat unexpected. However, the simple explanation is illustrated in Fig. 4; despite the wide geographic ranges of the breeding regions, the ranges of δD used to define (and therefore to discriminate between) breeding regions were relatively narrow, especially when considering the magnitude of the analytical uncertainty associated with δD measurements.

Although it is common practice to report some form of analytical precision for stable isotope measurements (often as ±SD or ±SE), I am aware of no studies that have directly considered or estimated the effects of analytical error on their results. Whereas it is likely that the actual δD value for tissue from an individual bird will fall within two standard deviations of the observed measurement (e.g. centered within a range of ~12‰ for most instrumentation), it remains possible that the observed measurement is greater than 15‰ different from the true value. Figure 2 shows that measurements of a highly homogenized standard keratin material can be off by nearly 20‰ (implying a range of 40‰). Unfortunately, in the case of making a single measurement for an unknown sample (which is the most common approach) there is no way to directly measure the accuracy of that particular measurement. Because of this, incorporating a full distribution of possible assignments for each individual directly into data analysis is more informative than using the original single assignment. I suspect that doing so would affect the conclusions of many studies published thus far.

The analytical error simulations resulted in a wider distribution of assignments for an individual than did the interpolation error simulations. This may be in part because the pre-defined breeding regions each contained a relatively large number of grid points (Fig. 1), thus reducing the estimated variance associated with the population of estimated

Reproduced with permission of the copyright owner. Further reproduction prohibited without permission.

precipitation values. This in turn dampens the effect of even relatively large interpolation errors associated with any grid point. Interpolation error is likely to have a bigger impact on studies that encompass either smaller assignment regions or assignment regions for which there is relatively greater interpolation uncertainty (e.g. fewer data stations or more complex topography).

Using pre-defined breeding regions can be an effective method to assign animals of unknown origin using δD but regions must be large enough to overcome the relatively high variability introduced from both the interpolation modeling process and natural heterogeneity in the landscape. A key advantage to the use of pre-defined breeding regions over range-matching or simple regression approaches is that it does not rely on a single δD value for a given location. The process of using modeled precipitation values for a given region to define assignment probability distributions for each region effectively divides a gradient of potential δD values into bins defined by assignment boundaries (Fig. 4). Whereas this is an efficient means for assignment, it masks the degree of assignment uncertainty that can be seen when the probability densities for each of the potential regions of origin are plotted together (Fig. 4). That is, in some areas along the gradient of potential δD values, the difference in density values between two or more regions can be small. This is of course exaggerated near the assignment boundaries between two regions. For example, a bird with a δD value between -80‰ and -100‰ may have originated from the NW, MW, or NE regions and a bird with a δD value between -50‰ and -70‰ could have originated from the MW, NE, or CE regions (Fig. 4). Moreover, if I accept that analytical uncertainty generates a range of values approximately 12‰ wide for a given measurement on an individual within unknown

Reproduced with permission of the copyright owner. Further reproduction prohibited without permission.

origin, I see that the ranges of δD for the MW and CE regions are on this same order of magnitude. That is, any assignment to either the MW or the CE region is likely tenuous.

My results also demonstrate that using a range of possible assignment values for a given individual can have important consequences on how these results are interpreted. Patterns of migratory connectivity will be important for predicting changes in population size of migratory animals (Webster and Marra 2005). Here, I coupled a simple model of habitat loss on the wintering grounds with the distributions of assignments from my simulations to predict changes in population size on the breeding grounds. I show that incorporating a distribution of assignment values leads to a wide range of potential population declines (e.g. Fig. 6). Although the predicted reduction in regional populations based on the original assignments fell within the range of possible outcomes from the simulation models, in some cases, the range of possible outcomes included zero. Some simulations also predicted regional population increases despite the fact that the only numeric manipulation in our simulations was removal of birds. Regional increases occurred under the following two conditions: (1) individuals wintering at non-affected sites were assigned to different breeding regions in the two comparative iterations and (2) few or no redstarts from the affected winter site were assigned to those breeding regions. These results suggest that ignoring both analytical and interpolation error may lead to erroneous conclusions about population dynamics of migratory species. Estimating probability densities of assignments thus allows the incorporation of stochastic effects into more complex population models, which in turn leads to more robust inference about potential population dynamics.

Reproduced with permission of the copyright owner. Further reproduction prohibited without permission.

There are, of course, other estimable sources of error that I did not consider here, but that are likely to affect conclusions from isotope-based assignments. Two known sources of error I did not consider include (1) temporal variation in the δD values in precipitation at any grid point (Farmer et al. 2002), and (2) variation in the discrimination factor between precipitation and animal tissue (Lott & Smith 2006). Both of these sources error will likely contribute additional uncertainty in assignments in animals of unknown origin and warrant investigation using an approach similar to what we have presented here.

In summary, certainty associated with likelihood-based assignment methods will depend on the level of understanding of any process that generates variance in either the measured δD value for an individual or in the values used to characterize a given region (a precipitation-based model in this example), especially for δD values near assignment boundaries. Likewise, any individual with a δD at an extreme end of the gradient will necessarily be assigned to the region at that end of the gradient, even though the individual may have actually derived from another, uncharacterized or unrecognized region. This means that the method is sensitive to how particular regions are pre-defined. Because of this sensitivity, considering distributions of individual-level assignments will lead to more robust inference than will the use of single assignments to the "most likely" region.

Reproduced with permission of the copyright owner. Further reproduction prohibited without permission.

LITERATURE CITED

Boulet, M.B., H.L. Gibbs, and K.A. Hobson. 2006. Integrated analysis of genetic, stable isotope and banding data reveal migratory connectivity and flyways in the northern yellow warbler (*Dendroica petechia; Aestiva* group). Ornithological Monographs **61**:29-78.

Bowen, G.J. and J. Revenaugh. 2003. Interpolating the isotopic composition of modern meteoric precipitation. Water Resources Research **39**:1-13.

Bowen, G.J., L.I. Wassenaar, and K.A. Hobson. 2005. Global application of stable hydrogen and oxygen isotopes to wildlife forensics. Oecologia **143**:337-348.

Chamberlain, C.P., J.D. Blum, R.T. Holmes, X. Feng, T.W. Sherry, G.R. Graves. 1997. The use of isotope tracers for identifying populations of migratory birds. Oecologia **109**:132-141.

Farmer, A., R. Rye, G. Landis, C. Bern, C. Kester, and I. Ridley. 2002. Tracing the pathways of neotropical migratory shorebirds using stable isotopes: A pilot study. Isotopes in Environmental and Health Studies **39**:1-9.

Hobson, K.A. 1999. Tracing origins and migration of wildlife using stable isotopes: a review. Oecologia **120**:314-326.

Hobson, K.A. 2005. Stable isotopes and the determination of avian migratory connectivity and seasonal interactions. Auk **122**:1037-1048.

Hobson, K.A. and L.I. Wassenaar. 1997. Linking breeding and wintering grounds of neotropical migrant songbirds using stable hydrogen isotopic analysis of feathers. Oecologia **109**:142-148.

Reproduced with permission of the copyright owner. Further reproduction prohibited without permission.

Kelly, J.F. 2000. Stable isotopes of carbon and nitrogen in the study of avian and mammalian trophic ecology. Canadian Journal of Zoology **78**:1-27.

Kelly, J.F., V. Atudorei, Z.D. Sharp, and D.M. Finch. 2002. Insights into Wilson's warbler migration from analyses of hydrogen stable-isotope ratios. Oecologia **130**:216-221.

Langin, K.M., M.W. Reudink, P.P. Marra, D.R. Norris, T.K. Kyser, and L.M. Ratcliffe. *In press* Hydrogen isotopic variation in migratory bird tissues of known origin: Implications for geographic assignment. Oecologia

Lott, C.A. and J.P. Smith. 2006. A geographic-information-system approach to estimating the origin of migratory raptors in North America using stable hydrogen isotope ratios in feathers. Auk **123**:822-835.

Meehan, T.D., R.N. Rosenfield, V.N. Atudorei, J. Bielefeldt, L.J. Rosenfield, A.C. Stewart, W.E. Stout, and M.A. Bozek. 2003. Variation in hydrogen stable-isotope ratios between adult and nestling Cooper's hawks. Condor **105**:567-572.

Norris, D.R., P.P. Marra, G.J. Bowen, L.M. Ratcliffe, J.A. Royle, and T.K. Kyser. 2006. Migratory connectivity of a widely distributed songbird, the American redstart (*Setophaga ruticilla*). Ornithological Monographs **61**:14-28.

Rocque, D.A., M. Ben-David, R.P. Barry, and K. Winker. 2006. Assigning birds to wintering and breeding grounds using stable isotopes: lessons from two feather generations among three intercontinental migrants. Journal of Ornithology **147**:395-404.

Reproduced with permission of the copyright owner. Further reproduction prohibited without permission.

Royle, J.A., and D.R. Rubenstein. 2004. The role of species abundance in determining breeding origins of migratory birds with stable isotopes. Ecological Applications **14**:1780-1788.

Rubenstein, D.R., C.P. Chamberlain, R.T. Holmes, M.P. Ayres, J.R. Waldbauer, G.R. Graves, and N.C. Tuross. 2002. Linking breeding and wintering ranges of a migratory songbird using stable isotopes. Science **295**:1062-1065.

Rubenstein, D.R. and K.A. Hobson. 2004. From birds to butterflies: animal movement patterns and stable isotopes. Trends in Ecology and Evolution **19**: 256-263.

Sauer, J.R., J.E. Hines, and J. Fallon. 2004. The North American Breeding Bird Survey, results and analyses 1966-2003, version 2004.1. [Online] U.S. Geological Survey, Patuxent Wildlife Research Center, Laurel, Maryland. Available at www.mbr-pwrc.usgs.gov/bbs/bbs2003.html

Wassenaar, L.I. and K. A. Hobson. 2003. Comparative equilibrium and online technique for determination of non-exchangeable hydrogen for keratins for use in animal migration studies. Isotopes in Environmental and Health Studies **39**:211-217.

Webster, M.S., P.P. Marra, S.M. Haig, S. Bensch and R.T. Holmes. 2002. Links between worlds: unraveling migratory connectivity. Trends in Ecology and Evolution **17**:76-83.

Webster, M.S., and P.P. Marra. 2005. The importance of understanding migratory connectivity and seasonal interactions. *In* R. Greenberg, and P.P. Marra. Birds of two worlds: the ecology and evolution of migration. The Johns Hopkins University Press, Baltimore.

Reproduced with permission of the copyright owner. Further reproduction prohibited without permission.

Wunder, M.B., C.L. Kester, F.L. Knopf and R.O. Rye. 2005. A test of geographic assignment using isotope tracers in feathers of known origin. Oecologia **144**:607-617.

Reproduced with permission of the copyright owner. Further reproduction prohibited without permission.

Table 1. Differences between the original outcome and the three simulation models in the proportional assignment of American redstarts to each of five breeding regions. Values are mean difference ± standard deviation and range ([minimum, maximum]). All units are in %, and represent the distribution of differences between the percent of all 188 redstarts assigned to a given breeding region in the original outcome and the percent assigned to that same region in each of the 1000 simulations.

	NW	MW	NE	CE	SE
Interpolation error	-17 ± 0.4	9 ± 1	-0.5 ± 0.8	3 ± 2	-1 ± 2
range	[-17, -13]	[5, 9]	[-3, 1]	[0, 8]	[-5, 0]
Analytical error	1 ± 9	5 ± 7	-6 ± 5	12 ± 12	-3 ± 9
range	[-26, 43]	[-26, 35]	[-22, 9]	[-35, 50]	[-26, 26]
Errors combined	-7 ± 9	6 ± 7	-7 ± 5	19 ± 12	-4 ± 9
range	[-30, 22]	[-21, 28]	[-22, 9]	[-15, 54]	[-26, 21]

Reproduced with permission of the copyright owner. Further reproduction prohibited without permission.

FIGURE LEGENDS

Fig. 1. Map of study area. Outlined areas are pre-defined breeding regions from Norris et al. (2006). Gray-scale surface shows the spatial distribution for the degree of interpolation uncertainty (interpolation error) in the expected δD values for precipitation; higher standard deviation values are darker in color and the dots show locations of data stations (after Bowen and Revenaugh 2003). Histograms in lower left show the frequency distributions of interpolation-associated standard deviations for the grid points in each of the five breeding regions. The histogram on the right shows the expected variation around the measured δD for an individual bird (the analytical error). All units are in ‰.

Fig. 2. Analytical error distributions. A) The residuals from per-run calibrations for the measurements of two keratin standards over the course of a year at the USGS stable isotope lab in Denver, CO. B) Histogram and fitted gamma distribution for standard deviations from 10,000 datasets simulated using the residuals in panel A. See methods for more detail.

Fig. 3. Numbers of wintering American redstarts (out of 188) assigned to each of the five pre-defined breeding regions. Solid dots show the values of the original outcome that does not incorporate error. Curves with dashed lines show the probability densities based on the interpolation error simulations; scaling is shown on the right y-axis. Solid line curves show the probability densities from the analytical error simulations and are scaled by the left y-axis. Curves with dash-dot lines are probability densities for simulations

Reproduced with permission of the copyright owner. Further reproduction prohibited without permission.

that considered both error types (scaled by the left y-axis). Labels on the right side inside each of the panels indicate the breeding regions shown in Figure 1.

Fig. 4. δD-based probability distributions used to assign individuals to each of the five breeding regions. Solid curves show the densities based on the values in the MAD grid (see methods). Dashed lines show the results from one of the 1000 simulations that incorporated interpolation error using the SD grid. Vertical lines are drawn at the assignment boundaries for the original outcome; the region to which individuals would be assigned is labeled across the top of the figure. Assignment boundaries would shift to where the dashed lines intersect for the single simulation result illustrated here.

Fig. 5. Proportions of American redstarts wintering in eastern Mexico that were assigned to each of the five breeding regions. Solid dots and curves are the same as in Figure 3.

Fig. 6. Distributions of the change in population size of American redstarts for each of the five breeding regions after loss of habitat in eastern Mexico (assuming that all the birds wintering in eastern Mexico perished; see methods). Solid dots and curves are the same as in Figure 3. Units are in %, and refer to the number of birds that wintered in eastern Mexico and that were assigned to the NW region relative to the overall number of birds that were assigned to the NW region for each given simulation.

Reproduced with permission of the copyright owner. Further reproduction prohibited without permission.

Figure 1

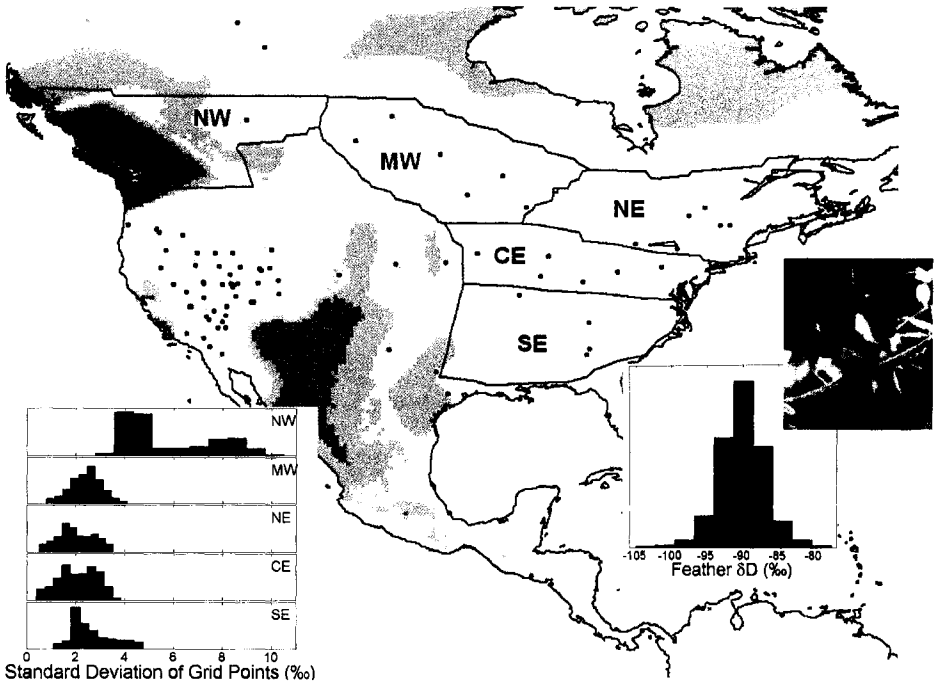

Reproduced with permission of the copyright owner. Further reproduction prohibited without permission.

Figure 2

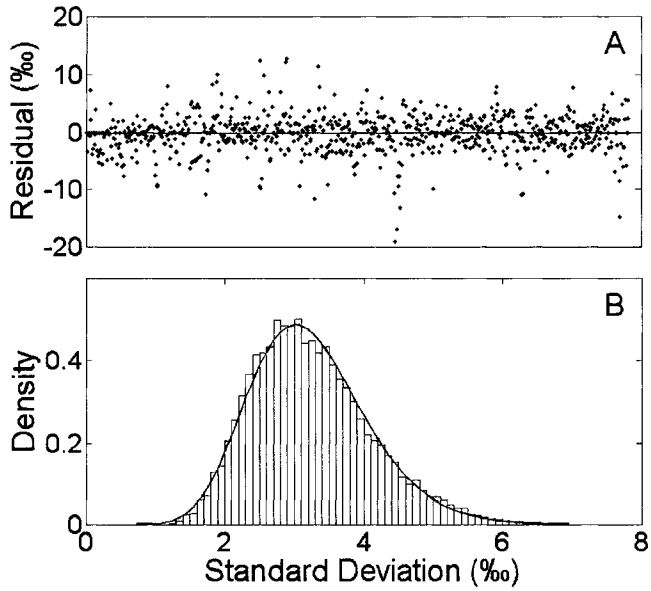

Reproduced with permission of the copyright owner. Further reproduction prohibited without permission.

Figure 3

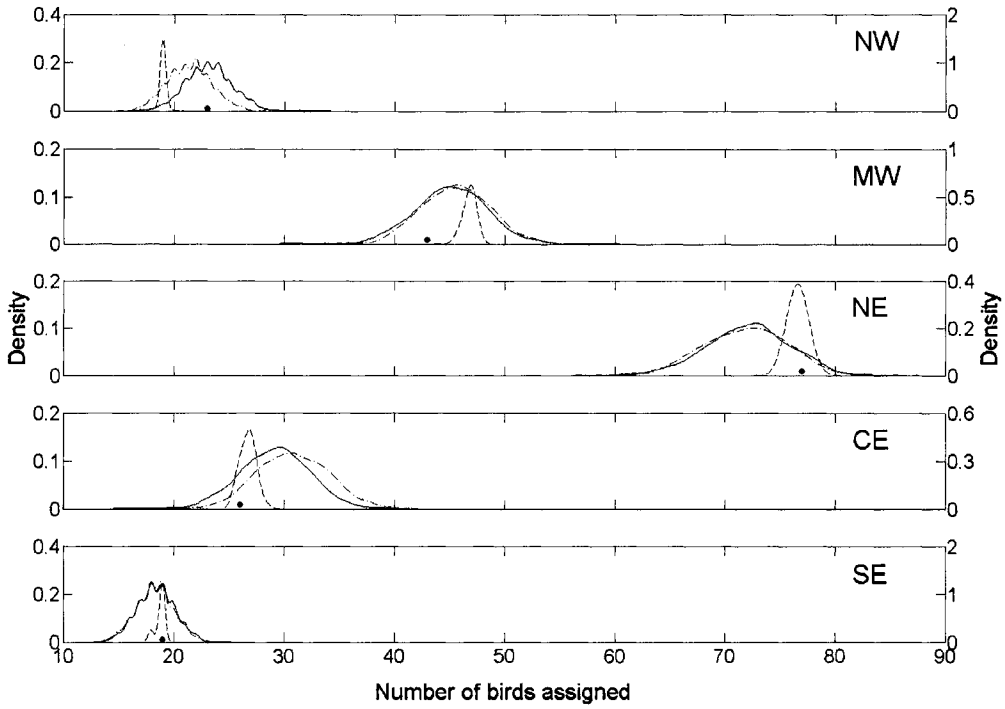

Reproduced with permission of the copyright owner. Further reproduction prohibited without permission.

Figure 4

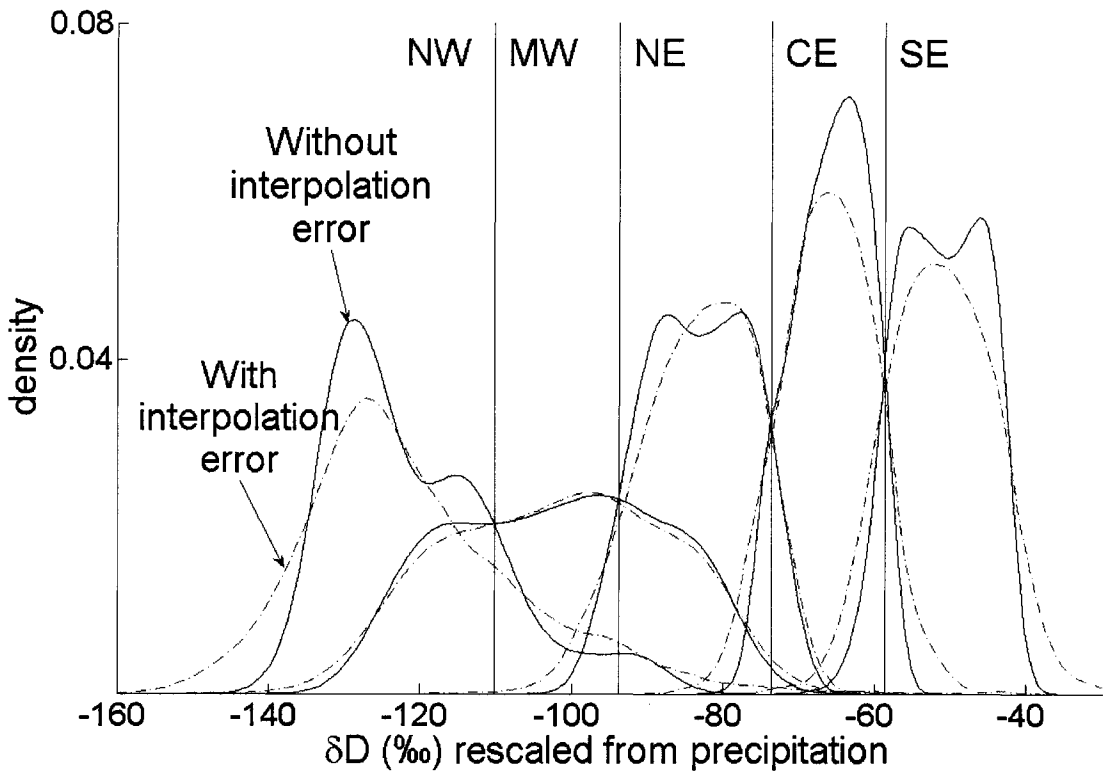

Reproduced with permission of the copyright owner. Further reproduction prohibited without permission.

Figure 5

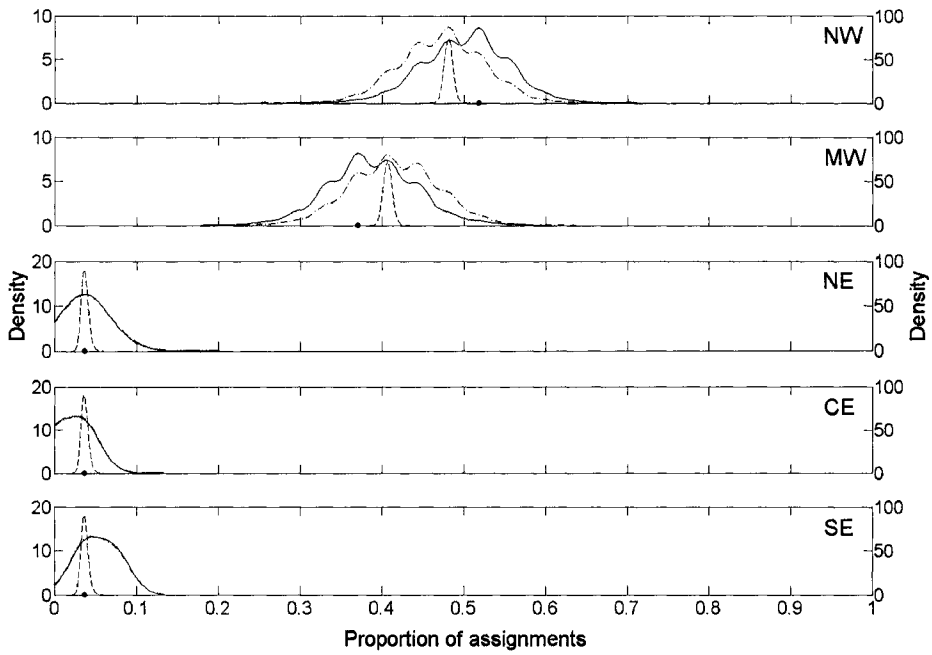

Reproduced with permission of the copyright owner. Further reproduction prohibited without permission.

Figure 6

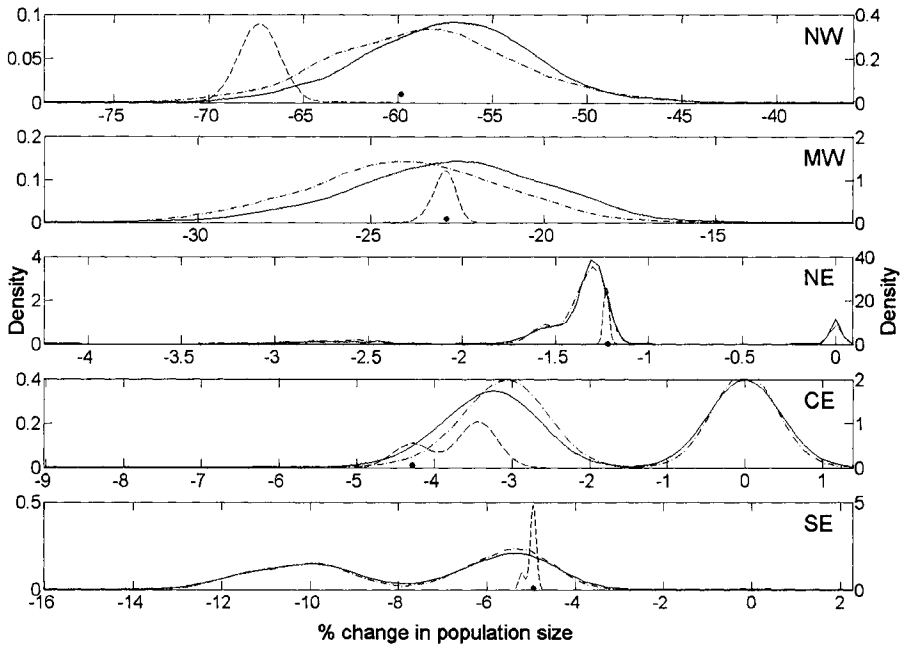

Reproduced with permission of the copyright owner. Further reproduction prohibited without permission.

CHAPTER THREE

GENERALIZED SPATIAL RESOLUTION LIMITS FOR INFERRING GEOGRAPHIC ORIGIN FROM STABLE HYDROGEN ISOTOPES

Reproduced with permission of the copyright owner. Further reproduction prohibited without permission.

Abstract. Stable hydrogen isotopes are increasingly used for estimating the geographic origins of a wide variety of organic materials, but especially for tissues from migratory animals. This approach takes advantage of widespread continental-scale patterning in the hydrogen isotopes of precipitation. Promising results have derived from some but not all studies and there are no consistent patterns to suggest the types of systems in which we can expect good results and those for which we cannot. Most studies fail to directly address known and nested sources of uncertainty. Frequently, measurement error rates and the degree of local variance in measurements are reported, but they are not integrated into subsequent modeling efforts, even though the degree of uncertainty is often not much smaller than the effect size reported. Because of this, there has been no clear sense of the general spatial resolution we can expect from this approach. I introduce a flexible simulation approach using a hierarchical error structure to explore the question of spatial resolution. I parameterize my model with values reported in the literature as well as with direct measurements. Deriving study-specific estimates of variance will improve the relevance of the findings, but I found that relatively large sample sizes (>30 per site) are required to estimate population-level variances with any precision. An uncertainty of about 5‰ is associated with sampling and measuring a single feather. Consequently, observed population-level estimates of standard deviation less than 5‰ will always be underestimates relative to the true value. I offer an odds-based risk analysis inferential framework that allows a tradeoff between spatial precision and accuracy. The generalized spatial resolution varies greatly depending geographic location of the study area and desired odds of circumscribing the true origin. Without further study-system-specific refinements, this approach is likely to work most effectively for inferences to locations in

Reproduced with permission of the copyright owner. Further reproduction prohibited without permission.

North America; differences between samples will need to be about 50‰ to reliably distinguish them as having distinct origins.

Keywords: error propagation, hierarchical model, simulation, avian migration, connectivity

Reproduced with permission of the copyright owner. Further reproduction prohibited without permission.

INTRODUCTION

The natural history and population dynamics of migratory species are characterized by persistent movement across space in an effort to continually optimize environmental conditions, a process that often strongly influences population structure. Understanding population structure is a foundational step for a wide range of research questions, forensic applications and management actions. Studying migration by direct observation is difficult and expensive for any species, and is impossible for many small species and for questions involving archaic systems. The use of stable isotope tracers, however, has proven useful for inferring geographic origins and spatial connections for a range of species and a variety of temporal extents. Examples include estimating single-season movement patterns of songbirds (Norris et al. 2004), reconstructing geographic histories for modern butterflies (Wassenaar and Hobson 1998), prehistoric humans (Muller et al. 2003, Sharp et al. 2003) and historic human trade routes (Giuliani et al 2000), as well as forensic work to determine recent human movement (Fraser et al. 2006), or the origin of illicit substances such as drugs or explosives (Ehleringer et al. 2000, Benson et al. 2006).

Although there are often distinct advantages to using multiple tracers for inferring geographic origins (Wunder et al. 2005 (chapter one)), it is becoming increasingly common to use only stable hydrogen isotopes for studies in ecology. The use of stable hydrogen isotopes is attractive for problems of geographic assignment because time-averaged patterns of hydrogen isotopes in precipitation are relatively predictable at continental scales (Dansgaard 1964). These patterns define geographic targets and comprise the basis for most contemporary work in hydrogen isotope forensics (Bowen et al. 2005a). Despite a rapid increase in the number of studies, there remains much room

Reproduced with permission of the copyright owner. Further reproduction prohibited without permission.

for refinement. For example, it is not possible to directly measure ratios of stable-hydrogen isotopes (deuterium and protium). Measurement values (δD) are scaled relative to an international standard (Vienna Standard Mean Ocean Water) via simple regression lines derived from internal lab standards run at the same time as samples (Wassenaar and Hobson 2002). The calibration residuals for those standards typically range from 1-5‰, but can extend upwards of 20‰ when considering individual outcomes, a substantial proportion of the overall range of observed values reported for most studies (Chapter two). Additionally, we know that whereas standards used to calibrate delta values are highly homogenized, samples are much less homogenized, so the magnitude of analytical error for samples is likely to be even higher than that for lab standards (Jardine and Cunjak 2005), complicating efforts to distinguish biophysical or ecological effect from measurement error.

Furthermore, time-averaged spatial models based on precipitation provide expected δD values for a given location, but they provide no information about the degree of isotopic heterogeneity in the population of interest at that location. Studies that use precipitation-based models of δD to determine the origin of individuals implicitly assume isotopic homogeneity in both time and space for geographical regions of interest. Recent work with a range of bird species has demonstrated that this assumption is regularly violated (Meehan et al. 2003, Farmer et al. 2004, Wunder et al. 2005 (Chapter one), Wassenaar and Hobson 2006, Langin et al. 2007). Although the growing number of such phenomenological studies helps characterize components of observed isotopic heterogeneity, they do not advance our understanding of causative agents which would help refine modeling efforts.

Reproduced with permission of the copyright owner. Further reproduction prohibited without permission.

Given these known and unavoidable contributions to naturally occurring isotopic heterogeneity, I asked how precisely the region of probable origin can be defined for an individual using hydrogen isotopes. Despite the fundamental nature of this question, to my knowledge it has not been studied in any theoretical way. This is likely because so many aspects of the isotope approach are still rapidly emerging. However, the need for application is great, particularly in the fields of disease ecology, conservation biology, archaeology, and forensics. Understanding current resolution limits and identifying relative advantages for refining various aspects of the method will clearly aid study design and evaluations of study potential.

In general, stable hydrogen isotopes have so far been used to address one of three different questions involving geographic origins: (1) the relative origin of samples, (2) what proportion of a population derived from some location, and (3) what is the origin of an individual. The first question relies on gradients and population-level statistics (e.g. Bearhop et al. 2005). The second question is also framed in population terms, but is often asked without a specific model of the structure-generating process for the population in question (e.g. Pain et al. 2004). I am concerned here with the third and most general question because if I can answer it, I have also answered the other two.

I present a flexible modeling framework to transform any raster model of water-based δD into a raster of probability distributions where the probabilities are probability of origin, given an individual δD value. I used these probability maps to define the geographic resolution from a risk analysis perspective where risk and error rate are inversely proportional. Because hydrogen isotopes have been commonly used to study migratory bird systems, I illustrate my model with an example for naturally occurring

Reproduced with permission of the copyright owner. Further reproduction prohibited without permission.

migratory bird systems. However, because this method appeals to a wide range of fields, I also discuss more general results that show how the resolution scales over a relatively wide range of the parameter space.

METHODS

I developed a stochastic modeling algorithm to propagate known sources of heterogeneity in the conversion of a raster map of values for expected hydrogen isotope ratios in precipitation (δD_p) into a raster map of values for probability of origin given an individual measured value of keratin (δD_k). I rescaled a raster of interpolated δD_p values for use as the data-generating process and modeled deviations from that output by simulating three interdependent random sampling processes, each with its own independent random error process. The algorithm generally contains four steps: (1) define probability distributions (from data or theory) to represent the variance-generating processes of interest, (2) use Monte Carlo simulations to approximate the posterior joint probability distribution for the combined sampling processes, (3) center these distributions over the data-generating process, and (4) calculate the probability density value for each raster cell (pixel), given the δD_k of interest.

Data-generating process

I based my analyses on the expected geographic distribution in δD_p from the model described in Bowen et al. (2005a). This commonly-used model is a carefully considered spatial interpolation of δD_p based on data collected over ca. 40 years during months with mean temperatures greater than 0°C. The spatial extent of the model output includes

Reproduced with permission of the copyright owner. Further reproduction prohibited without permission.

nearly all terrestrial surfaces on earth excluding Antarctica. The spatial resolution of this grid is 20', theoretically the finest geographic resolution at which I can infer origin using this tool. This resolution yielded 486 000 pixels for the globe, 133 628 of which contained model output. Following Bowen et al. (2005a) I refer to this model as the $GS\delta D_p$ grid (Growing Season δD_p) and use it as the data generating process. That is, I assume the $GS\delta D_p$ grid reflects the true pattern of spatial variation in δD_p. I believe this assumption is not entirely reasonable because the degree of temporal variation in δD_p at any location can be large, particularly when comparing among seasons or among years (Farmer et al. 2002); using a single long-time-averaged value is not as informative as using temporal distributions for each grid point. However, a spatially explicit model of time-specific functions of expected δD_p is not readily available and my interest was in defining resolution limits based on the current state of the science. The precision of my generalized estimates of resolution limits is therefore biased high; incorporating temporal uncertainty into the data-generating model will decrease the precision for the general case I present here.

I rescaled the GS δD_p grid from expected precipitation values (δD_p) to expected keratin values (δD_k) using the commonly applied assumption that the difference between keratin and precipitation is a simple relocation (Rubenstein and Hobson 2004). That is, I assumed a slope of one and an offset of 25‰ in the rescaling ($\delta D_k = \delta D_p - 25$). This gave me a grid I call the $GS\delta D_k$ grid. I used this simple rescaling purposely because I was interested in the resolution limit results for the most general case in the use of the $GS\delta D_p$ model. I note that, in general, any rescaling involving a slope less than one will map δD_p values onto a narrower range of the δD_f field, reducing the generalized spatial precision.

Reproduced with permission of the copyright owner. Further reproduction prohibited without permission.

Rescaling involving slopes greater than one will have the opposite effect. For specific case studies, however, I do not advocate such a generalized rescaling; it is more appropriate to rescale δD_p for each study using samples of known origin collected consistent with the samples of interest (of unknown origin) because compressions or expansions in the rescaling will alter the spatial configuration of inference and the degree of compression or expansion will vary with time, species, location, trophic level, and other study-specific attributes (Chapter four).

Empirical model structure

The structure of my simulation models reflects a typical sampling process where variance is introduced at multiple stages. I model these variance components by nesting probability distributions. This hierarchical structure allowed me to give prior distributions to parameters that typically are thought to be fixed. I identified three empirically estimable components of variance: (1) analytical, (2) within-individual, and (3) within-population (Fig. 1). Isotopic heterogeneity is introduced by all of these processes, none of which can be controlled for in studies of natural systems. I structured my model to simulate these variance-generating processes using three inter-dependent random variables:

$$X_{pop} \left| GS\delta D_k, \sigma_{population}, \sim N\left(GS\delta D_k, \sigma_{population}\right) \right. \quad (1.1)$$

$$X_{ind} \left| X_{pop}, \sigma_{individual} \sim N\left(X_{pop}, \sigma_{individual}\right) \right. \quad (1.2)$$

$$X_{obs} \left| X_{ind}, \sigma_{analytical} \sim N\left(X_{ind}, \sigma_{analytical}\right) \right. \quad (1.3)$$

and three independent random variables:

Reproduced with permission of the copyright owner. Further reproduction prohibited without permission.

$$\sigma_{population} | \alpha_p, \beta_p \sim \Gamma(\alpha_p, \beta_p) \quad (1.4)$$

$$\sigma_{individual} | \alpha_i, \beta_i \sim \Gamma(\alpha_i, \beta_i) \quad (1.5)$$

$$\sigma_{analytical} | \alpha_a, \beta_a \sim \Gamma(\alpha_a, \beta_a) \quad (1.6)$$

X_{obs} represents the δD_k value that I observe for a sampled individual. In my model this value depends on random processes that generate error resulting from (1) the measurement of δD_k ($\sigma_{analytical}$), (2) the sampling of tissue from an individual (X_{ind}), and (3) the sampling of individuals at a given location (X_{pop}). $GS\delta D_k$ is the geographical data-generating process described in the previous section ($GS\delta D_k = GS\delta D_p - 25$).

I estimated the shape and scale parameters for the gamma distributions in 1.4 and 1.5 as follows. First, I used maximum likelihood to estimate parameters for the set of observed standard deviations from the literature and my own work with mountain plovers (*Charadrius montanus*; Table 1) for 1.4 and from Wassenaar and Hobson (2006) for 1.5. Next, I simulated 10 000 values from each fitted distribution and squared each element to obtain vectors of observed variances. Because I assumed the population level variance was independent from that for an individual and that analytical variance does not depend on either the population or individual level variances, these components are additive and I wrote

$$\sigma^2_{observed-population} = \sigma^2_{population} + \sigma^2_{individual} + \sigma^2_{analytical} \quad (1.7)$$

$$\sigma^2_{observed-individual} = \sigma^2_{individual} + \sigma^2_{analytical} \quad (1.8)$$

$$\sigma^2_{observed-analytical} = \sigma^2_{analytical} \quad (1.9)$$

I used the observed estimates and the equality in equation 1.9 to solve for the vectors of interest (e.g. $\sigma_{population}$, $\sigma_{individual}$ and $\sigma_{analytical}$) and again used maximum

Reproduced with permission of the copyright owner. Further reproduction prohibited without permission.

likelihood to fit the parameters α and β to these vectors of "true" values for use in model simulations (Fig 2).

To estimate α and β for 1.6, I used a series (n = 782) of δD_k measurements made over the course of a year for two different in-house keratin standards using continuous-flow isotope ratio mass spectrometry (CFIRMS; see Chapter two). These standards are used to calibrate organic samples analyzed at the U.S. Geological Survey Stable Isotope Laboratory in Denver, CO. Each standard was cryogenically ground and homogenized black bear (*Ursus americanus*) hair, one from a bear collected in Alaska and the other from a bear collected in Louisiana. Stable isotope labs in Denver, Flagstaff, and Saskatoon each independently measured δD_k for the non-exchangeable hydrogen in these keratin standards, which gave the "known" value for each standard. These known values were then regressed on the measured values for each auto-run (carousel) to generate per-auto-run curves for calibrating samples in the run; the collection of per-auto-run residuals from these regressions describe the analytical error. A typical auto-run for measuring δD_k at the Denver lab includes 16 samples and between two and five of each of the standards. Just as is done when we collect data for samples, I assumed that the variance observed for standards represents that for samples. Thus, I simulated analytical error associated with CFIRMS by drawing 10 000 sets of 16 values each from the set of 782 residuals described above. I calculated the standard deviation for each set of 16 samples. This gave me a set of 10 000 standard deviations from which I estimated the parameters α and β for 1.6 using maximum likelihood.

Generalized model structure

Reproduced with permission of the copyright owner. Further reproduction prohibited without permission.

Because these hydrogen models are used for a wide variety of problems that extend well beyond the taxonomic range of birds, I generalized my model to systematically explore a range of the parameter space for population-level isotopic heterogeneity. I assumed that local variance in δD_k among individuals of any species in a population at any geographic location derived from differences in the ages of individuals, year of sampling, trophic foraging level, relative water stress, and other processes about which I am unaware. In contrast to the preceding approach, I modeled these population-level effects collectively for each pixel. I again used a normally-distributed random variable with $GS\delta D_k$ for the mean, but for this model, I iterated through 25 different integer values for the standard deviation. I covered this relatively wide range of the parameter space for the standard deviation to quantify the individual-level assignment resolution as a function of localized population-level variance in the δD_k of sampled individuals, regardless of the cause of the variance. As before, I modeled the random process of measuring δD_k for X_{pop} using a normally distributed random variable (X_{obs}) that depended on X_{pop} and $\sigma_{analytical}$ as follows:

$$X_{pop} | GS\delta D_k \sim N\left(GS\delta D_k, \sigma_{population}\right) \tag{1.10}$$

$$\sigma_{population} \sim [1..25] \tag{1.11}$$

$$X_{obs} \left| X_{pop}, \sigma_{analytical} \sim N\left(X_{pop}, \sigma_{analytical}\right)\right. \tag{1.12}$$

$$\sigma_{analytical} | \alpha_a, \beta_a \sim \Gamma\left(\alpha_a, \beta_a\right) \tag{1.13}$$

Probability of origin grids

Reproduced with permission of the copyright owner. Further reproduction prohibited without permission.

I simulated X_{obs} 10 000 times for each of the 133 628 pixels for each of the models described above. For each model, I used these sets of 10 000 values to define the probability density for X_{obs} for every pixel. I arbitrarily chose a δD_k to represent a sampled individual and evaluated the density functions for every pixel to derive a continuous surface of probabilities of origin. I refer to this transformed surface as the probability of origin grid.

I rescaled the probability density value for each pixel in the probability of origin grid relative to the maximum density value on a per-model basis. Thus, each probability of origin grid describes the global relative odds of any given pixel as the origin for an individual with the specified δD_k. I purposely did not constrain the spatial extent of the model output to study the geographical precision as a function of δD_k. I rescaled on a per-pixel basis because I was interested in the finest resolution possible for any given δD_k. Because each pixel was independently rescaled, the pixel values in the probability of origin grid ranged from zero to one. In doing this, I could define the maximum effective theoretical geographical precision by limiting my assignments to only those pixels with probability = 1. However, this ignores assignment uncertainty and I do not advocate this approach; indeed, it seems unreasonable to claim that the pixels with probability = 1 represent the origin, but pixels with probability = 0.99 do not. Instead, I used odds ratios as a more flexible way to explore the results. For example, I can approximate spatially explicit 95% confidence intervals by identifying all pixel values greater than 1/20 (i.e. representing odds better than 19:1 that the pixel is the origin, implying an error rate of 5%).

Reproduced with permission of the copyright owner. Further reproduction prohibited without permission.

RESULTS AND DISCUSSION

Empirically-based results

Estimates of spatial resolution have thus far been case-specific for North American bird species. For example, Meehan et al. (2001) estimated a spatial resolution of about 1.5° of latitude for predicting the geographic origin of Cooper's hawks (*Accipiter cooperi*) and Langin et al. (2007) estimated 6°-8° of latitude as the resolution for American redstarts (*Setophaga ruticilla*). Estimating resolution in terms of latitude is only appropriate for North America where monotonic gradients exist in predicted patterns of δD_p across latitude. Here, I estimate the geographic resolution in terms of area, assuming the range of case studies from Europe and North America is representative for migratory bird populations.

Chapter two demonstrated that propagating analytical error can lead to relatively large uncertainties in the assignment of individuals to pre-defined geographic regions. Here I show that propagating within-population isotopic heterogeneity results in a much coarser resolution than does the propagation of only analytical error (Figure 3). Most of the heterogeneity in the empirically-parameterized model I explored was attributed to within-population variance as measured for single locations (Fig 2); analytical variance and within-individual heterogeneity only marginally affected the overall resolution associated with assigning an area of probable origin (Table 2). Thus, whereas improvements in the ability to constrain the degree of variance derived from measuring δD (e.g. Bowen et al. 2005b) will improve the spatial resolution in problems of assigning geographic origins to some degree, the gains are minimal relative to gains from a better

Reproduced with permission of the copyright owner. Further reproduction prohibited without permission.

understanding of mechanisms that generate variance among individuals in local populations (Table 2).

Heterogeneity within populations at discrete geographic locations depends on the age of sampled individuals (Meehan et al. 2003, Langin et al. 2007), sample year (Pain et al. 2004, Wunder et al. 2005 (Chapter one)), degree of water stress (McKechnie et al. 2004), and potentially trophic position (Birchall et al. 2006). This reinforces that experimental work to identify heterogeneity-generating mechanisms for δD in tissues (e.g. McKechnie et al. 2004) and local environmental systems involving animals is still badly needed. Until more such work is done, the foundational assumption of isotopic homogeneity is essential, though never met, for any application of hydrogen isotopes to predict geographic origins.

Geographic resolution as a function of risk

Probability-based approaches to data analysis can be used to quantify the consequences of assuming isotopic homogeneity despite unknown or unmeasured variance-generating factors. Assignment approaches based on Bayes' rule effectively consider unknown sources of within-population isotopic heterogeneity, but require tissue samples of known origin to estimate variance for all possible target populations (Wunder et al. 2005 (Chapter one)). My probability of origin grids present another means to quantify the consequences of violating the assumption of isotopic homogeneity, and are especially useful in cases where all possible origins are not known or where all possible locations cannot be sampled. In both cases, potential areas of origin can be characterized by probabilities, rather than binary "yes/no" decision responses.

Reproduced with permission of the copyright owner. Further reproduction prohibited without permission.

By estimating probabilities for each pixel, I can frame the assignment problem from a risk analysis perspective. That is, I can evaluate the area of probable origin associated with odds appropriate to the stakes at hand. For example, suppose the goal was to use the isotopic profile in the hair of a fugitive to determine the probable geographic region of recent use in order to entrap associates or to gather evidence, I might prefer relatively high odds of identifying the correct region, say 100:1. In contrast, suppose a graduate student wanted to use feathers to determine the migratory pathway of a small but common passerine. In this case, the stakes are relatively low and can tolerate much lower odds of identifying the correct region, say 3:1. Both the probability of origin grids I present here and probabilistic assignment tests described in chapter one can be used to identify the potential geographic range associated with each risk level. For example, assuming the empirically-based probability of origin grid, the resolution associated with odds of 19:1 (risk of 5% error rate) for samples that are 50‰ apart is such that the regions of origin overlap everywhere they are adjacent; however, some geographic separation exists between the ranges for the same samples with odds 9:1 (10% error rate), and there is nearly universal separation for odds 2:1 (Figure 4).

More generally, I used the model described by equations 1.10-1.13 to quantify the resolution in terms of risk and degree of within-population heterogeneity (Figure 5). Naturally, the response of the resolution depends on the δD value because the distribution of δD values is not uniform across the globe. Lower δD values occur at high latitude and high elevation, regions that contain relatively small amounts of terrestrial surface, whereas higher δD values are associated with tropical regions, which contain disproportionately more land mass. Thus, the resolution associated with low δD values

Reproduced with permission of the copyright owner. Further reproduction prohibited without permission.

responded more strongly to change in odds than did that for higher δD values because there are more pixels associated with high δD values, resulting in a more uniform distribution over the range of odds for a given level of variance. Not surprisingly, the spatial resolution for all levels of δD responded most strongly to the degree of variance. The values on the z-axes for the δD values in figure 5 will change depending on the geographic region of the study area (which presumably will not be the entire earth), but the relative patterns of response by the resolution in the x (odds) and y (variance) directions will remain the same for a given δD value because the probabilities were estimated on a per-pixel basis and the underlying data-generating process is smooth.

Although I used this per-pixel rescaling, it is not required, and indeed may not be desirable in some cases. For example, I can evaluate any individual pixel relative to another or to a specified probability density value of interest (e.g. that for a pixel known to be the origin for a given δD_k). Or if the geographic extent of inference is restrained (say to the known range for a species), it is a simple matter to rescale each pixel within that range using the sum of all pixel values contained in the restrained grid such that the grid represents a proper probability surface for that restricted geographic range. In all cases, the use of odds and probability fields can quantify the expected resolution for a given risk level determined by the question at hand.

Study design considerations

In constructing the probability of origin grids I assumed that among-individual heterogeneity is constant in time and space, and I approximated the asymptotic estimate for variance under these static conditions. This is almost certainly never realized, and I

Reproduced with permission of the copyright owner. Further reproduction prohibited without permission.

suggest estimating within-population heterogeneity on a per-case basis. However, logistical constraints frequently prevent large sample collections for estimating per-case variances. So to elucidate the effect of sample size on estimating within-population variance, I used equation 1.3 to simulate 10 000 sets of observations for each sample size from 2-100 (Figure 6). If I assume that the set of estimated standard deviations in Table 1 is representative of typical wild bird populations, relatively large sample sizes (e.g. > ~30) will be required to generate reliable estimates of within-population heterogeneity.

Because of the persistent effects of analytical error and within-individual heterogeneity, there will always be some reliable lower bound for the estimated standard deviation of a population sample. In other words, just because I sampled eight individuals and calculated a standard deviation of 3‰, that does not mean the true population standard deviation is 3‰. It is possible to underestimate the standard deviation, and in cases where the estimated value is less than 5‰, it has likely been underestimated by as much as 20-300% (Figure 7).

Reproduced with permission of the copyright owner. Further reproduction prohibited without permission.

LITERATURE CITED

Bearhop S., W. Fiedler, R.W. Furness, S.C. Votier, S. Waldron, J. Newton, G.J. Bowen, P. Berthold, and K. Farnsworth. 2005. Assortative mating as a mechanism for rapid evolution of a migratory divide. Science **310**:502-504.

Benson S., C. Lennard, P. Maynard, and C. Roux. 2006. Forensic applications of isotope ratio mass spectrometry – a review. Forensic Science International **157**:1-22.

Bowen, G.J., L.I. Wassenaar, and K.A. Hobson. 2005a. Global application of stable hydrogen and oxygen isotopes to wildlife forensics. Oecologia **143**:337-348.

Bowen, G.J., L. Chesson, K. Nielson, T.E. Cerling, and J.R. Ehleringer. 2005b. Treatment methods for the determination of δ^2H and $\delta^{18}O$ of hair keratin by continuous-flow isotope-ratio mass spectrometry. Rapid Communications in Mass Spectrometry **19**:2371-2378.

Chamberlain C.P., J.D. Blum, R.T. Holmes, X. Feng, T.W. Sherry, and G.R. Graves. 1997. The use of isotope tracers for identifying populations of migratory birds. Oecologia **109**:132-141.

Clegg S.M., J.F. Kelly, M. Kimura, and T.B. Smith. 2003. Combining genetic markers and stable isotopes to reveal population connectivity and migration patterns in a Neotropical migrant, Wilson's warbler (*Wilsonia pusilla*). Molecular Ecology **12**:819-830.

Dansgaard W. 1964. Stable isotopes in precipitation. Tellus **16**:436-468.

Ehleringer J.R., J.F. Casale, M.J. Lott, and V.L. Ford. 2000. Tracing the geological origin of cocaine. Nature **408**:311-312.

Reproduced with permission of the copyright owner. Further reproduction prohibited without permission.

Farmer, A., R. Rye, G. Landis, C. Bern, C. Kester, and I. Ridley. 2002. Tracing the pathways of neotropical migratory shorebirds using stable isotopes: A pilot study. Isotopes in Environmental and Health Studies **39**:1-9.

Farmer A., M. Abril, M. Fernandez, J. Torres, C. Kester, C. Bern. 2004. Using stable isotopes to associate migratory shorebirds with their wintering locations in Argentina. Ornitologia Neotropical **15**:377-384.

Fraser I., W. Meier-Augenstein, and R.M. Kalin. 2006. The role of stable isotopes in human identification: a longitudinal study into the variability of isotopic signals in human hair and nails. Rapid Communications in Mass Spectrometry **20**:1109-1116.

Giuliani G., M. Chaussidon, H.J. Schubnel, D.H. Piat, C. Rollion-Bard, C. France-Lanord, D. Giard, D. deNarvaez, and B. Rondeau. 2000. Oxygen isotopes and emerald trade routes since antiquity. Science **287**:631-633.

Hobson K.A. and L.I. Wassenaar. 1997. Linking breeding and wintering grounds of neotropical migrant songbirds using stable hydrogen isotopic analysis of feathers. Oecologia **109**:142-148.

Hobson K.A., R.B. Brua, W.L. Hohman, and L.I. Wassenaar. 2000. Low frequency of "double molt" of remiges in ruddy ducks revealed by stable isotopes: implications for tracking migratory waterfowl. Auk **117**:129-135.

Hobson K.A., L.I. Wassenaar, B. Mila, I. Lovette, C. Dingle, and T.B. Smith. 2003. Stable isotopes as indicators of altitudinal distributions and movements in an Ecuadorean hummingbird community. Oecologia **136**:302-308.

Reproduced with permission of the copyright owner. Further reproduction prohibited without permission.

Hobson K.A., G.J. Bowen, L.I. Wassenaar, Y. Ferrand, and H. Lormee. 2004. Using stable isotope measurements of feathers to infer geographical origins of migrating European birds. Oecologia **141**:477-488.

Jardine T.J. and R.A. Cunjak. 2005. Analytical error in stable isotope ecology. Oecologia **144**:528-533.

Langin, K.M., M.W. Reudink, P.P. Marra, D.R. Norris, T.K. Kyser, and L.M. Ratcliffe. 2007. Hydrogen isotopic variation in migratory bird tissues of known origin: Implications for geographic assignment. Oecologia *In Press*

McKechnie A.E., B.O. Wolf, and C. Martinez del Rio. 2004. Deuterium stable isotope ratios as tracers of water resource use: an experimental test with rock doves. Oecologia **140**:191-200.

Meehan, T.D., R.N. Rosenfield, V.N. Atudorei, J. Bielefeldt, L.J. Rosenfield, A.C. Stewart, W.E. Stout, and M.A. Bozek. 2003. Variation in hydrogen stable-isotope ratios between adult and nestling Cooper's hawks. Condor **105**:567-572.

Muller W., H. Fricke, A.N. Halliday, M.T. McColluoch, and J.A. Wartho. 2003. Origin and migration of the Alpine Iceman. Science **302**:862-866.

Norris D.R., P.P. Marra, R. Montgomerie, T.K. Kyser, and L.M. Ratcliffe. 2004. Reproductive effort, molting latitude, and feather color in a migratory songbird. Science **306**:2249-2250.

Pain D.J., Green R.E., Gießing B., Kozulin A., Poluda A., Ottosson U., Flade M., and Hilton G.M. 2004. Using stable isotopes to investigate migratory connectivity of the globally threatened aquatic warbler *Acrocephalus paludicola*. Oecologia **138**:168-174.

Reproduced with permission of the copyright owner. Further reproduction prohibited without permission.

Rubenstein, D.R. and K.A. Hobson. 2004. From birds to butterflies: animal movement patterns and stable isotopes. Trends in Ecology and Evolution **19**:256-263.

Sharp Z.D., V. Atudorei, H.O. Panarello, J. Fernandez, and C. Douthitt. 2003. Hydrogen isotope systematics of hair: archeological and forensic applications. Journal of Archaeological Science **30**:1709-1716.

Wassenaar, L.I. and K. A. Hobson. 2002. Comparative equilibrium and online technique for determination of non-exchangeable hydrogen for keratins for use in animal migration studies. Isotopes in Environmental and Health Studies **39**:211-217.

Wassenaar L.I. and K.A. Hobson. 1998. Natal origins of migratory monarch butterflies at wintering colonies in Mexico: new isotopic evidence. Proceedings of the National Academy of Sciences, USA **95**:15436-15439.

Wassenaar L.I. and K.A. Hobson. 2006. Stable-hydrogen isotope heterogeneity in keratinous materials: mass spectrometry and migratory wildlife tissue subsampling strategies. Rapid Communications in Mass Spectrometry **20**:2505-2510.

Wunder M.B., C.L. Kester, F.L. Knopf, and R.O. Rye. 2005. A test of geographic assignment using isotope tracers in feathers of known origin. Oecologia **144**:607-617.

Reproduced with permission of the copyright owner. Further reproduction prohibited without permission.

Table 1. Standard deviations used to estimate within-population heterogeneity for δD_k. Each study used given values to characterize specific (single) geographic regions in terms of δD_k. The last column describes whether the feathers were of known or assumed origin.

Reproduced with permission of the copyright owner. Further reproduction prohibited without permission.

Study	Species	N	SD (‰)	Origin
Hobson and Wassenaar 1997	Swainson's thrush (*Catharus ustulatus*)	15	11	Assumed
	Swainson's thrush, American redstart (*Setophaga ruticilla*)	6	8	Assumed
	Swainson's thrush, American redstart, Tenessee warbler (*Vermivora peregrinus*)	14	10	Assumed
	Swainson's thrush, American redstart, ovenbird (*Seiurus tulatus*)	29	10	Assumed
	least flycatcher (*Empidonax minimus*)	9	8	Known
	ovenbird	17	13	Assumed
	ovenbird	5	4	Assumed
	ovenbird, wood thrush (*Hylocichla mustelina*)	17	6	Assumed
	Swainson's thrush, American redstart, ovenbird	14	12	Assumed
	Swainson's thrush, American redstart	12	9	Assumed
	Swainson's thrush, American redstart	12	10	Assumed
	not reported	13	13	Assumed
	not reported	5	5	Assumed
	not reported	6	8	Assumed
Chamberlain et al. 1997	black-throated blue warbler (*Dendroica caerulescens*)	15	10	Assumed
	black-throated blue warbler	14	14	Assumed
	black-throated blue warbler	17	9	Assumed
	black-throated blue warbler	15	9	Assumed
	black-throated blue warbler	12	11	Assumed
	black-throated blue warbler	19	10	Assumed
	black-throated blue warbler	19	9	Assumed
	black-throated blue warbler	17	13	Assumed
	black-throated blue warbler	15	10	Assumed
Hobson et al. 2000	thick-billed murre (*Uria lomvia*), black-legged kittiwake (*Rissa tridactyla*)	13	11	Assumed
Hobson et al. 2003	*Phaethornis malaris*	13	8	Assumed
	P. malaris	6	12	Assumed
	P. malaris	11	8	Assumed
	P. malaris	12	6	Assumed
	P. guy	10	18	Assumed
	Adelomyia melanogenys	3	3	Assumed
	A. melanogenys	7	9	Assumed
	P. syrmatophorus	11	8	Assumed
	A. melanogenys	6	5	Assumed
	P. syrmatophorus	1	2	Assumed
	A. melanogenys	6	6	Assumed
	Coeligena torquata	4	5	Assumed
	C. torquata	5	5	Assumed
	A. melanogenys	6	6	Assumed
	Metallura baroni	4	5	Assumed
	C. luteliae	4	4	Assumed
	M. williami	4	3	Assumed
Clegg et al. 2003	Wilson's warbler (*Wilsonia pusilla*)	20	14	Assumed
	Wilson's warbler	18	17	Assumed
	Wilson's warbler	24	8	Assumed
	Wilson's warbler	15	7	Assumed
	Wilson's warbler	27	11	Assumed
	Wilson's warbler	13	17	Assumed
Hobson et al. 2004	Blue tit (*Parus caeruleus*)	6	8	Known
	house sparrow (*Passer domesticus*)	4	11	Known
	pheasant (*Phasianus colchicus*)	7	6	Assumed
	red grouse (*Lagopus lagopus*)	4	4	Assumed
	tit species	3	9	Known
	lapwing (*Vanellus vanellus*)	3	6	Assumed
	Eurasian blackbird (*Turdus merula*)	3	1	Known
	thrush species	3	2	Known
	carrian crow (*Corvus corone*)	3	5	Known
	jackdaw (*Corvus monedula*)	3	9	Known
	common wood pigeon (*Columba palumbus*)	5	3	Known
	common wood pigeon	3	4	Known
	common wood pigeon	5	5	Known
	common wood pigeon	5	6	Known
	hazel grouse (*Tetrastes bonasia*)	5	6	Assumed
	hazel grouse	5	13	Assumed
	partridge (*Perdix perdix*)	5	3	Assumed
	mallard (*Anas platyrhynchos*)	4	11	Assumed
	Eurasian curlew (*Numenius arguata*)	4	5	Known
	redwing (*Turdus iliacus*)	5	4	Known
	willow grouse (*Lagopus lagopus*)	5	6	Known
	black grouse (*Tetrao tetrix*)	5	5	Known
	willow grouse	5	9	Known
	black grouse	6	5	Known
	black grouse	6	4	Known
Wunder et al. 2005 & unpubl	mountain plover (*Charadrius montanus*) chick	2	7	Known
	mountain plover chick	17	8	Known
	mountain plover chick	6	11	Known
	mountain plover chick	8	4	Known
	mountain plover chick	9	8	Known
	mountain plover chick	17	8	Known
	mountain plover chick	34	8	Known
	mountain plover chick	66	13	Known
	mountain plover chick	7	2	Known
	mountain plover chick	3	10	Known
	mountain plover chick	2	6	Known
	mountain plover chick	8	5	Known
	mountain plover chick	2	5	Known
	mountain plover chick	3	7	Known
	mountain plover chick	11	9	Known
	mountain plover chick	3	14	Known
	mountain plover chick	8	14	Known
	mountain plover chick	5	14	Known
	mountain plover chick	22	7	Known
	mountain plover chick	6	10	Known
	mountain plover chick	17	8	Known
	mountain plover chick	14	18	Known
	mountain plover chick	2	11	Known
	mountain plover chick	62	12	Known
	mountain plover chick	7	6	Known
	mountain plover chick	9	6	Known
	mountain plover adult	17	17	Known
	mountain plover adult	10	16	Known
	mountain plover adult	2	19	Known
	mountain plover adult	2	18	Known
	mountain plover adult	6	14	Known
	mountain plover adult	5	9	Known
	mountain plover adult	6	21	Known
	mountain plover adult	6	15	Known
	mountain plover adult	30	12	Known
	mountain plover adult	5	12	Known
	mountain plover adult	20	13	Known
Langin et al. 2007	American redstart nestling	20	8	Known
	American redstart fledgeling	14	5	Known
	American redstart adult	42	4	Known

Reproduced with permission of the copyright owner. Further reproduction prohibited without permission.

Table 2. Empirical-based results showing resolution gains in terms of modeled variance components, δD value, and relative odds of correct assignment. Modeled components shows which of the three variance components were propagated. SD is the asymptotic gamma-based mean (±SD) of the standard deviation for that model. Proportion of total area is proportion of terrestrial surface of the earth included in the assignment range for the specified odds. δD values are used here as a proxy for geographic location.

			Proportion of total area		
Modeled components	SD	δD	odds 19:1	odds 9:1	odds 2:1
all	10.59 ± 0.14	-150	0.11	0.09	0.06
		-100	0.28	0.25	0.18
		-50	0.57	0.53	0.43
exclude analytical	10.04 ± 0.14	-150	0.10	0.09	0.06
		-100	0.27	0.24	0.17
		-50	0.55	0.51	0.40
exclude within-individual	9.73 ± 0.16	-150	0.10	0.09	0.06
		-100	0.27	0.23	0.17
		-50	0.55	0.52	0.40
exclude within-population	5.37 ± 0.10	-150	0.05	0.04	0.03
		-100	0.15	0.13	0.08
		-50	0.36	0.32	0.24

Reproduced with permission of the copyright owner. Further reproduction prohibited without permission.

Figure 1. Schematic of hierarchical model structure showing dependencies of random variables used to model sampling an individual from a population, then sampling tissue from an individual, then calibrating CFIRMS measurement.

Figure 2. Empirical based error distributions for the three modeled error processes.

Figure 3. Probability of origin grids for model that assumes isotopic homogeneity, incorporating only analytical error (left panels) and for model additionally considering individual and population level heterogeneity (right panels). Color bar indicates probability value for pixels in grids. The top row shows results for an observed δD_k of -150‰, the middle row for -100‰, and the bottom row for -50‰.

Figure 4. Geographic resolutions for observed δD_k of -150‰ (light green), -100‰ (yellow), and -50‰ (brown), considering odds of 19:1 (top panel), 9:1 (middle panel), and 2:1 (bottom panel), assuming empirically estimated heterogeneity.

Figure 5. Geographic resolution as a function of risk (relative odds), degree of heterogeneity (standard deviation), and δD_k value. The z-axis shows proportion of global landmass.

Figure 6. Asymptotic estimates of population-level heterogeneity as a function of sample size. Bars indicate log-based 95% CI range.

Figure 7. Difference between standard deviations with and without error propagation. Solid dots show the standard deviation when considering the analytical error (y-direction) as a function of sample-based population standard deviation (x-direction). Plus symbols show the same for considering within-individual heterogeneity.

Reproduced with permission of the copyright owner. Further reproduction prohibited without permission.

Figure 1

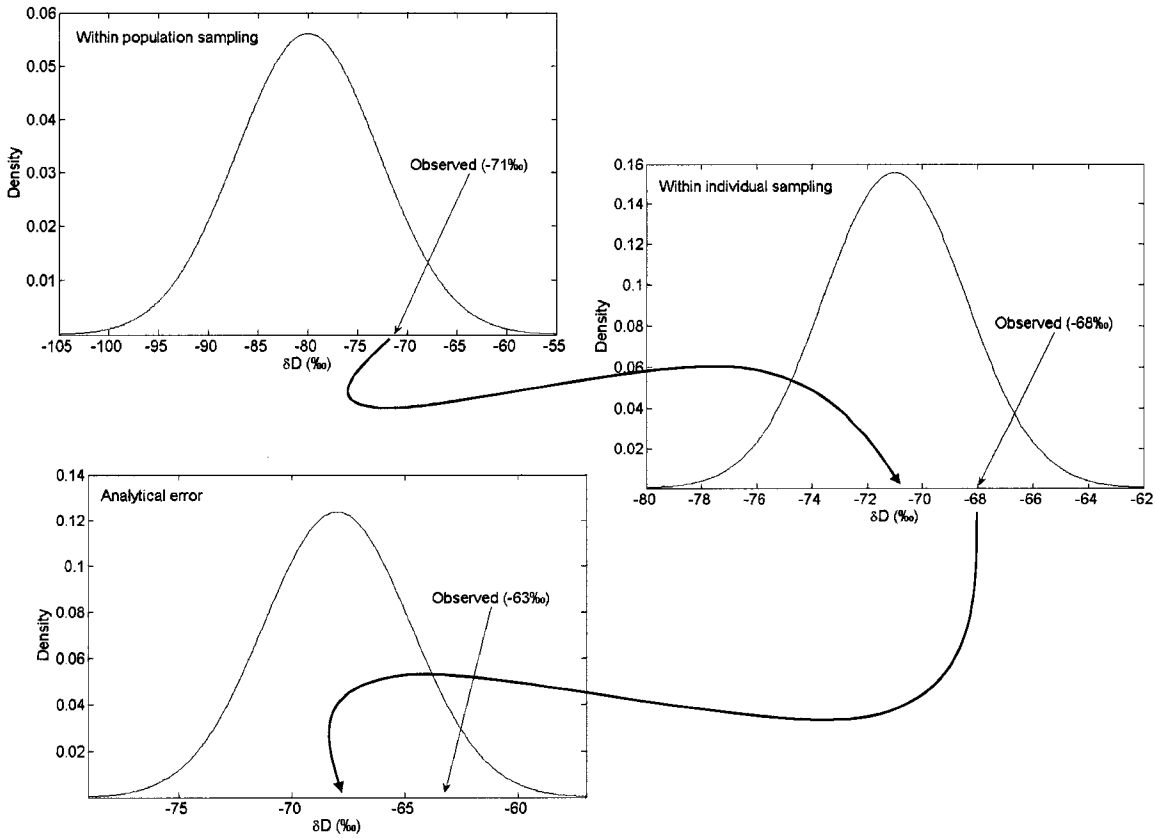

Reproduced with permission of the copyright owner. Further reproduction prohibited without permission.

Figure 2

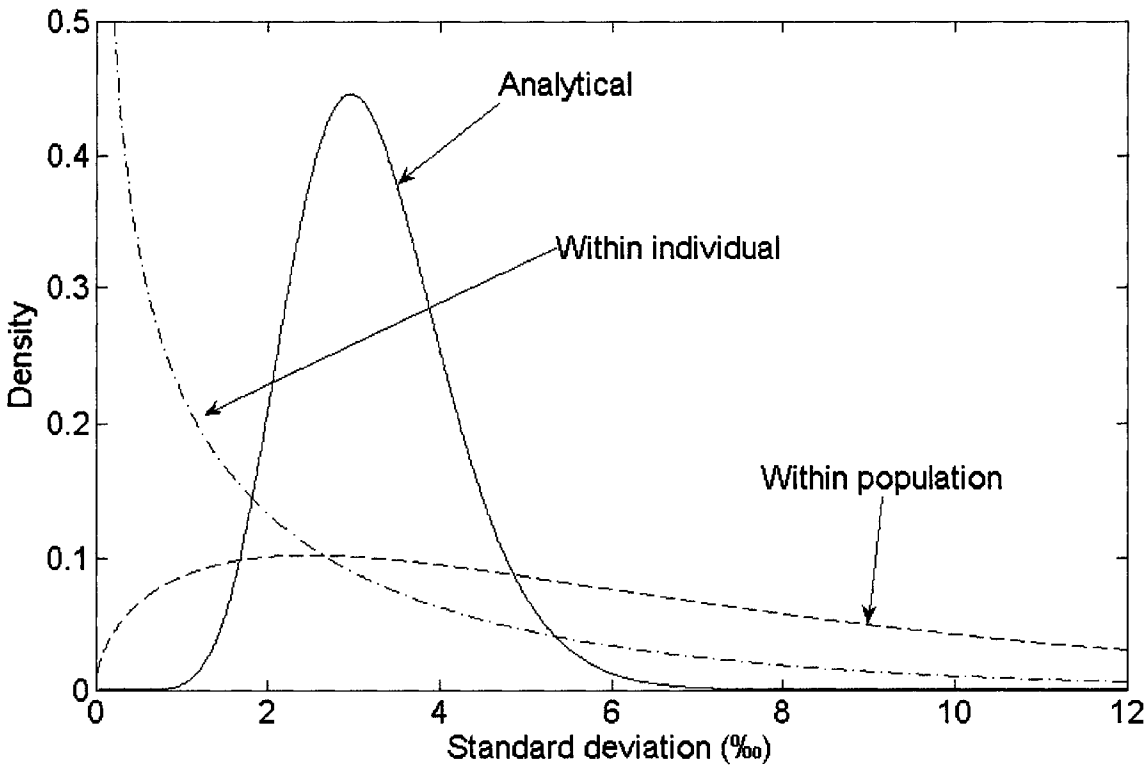

Reproduced with permission of the copyright owner. Further reproduction prohibited without permission.

Figure 3

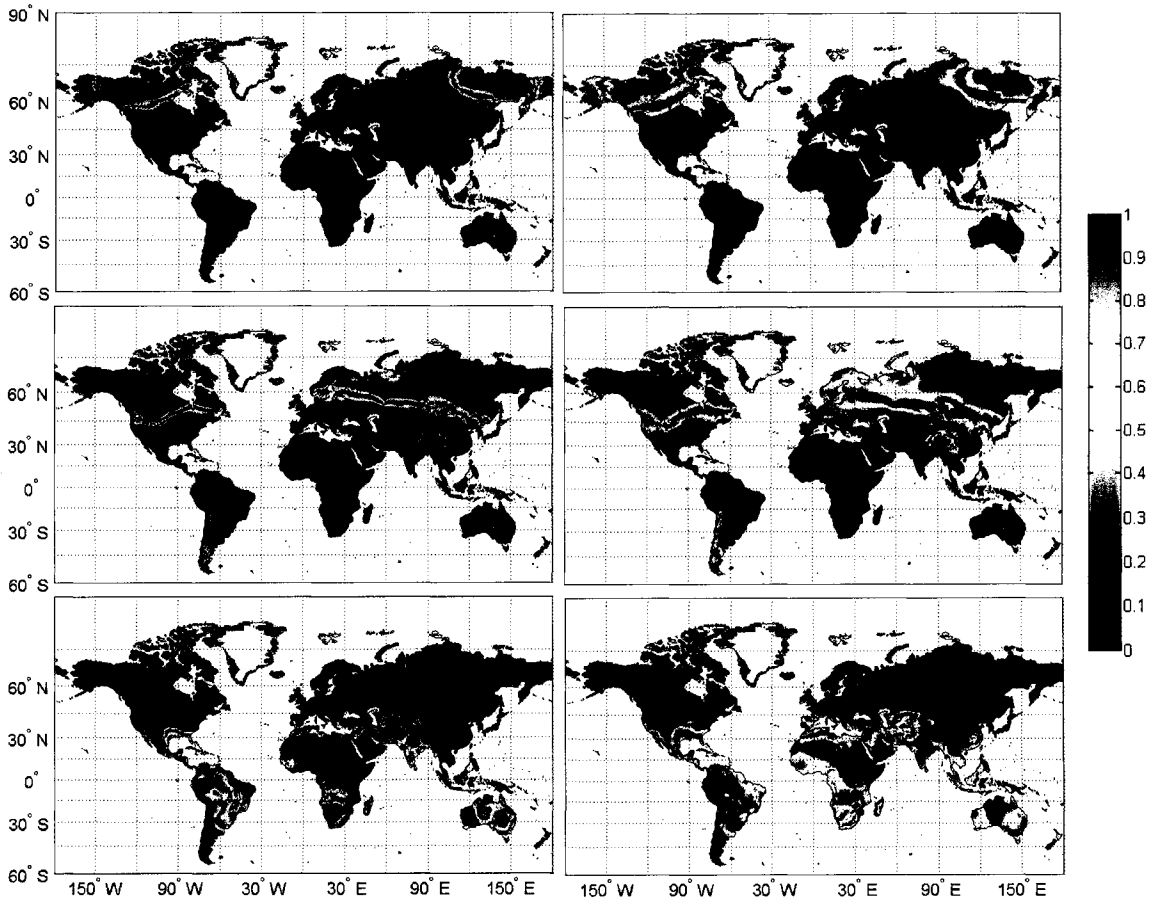

Reproduced with permission of the copyright owner. Further reproduction prohibited without permission.

Figure 4

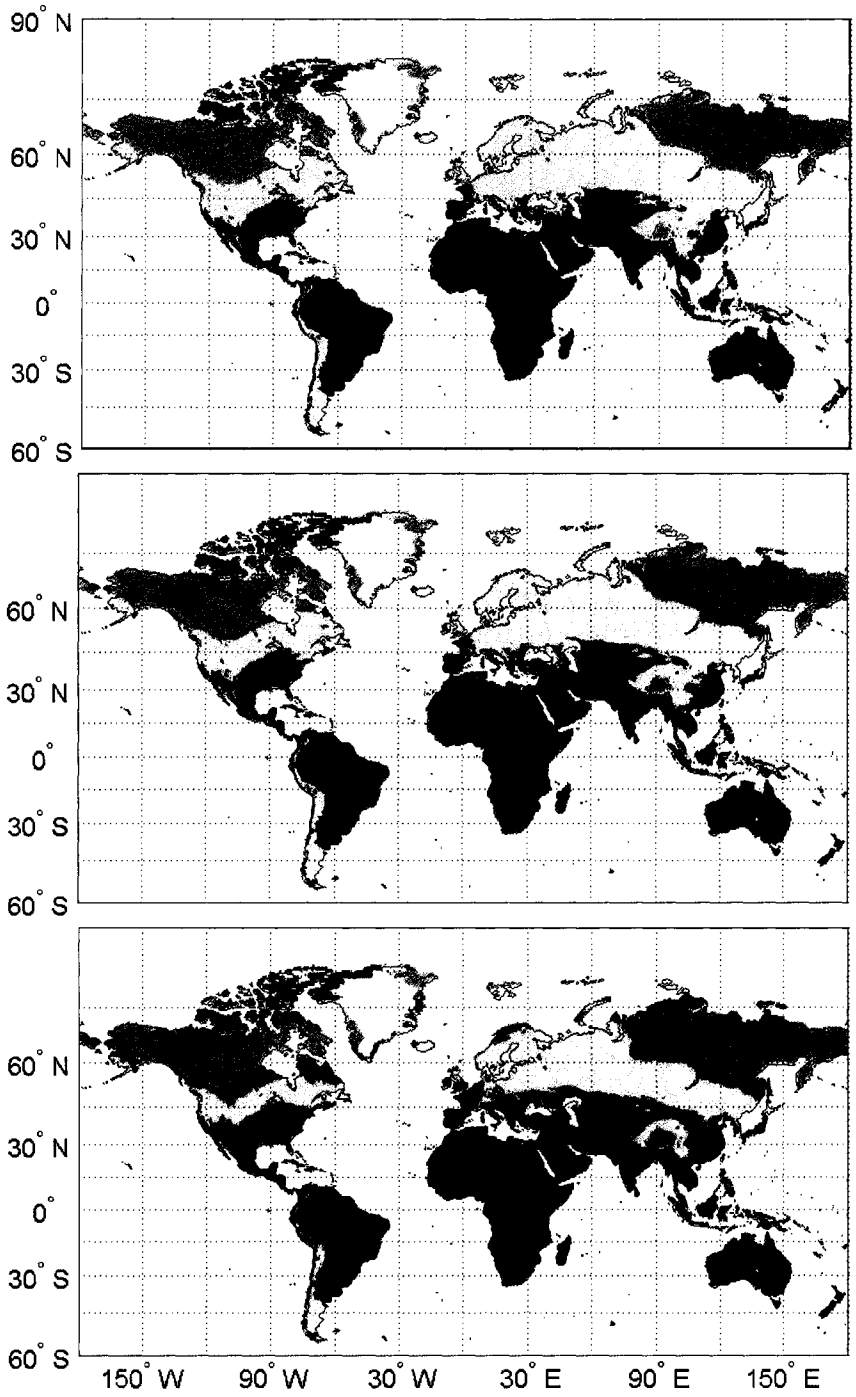

Reproduced with permission of the copyright owner. Further reproduction prohibited without permission.

Figure 5

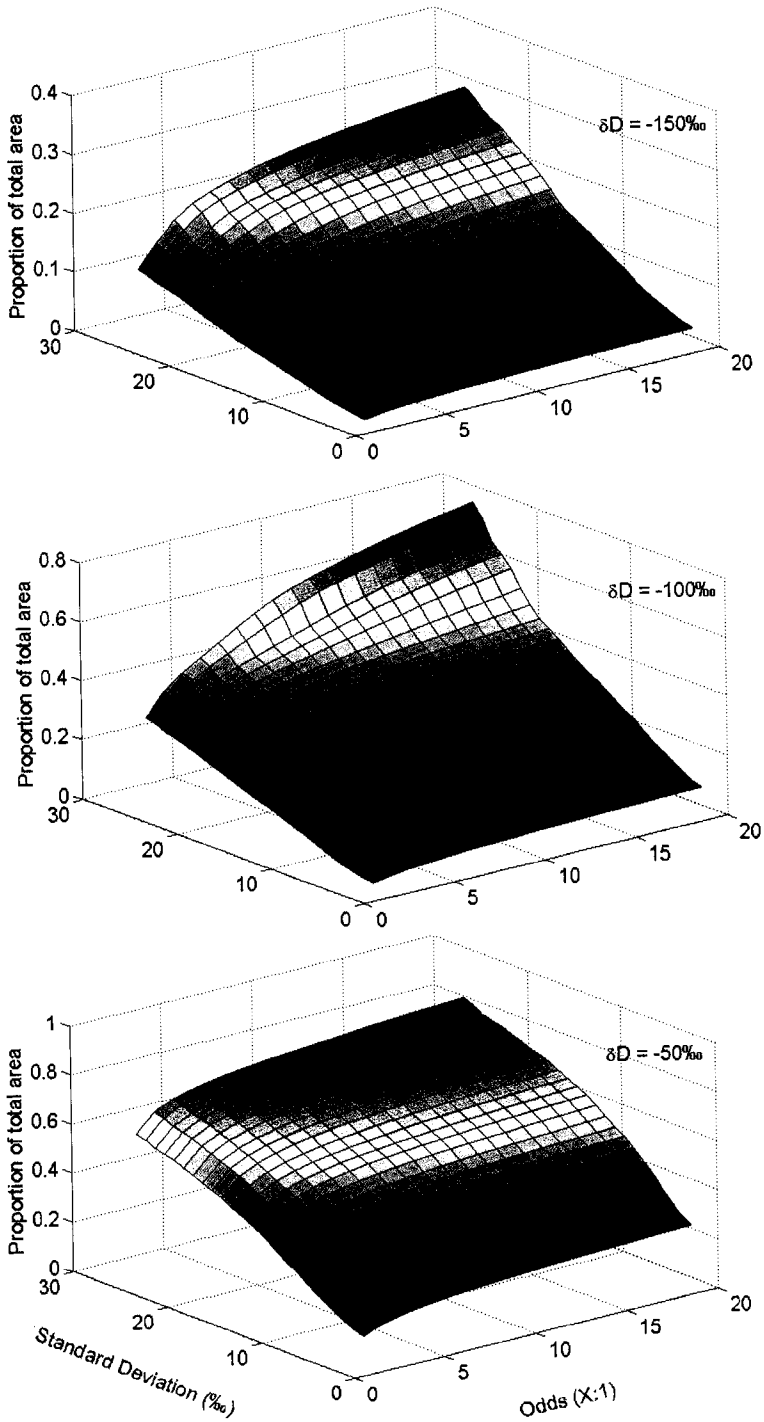

Reproduced with permission of the copyright owner. Further reproduction prohibited without permission.

Figure 6

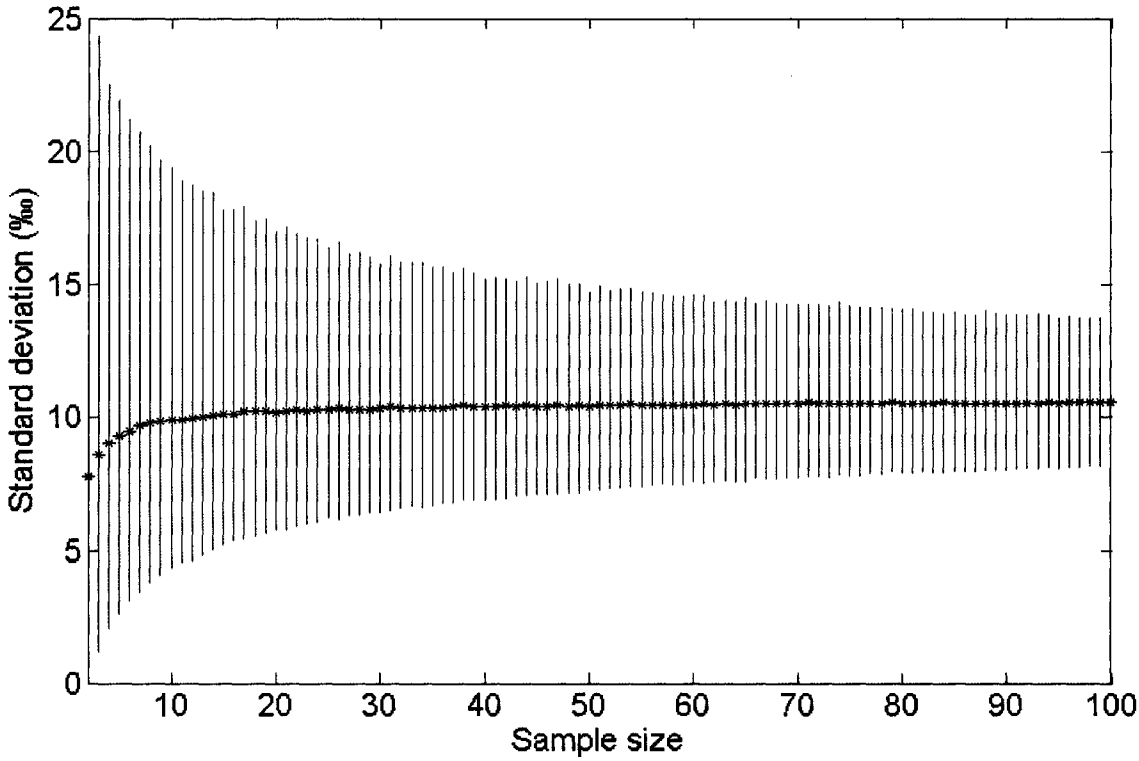

Reproduced with permission of the copyright owner. Further reproduction prohibited without permission.

Figure 7

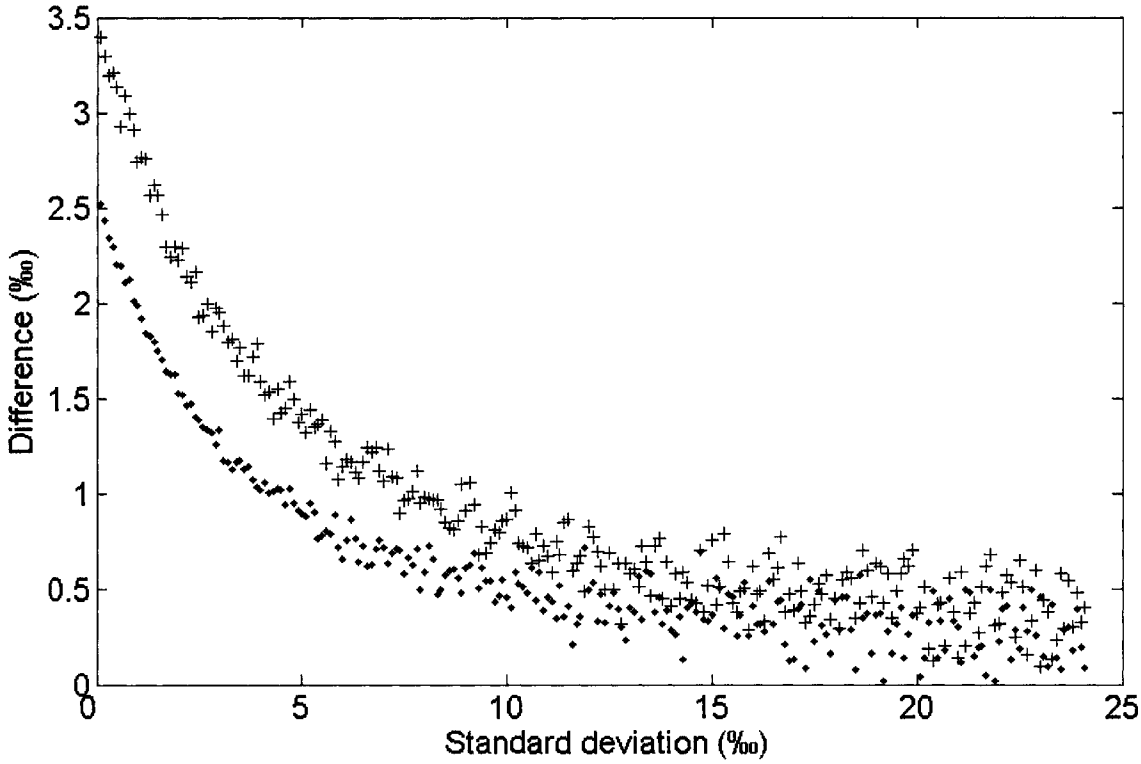

Reproduced with permission of the copyright owner. Further reproduction prohibited without permission.

CHAPTER FOUR

DYNAMICAL GEOGRAPHIC STRUCTURE IN MOUNTAIN PLOVER

Reproduced with permission of the copyright owner. Further reproduction prohibited without permission.

Abstract

Mountain plovers (*Charadrius montanus*) breed across the western edge of the Great Plains from Canada south into Mexico and winter across northern Mexico into the Imperial and Central Valleys of California. Little is known about spring and fall migratory routes between the ranges. A large portion of the population winters in the highly agricultural landscape of Imperial County, CA, but nothing is known about the compositional structure of breeding origins among individuals wintering there. I used color band relocations across 12 years to suggest potential migratory routes. Applying a novel modeling approach based on stable hydrogen isotopes in feathers and precipitation, I quantified the structural dynamics of the composition of breeding origin for birds wintering in Imperial County during four winters. I found evidence for widespread breeding population mixing during winter and offer that migration from the breeding grounds to the wintering ground follows a north-south corridor along the eastern flanks of the Rocky Mountains, followed by a westerly route across the Chihuahuan desert and into the central plains of California. I found unanticipated evidence for rapid geographic turnover of the adult population driven by drought-induced recruitment of young in response to the El Niño Southern Oscillation.

Keywords: Charadrius montanus, migration, connectivity, stable isotopes, color banding, climate effects, ENSO

Reproduced with permission of the copyright owner. Further reproduction prohibited without permission.

INTRODUCTION

Studying populations of migratory birds presents an array of logistical challenges. Because migratory birds spend different parts of the year in different geographic locations, it is often logistically difficult but important to fully define the annual substructures within populations in order to study influences and interactions of seasonal factors (Holmes et al. 1989). Inference to populations of migratory birds cannot be made without an understanding of the underlying time-space substructure (Gill et al. 2001) because events during one season can strongly influence dynamics in another (Marra et al. 1998, Sillet et al. 2000, Norris et al. 2004a). A growing number of reports have implicated well known climate-related dynamics at wide geographic scales (El Niño Southern Oscillation and North Atlantic Oscillation) as directly limiting many if not most ecological processes (Stenseth et al. 2002), including studies that show very direct influences of climate flux on recruitment in migratory bird populations (e.g. Sillet et al. 2000).

Here, I am interested in elucidating the geographic structural composition in wintering aggregations of mountain plover (*Charadrius montanus*), an arid lands migratory shorebird. The breeding range for mountain plovers extends from Canada south into Mexico along the transition from high plains to cold desert (Figure 1). The largest reported wintering concentrations occur in the Imperial Valley, Imperial County, CA, a highly agricultural region where plovers almost exclusively rely on habitats maintained largely according to human economic fluctuations (Wunder and Knopf 2003). Because of the fickle nature of such economics and the potential for impacting a relatively large portion of the world's mountain plovers, I wanted to better understand the

Reproduced with permission of the copyright owner. Further reproduction prohibited without permission.

annual dynamics of wintering aggregations and how widely the effects of land use change would extend across the breeding range.

In general, it is not possible to directly track most migratory species through the complete annual cycle, nor across the full extent of the breeding or wintering ranges; the understanding of seasonal geographic connections is often based on a paucity of information scattered across time. Banding birds has a long tradition of trying to address this problem, but it is not possible to control the time or space aspects of design; the use of bands relies on what really amounts to chance encounters after the initial capture and banding. As such, band-based inference is usually poorly developed or restricted to the population of marked individuals. More recently, a flood of effort has poured into research on using intrinsic tracers to make connections over time and space (Webster et al. 2002). Intrinsic tracers effectively offer a "mark" for every encountered individual, but using this mark to infer geographic connections over time it is not as straightforward as with band encounters; there is substantially more potential for variance associated with the use of intrinsic markers. For example, the effective use of stable isotopes to link breeding and wintering areas for migratory birds requires geographic structure in the isotope ratios at a scale compatible with the investigation, such as that present in the hydrogen and oxygen isotopes of precipitation (Dansgaard 1964). It also requires knowledge of turnover time in various tissues; the timing and location of tissue sampling must account for this turnover (Hobson 2005). Additionally, there should be some prior knowledge of where in the life cycle the tissue was developed; in the case of feathers the molt sequence must be known (Norris et al. 2004b)

Reproduced with permission of the copyright owner. Further reproduction prohibited without permission.

I used a combination of color-marked birds and stable hydrogen isotopes in feathers to describe the geographic structural dynamics for mountain plovers wintering in Imperial County, CA across four years. In so doing, I illustrate and evaluate the application of a new modeling approach for inferring geographic origins from stable isotopes. Ratios of stable hydrogen isotopes in water show a strong latitudinal pattern across the breeding range for plovers (Bowen et al. 2005). I clipped the raster model of expected geographic distribution of δ^2H_{precip} described in Bowen et al. (2005) for the breeding range of plovers. Through an iterative series of steps to simulate the effects of three nested sampling processes I transformed this model into a raster populated with relative probabilities of origin for individual plovers wintering in Imperial County. I combined these individual-level maps to provide insight to the structural dynamics of the mountain plover breeding population.

METHODS

Study Area

I captured and banded plovers at sites distributed across most of the northern extent of the breeding range for mountain plovers and at locations scattered across the wintering range. Locations of long-term breeding biology studies in Montana and Colorado are indicated in Figure A. I am aware of plovers breeding in Nuevo Leon, Mexico and in the Davis Mountain of Texas. Little is known about the population status or distribution between these sites and those where I trapped plovers in northern New Mexico. It is possible that the breeding range is disjoint, but not likely; suitable breeding habitat exists in southern New Mexico and northern Mexico; relatively little effort has been put forth to search for

Reproduced with permission of the copyright owner. Further reproduction prohibited without permission.

breeding plovers in these areas. For this reason, the southern portion of the breeding range has been conservatively outlined and differs from the range map in Knopf and Wunder (2006). Although I worked at sites across the wintering range, the largest concentrations of wintering plovers consistently occurred in Imperial County, CA. Consequently, I focused on this wintering site for the study presented here.

Generally, habitats across the breeding range were characterized as arid tablelands along the transition between high prairie and cold desert and have been described for some of these locations elsewhere (Finzel 1964, Graul 1975, Olsen-Edge 1987, Parrish et al. 1993, Plumb et al. 2005, Wunder et al. 2003). Wintering sites were predominantly agricultural, but habitats in Mexico additionally included black-tailed prairie dog (*Cynomys ludovicianus*) and Mexican prairie dog (*Cynomys mexicanus*) colonies. Habitat in the Imperial Valley was almost exclusively agricultural (Wunder and Knopf 2003).

Mountain Plover Sampling

Mountain plovers molt flight feathers once per year on the breeding grounds except for cases where molt is induced from aberrant feather loss. This molt begins in the late incubation stages for most birds, but can be postponed until after the nest hatches for early nesters; we frequently caught birds in molt while on the nest. The wing molt sequence is initiated at the center of the wing and proceeds outward in both directions. Thus, the innermost primary is almost always grown on the breeding grounds. Body feathers are molted twice per year, once before and during fall migration and again immediately prior to and during spring migration. Young are precocial and molt into juvenal plumage within ~21 days after hatching. All juvenal feathers reflect local patterns

Reproduced with permission of the copyright owner. Further reproduction prohibited without permission.

in isotope values for their natal grounds. First year (young) birds can be distinguished from older (adult) birds by the presence of a wide buff fringe on the primary coverts, which are generally molted after the first full breeding season (Knopf and Wunder 2006). My feather sampling strategy for isotopes was designed around this molt pattern.

I wanted to link wintering birds to the breeding grounds, so I sampled only feathers I knew were grown on the breeding grounds from birds caught in all seasons. During winter, I captured plovers with low-profile walk-in mist-nets and by spotlighting and hand-netting individual birds at night roosts. During the breeding season, I captured adult plovers with mesh walk-in traps and I caught young of the year by hand.

An aluminum USFWS band and a combination of 3-4 color bands was affixed to 3015 mountain plovers during the 1995-2006 breeding seasons at sites in Montana, Wyoming, Colorado, and New Mexico (Figure 1). Individual color band combinations were used in cases from Phillips County, MT and Park County, CO, but for most cases the combination indicated band location and year. I measured δ^2H for breast feathers sampled from 352 pre-fledged young from across the breeding range during the 2001-2004 breeding seasons. I measured δ^2H for P1 (the innermost primary) from both wings taken from 110 adult plovers that were recaptured at the same location in a subsequent breeding season during the same 2001-2004 time span, bringing my known-origin sample size to 462, and dividing it across age classes. I color-banded an additional 349 plovers during the 2001-2004 winters in Imperial County, CA; color band combinations indicated band year. I measured δ^2H for P1 feathers taken from 298 plovers caught during the winter banding periods in Imperial County. Of these individuals, 138 were first-year birds (referred to here as "young") and the other 160 were in at least their second winter

Reproduced with permission of the copyright owner. Further reproduction prohibited without permission.

(referred to here as "adult"). These samples were distributed across years 2001-2004 respectively as follows: 24, 71, 21 and 22 young, and 34, 67, 38, and 21 adults.

One individual was caught and banded as an adult on a nest in Weld County, CO in June 2001, then caught it again in January 2002 in Imperial County, CA. A second individual was caught and banded as a first-winter bird in February 2002 in Imperial County, CA, then caught on a nest in Phillips County, MT in June 2002. A third individual was caught and banded prior to fledging in Lincoln County, CO in June 2003, then caught again in February 2004 in Imperial County, CA, then once again May 2005 when it returned to nest at its natal breeding site in Lincoln County. A fourth bird was caught and banded as an adult during winter in February 2004 in Imperial County, and then caught again on a nest in June 2005 in Park County, CO.

Stable Isotope Measurements

Feathers were washed of surface oils with a 2:1 chloroform/methanol solution and allowed to air dry overnight under a fume hood. Approximately 0.5mg of feather tissue was loaded into pressed silver capsules. Samples were then analyzed by continuous flow isotope ratio mass spectrometry using a Finnigan TC/EA coupled to a Finnigan Delta Plus XL mass spectrometer at the USGS stable isotope lab in Denver, CO. Non-exchangeable hydrogen isotopic compositions were determined by comparative equilibration techniques using internal keratin standards that were calibrated to the VSMOW-SLAP scale via the CFS-CHS-BWBII scaling as described in Wassenaar and Hobson (2003). I report stable isotope ratios for bulk non-exchangeable hydrogen as delta values relative to the Vienna Standard Mean Ocean Water (VSMOW) scaling in parts per

Reproduced with permission of the copyright owner. Further reproduction prohibited without permission.

mil (‰) using the standard delta scale $\delta^2H = (R_{feather}/R_{VSMOW} - 1) \times 1000$, where R is the ratio of $^2H:^1H$. Analytical error associated with this measurement process was stochastically propagated in the data analysis model as described in chapter three and briefly below.

Error Propagation Model

I compared the expected geographic distribution of δ^2H from the model described in Bowen et al. (2005) with the values we measured in feathers from plovers of known origin (young and recaptured adults). For each individual, I looked up the precipitation value for the latitude/longitude coordinate where the plover was captured and calculated the difference between the values ($\delta^2H_{feather} - \delta^2H_{precip}$). Although plovers are precocial (and thus adults and chicks independently take similar prey items), I suspected that differences in the energetic demands associated with structural growth in young and mass maintenance in adults would generate age specific differences in the incorporation of δ^2H into feathers. For this reason, I compared the distributions of differences for adult recaptures and young separately.

Juveniles were captured across a wide extent of the breeding range whereas recaptured adults were generally restricted to three sites in Colorado; this meant that the δ^2H_{precip} values spanned a wider range for the young than for the recaptures. I therefore used the data from young birds to estimate slope and intercept parameters for a linear rescaling from δ^2H_{precip} to $\delta^2H_{feather}$. Because the age specific distributions of differences between $\delta^2H_{feather}$ and δ^2H_{precip} varied in location (mean value) but not appreciably in

Reproduced with permission of the copyright owner. Further reproduction prohibited without permission.

scale (Figure 2), I adjusted the intercept, but not the slope for adults and obtained the following age specific rescalings:

$$\delta^2 H_{young\ feather} = 1.257\left(\delta^2 H_{precip}\right) + 17.361 \quad (1.1)$$

$$\delta^2 H_{adult\ feather} = 1.257\left(\delta^2 H_{precip}\right) + 50.4584 \quad (1.2)$$

I used the rescaled raster to describe the mean geographic distribution for $\delta^2H_{feather}$ and incorporated three sources of estimable error as described in chapter three. Briefly, I modeled three nested stochastic sampling processes to simulate (1) sampling an individual bird of known origin from a single location, (2) taking a feather sample from that bird, and (3) measuring δ^2H for that feather. My model incorporated three dependent and three independent variables and was structured as follows:

$$X_{pop} \left| \delta^2 H_{rescale}, \sigma_{population}, \sim N\left(\delta^2 H_{rescale}, \sigma_{population}\right) \right. \quad (1.3)$$

$$X_{ind} \left| X_{pop}, \sigma_{individual} \sim N\left(X_{pop}, \sigma_{individual}\right) \right. \quad (1.4)$$

$$X_{obs} \left| X_{ind}, \sigma_{analytical} \sim N\left(X_{ind}, \sigma_{analytical}\right) \right. \quad (1.5)$$

where

$$\sigma_{population} \left| \alpha_p, \beta_p \sim \Gamma\left(\alpha_p, \beta_p\right) \right. \quad (1.6)$$

$$\sigma_{individual} \left| \alpha_i, \beta_i \sim \Gamma\left(\alpha_i, \beta_i\right) \right. \quad (1.7)$$

$$\sigma_{analytical} \left| \alpha_a, \beta_a \sim \Gamma\left(\alpha_a, \beta_a\right) \right. \quad (1.8)$$

X_{obs} represents the δ^2H value I observe for a sampled individual, and $\delta^2H_{rescale}$ is the age-appropriate rescaling (equation 1.1 or 1.2). I used published estimates of within-location variance and data from mountain plovers to estimate the shape and scale parameters for the gamma distributions in 1.6 and 1.7 as described in chapter three. Briefly, I wrote

Reproduced with permission of the copyright owner. Further reproduction prohibited without permission.

$$\sigma^2_{observed-population} = \sigma^2_{population} + \sigma^2_{individual} + \sigma^2_{analytical} \quad (1.9)$$

$$\sigma^2_{observed-individual} = \sigma^2_{individual} + \sigma^2_{analytical} \quad (1.10)$$

$$\sigma^2_{observed-analytical} = \sigma^2_{analytical} \quad (1.11)$$

and used the observed estimates along with the equality in equation 1.9 to solve for $\sigma_{population}$, $\sigma_{individual}$ and $\sigma_{analytical}$, then used maximum likelihood to estimate the parameters α and β from these "true" values for model simulations (equations 1.6 and 1.7).

To estimate α and β for 1.8, I used a series (n = *782*) of δ^2H measurements made over the course of a year for two different in-house keratin standards using continuous-flow isotope ratio mass spectrometry (CFIRMS; see chapter two). Stable isotope labs in Denver, Flagstaff, and Saskatoon independently measured δ^2H for the non-exchangeable hydrogen in these keratin standards, which gave the "known" value for each standard. Known values were regressed on the measured values for each auto-run (carousel) for calibrating samples in the run; the collection of residuals from these regressions described the analytical error. A typical auto-run at the Denver lab includes 16 samples and between two and five of each of the standards. Thus, I simulated analytical error associated with CFIRMS by drawing 10 000 sets of 16 values each from the set of 782 residuals described above. I calculated the standard deviation for each set of 16 samples and I used maximum likelihood to estimate α and β for 1.8 from the set of 10 000 standard deviations.

Determining Probabilities of Origin for Individual Wintering Birds

I simulated 10 000 values of X_{obs} to generate a distribution that was centered on values for each pixel in the raster. I used these as probability densities for determining the

Reproduced with permission of the copyright owner. Further reproduction prohibited without permission.

probability density for each pixel as the origin for a wintering bird with a measured $\delta^2H_{feather}$ as follows:

$$P\left(pixel_{i,j} \middle| \delta^2 H_{rescale}, \boldsymbol{\alpha}, \boldsymbol{\beta}\right) \propto X_{obs} \quad (1.12)$$

where *i,j* are the row/column index for the pixel, $\delta^2H_{rescale}$ is determined by the age of the wintering bird in question and $\boldsymbol{\alpha}$ and $\boldsymbol{\beta}$ are vectors of hyper-parameters.

Distributions of δ^2H vary widely among individual birds at any given location (see Table 1 in chapter three). Incorporating this variance directly into the probability models resulted in an appropriately flat posterior density for any given pixel. For this reason, I evaluated the densities for each pixel relative to the global maximum. This effectively established the odds for each pixel as the origin relative to the most likely pixel(s). I refer to these odds interchangeably as relative probabilities here. I used the offsite winter recaptures and the known-origin samples to evaluate the performance of the models in determining the probability of origin for individual plovers. To describe the proportional composition of annual wintering bird concentrations, I averaged the probability rasters on a per-pixel basis. This provided a surface of probability-weighted proportions where broad spatial ranges were associated with any given proportion.

RESULTS AND DISCUSSION

Model Rescaling and Diagnostics

Mountain plover adult feathers were more enriched in ^2H relative to expected precipitation values than were feathers from pre-fledged chicks (Figure 2). This is consistent with findings for raptors (Meehan et al. 2003) and passerines (Langin et al. 2007). However, in contrast to one proposed explanation in those studies, difference in

Reproduced with permission of the copyright owner. Further reproduction prohibited without permission.

diet cannot explain the difference observed here as plovers are precocial so young forage independently from and take similar diet items as adults. Young plovers grow juvenal plumage concurrent with skeletal growth and mass gain, whereas adults are post-nesting and replacing feathers while maintaining, replenishing, or adding mass, but skeletal growth has been complete for more than a year. I suggest that the difference is related to differences in metabolic demands between the two age groups, be it from the demands of structural growth in young, periods of differential relative heat stress (McKechnie et al. 2004), food deprivation while sitting on eggs as suggested by Meehan et al. (2003), or by some other unspecified mechanism.

The poor mechanistic understanding of this difference among ages did not preclude the relatively effective use of the precipitation-based model for determining origins, but it did mandate age- and species-specific rescaling from precipitation to feather. The precision and accuracy of my approach depend strongly on the functional form of the rescaling from precipitation to feathers. Although I had only four offsite recaptures of known origin birds during winter, two were recaptured as adults and two were recaptured in their first winter, providing a unique opportunity to compare the performance of the two age-specific rescalings along with the one suggested as a general guideline by others (e.g. $\delta^2H_{feather} = \delta^2H_{precip}$ -25‰; Rubenstein and Hobson 2005). Importantly, in these four cases, I am evaluating my model with precisely the sort of information I hope to gain from the model rather than using a proxy such as known-origin birds sampled during the breeding season (e.g. Wunder et al. 2005 (chapter one)).

In the case of the adult recapture from Weld County, CO, the relative probability of the true origin based on the rescaling suggested in the literature was 1.98×10^{-15}; the

Reproduced with permission of the copyright owner. Further reproduction prohibited without permission.

rescaling based on young feathers gave a relative probability of 1.03×10^{-6}. In strong contrast, the relative probability based on the adult rescaling was 0.37. The results for the adult plover from Park County, CO, were similar: the literature-based rescaling yielded a relative probability of 6.42×10^{-13} for the true origin; the rescaling based on young feathers gave a relative probability of 2.82×10^{-5}, and the relative probability was 0.82 when using the adult-specific rescaling. Similar disparities among rescaling forms were observed for the young of the year birds from Lincoln County, CO and Phillips County, MT. In the case of the Lincoln County bird, the literature-based rescaling yielded a relative probability of 0.00029, the adult feather rescaling yielded 0.00010, and the young feather rescaling yielded a relative probability of 0.96 for the true origin. In the case of the Phillips County bird, the literature-based rescaling gave a relative probability of 0.00058, the adult rescaling yielded 0.00021, and the young feather rescaling gave a relative probability of 0.99 for the true origin.

When using the correct rescaling in these cases, the proportion of the breeding range with relative probabilities greater than or equal to that for the true origin was 0.47, 0.09, 0.05, and 0.02 for the Weld, Park, Lincoln, and Phillips birds respectively. This means that in these cases, my model reduced the probable range of origin to 47%, 9%, 5%, and 2% respectively, of the entire breeding range. The literature-based rescaling reduced the probable ranges to 70%, 70%, 61%, and 84% of the breeding range respectively, whereas the age-inappropriate rescaling reduced the ranges to 70%, 99%, 39%, and 8% respectively. As expected, in all cases the literature-based rescaling predicted that the range of origin was much further south than the true origin, whereas the

Reproduced with permission of the copyright owner. Further reproduction prohibited without permission.

age-inappropriate rescaling predicted the range to be further north for adults and further south for the young (Figure 3).

Although these cases provided the only opportunity to directly explore the performance of the model as intended, the adults that were banded and recaptured on the breeding grounds and the pre-fledged young provided surrogate opportunities to explore the reliability of our model. To determine the error rates of the model for these 462 known-origin birds, I first determined the probable geographic range of origin in terms of odds of correctly encompassing the geographic origin (referred to here as the nominal odds) for each bird (see chapter three) and then asked whether the true origin was circumscribed by this geographic area. The geographic resolution for assignment is inversely proportional to the nominal odds (chapter three). That is, as I increase the odds of correctly including the true origin, I increase the geographic extent of the identified probable range; this is why I observed the inverse relationship between nominal odds and error rate as I measured it here (Figure 4). The age appropriate rescaling generated error rates that aligned reasonably well with the nominal odds, whereas the literature-based rescaling and the inappropriate age rescaling both yielded consistently high error rates, regardless of choice of odds (Figure 4).

Summarizing these diagnostics, it is clear that failing to use system-specific rescaling results in both poor accuracy and precision. Although I would have preferred higher relative probability values associated with the true origins for the offsite recaptures, especially for the case of the Weld County bird, I point out that my approach represents a substantial improvement over currently used approaches. I need only look at the proportions of the probabilities for the true origin to get some sense for the magnitude

Reproduced with permission of the copyright owner. Further reproduction prohibited without permission.

of the gain in accuracy. For example, even though the relative probability of the Weld County bird was 0.37 using the most appropriate rescale, this represents a 1.8×10^{14}-fold ($0.37/1.98 \times 10^{-15}$) improvement over the literature-based rescaling. Only through age- and species-specific rescaling was I able to obtain relatively accurate, precise and predictable results. Consequently, until more is known about the mechanisms that influence incorporation rates of ^{2}H from precipitation into feather tissue, it will be necessary to use known-origin feathers for constructing an age- and species-appropriate rescaling for the unknown-origin birds of interest.

Band Encounter Patterns

From 1995-2006, I recorded 57 offsite relocations of wintering plovers that were banded on the breeding grounds and 19 offsite relocations of winter-banded plovers during the breeding season. Figure 5 illustrates the spatial connections implied by these records and from an additional recovery from 1965 in Austin, TX of a bird banded in Montana that same year (Knopf and Wunder 2006). Of note among these records include a plover seen in Tulare County, CA during December 2006 that was originally banded in February 2002 in Imperial County, CA, and the observation in February 2006 of seven color-banded birds in the same flock of about 100 plovers on a cotton/hay field in Madera County, CA. These seven birds were banded in Phillips County, MT in 2003, Weld County, CO in 2003, Park County, CO in 2005, and Lincoln County, CO in 2002, 2003 (2 such birds), and 2004. Additionally, a plover banded in Phillips County, MT in 1998 was relocated during spring migration in Baca County, CO in April 1999 and a plover banded in Park County, CO in 2000 was relocated during spring migration in Pueblo

Reproduced with permission of the copyright owner. Further reproduction prohibited without permission.

County, CO in May 2001; neither of these plovers was relocated after a few days at those locations, suggesting they continued north to Phillips and Park Counties, respectively.

The band relocation data, although sparse, suggest three dynamical features of mountain plover biogeography. First, that there is extensive and widespread population mixing during winter. Second, that the likely route of spring and fall migrations is north-south along the western edge of the Rocky Mountains, northeast-southwest across New Mexico, Texas, and northern Mexico and again north-south within the Imperial and Central Valleys of California. And lastly, that plovers will use alternate winter sites among years. This last conclusion complements the findings of Knopf and Rupert (1995) that site fidelity is poor during winter with plovers regularly moving long distances and using alternate sites even within a single winter season. The first conclusion also supports the suggestion by Knopf and Rupert (1995) that there is little structural integrity in wintering flocks; despite affixing radio transmitters to birds captured simultaneously in the same flock, they never again found any two radio-marked birds in the same flock. It appears as though winter flocks are relatively fluid in terms of both individual and geographic composition. Although these band data provide useful hints about direct seasonal linkages, they are scattered across time such that it is difficult to determine fine-scale (e.g. annual) temporal dynamics of that fluidity.

Isotope-based Patterns

The feathers I sampled from plovers caught during winters 2001-2004 were grown during the breeding seasons 2000-2003; all isotope-based inferences are to these breeding seasons. The spatial pattern of relative proportional composition of breeding

Reproduced with permission of the copyright owner. Further reproduction prohibited without permission.

origins shifted annually for both adults and first winter plovers (Figure 6). In 2000, the composition of young plovers was relatively peaked over natal origins across the southern plains, whereas the composition of adults was more flatly distributed among more northerly breeding origins. In 2001 both the adult and young wintering compositions were flatter and more widely distributed across the breeding range than in the previous year; the adult population appears to have absorbed some of the young distribution from the previous year, suggesting successful recruitment into the adult population at those southern sites.

In 2002, there was a strong shift in composition toward the southern plains for both young and adults with a reasonable amount of the adult mass still deriving from Wyoming; the adult pattern here again looks to have absorbed the mass from the young distribution in the prior year. Moreover, distributions are more peaked than in 2000 and 2001, suggesting that there was relatively little contribution from the northern extent of the range in 2002. Life expectancy for mountain plovers is 1.92 ± 0.17 years (Dinsmore et al. 2003). Additionally, at the Phillips County, MT study site, Dinsmore et al. (2002) documented that daily precipitation strongly and negatively influenced nest survival; most documented nest losses occurred within 24 hours of a rain event. Taking these findings together with the pattern of relatively heavy precipitation in the north during the 2000 and 2001 breeding seasons (Figure 6), it seems reasonable to conclude that most of the recruitment in the mountain plover population from 2000-2002 was from the drier regions further south. The compositional distributions in 2003 are again relatively peaked and may be explained by my suggestion that the center of mass in the adult population

Reproduced with permission of the copyright owner. Further reproduction prohibited without permission.

shifted south over the previous two years. The majority of wintering plovers likely derived from the central portion of the range in 2003.

The El Niño Southern Oscillation (ENSO) drove the precipitation patterns I observed. There was a strong El Niño effect during May-July 2000 (Data available from http://www.cpc.ncep.noaa.gov/products/monitoring_and_data/ENSO_connections.shtml, accessed 22 February, 2007) resulting in a much more even and widespread distribution of rainfall across the breeding season than in other years (Figure 6). Strong La Niña effects occurred in 2002, resulting in a more even pattern of low precipitation and widespread drought across the extent of the range (Figure 6). These climatic patterns appear to have driven recruitment and the subsequent compositional dynamics of the mountain plover population. However, an alternative explanation would be that the varying precipitation levels caused differential stresses on the water use efficiency in either the plovers themselves during molt or at some lower level in the food web. This could generate systematic offsets which in turn might, for example, elevate δ^2H values in feathers for drought years (McKechnie et al. 2004); these higher values would have then been mapped further south than the true origin in 2002. However, if this were the case, my observed pattern of more young birds deriving from further south in 2000 (a cool wet year) relative to 2002 (an extreme drought year) is contradictory.

As added evidence against a precipitation-based bias, the distribution of young appears to respond to precipitation levels in a manner consistent with what I would expect from studies of nesting biology, but the adult distribution does not. It appears instead to represent a combination of adult turnover and recruitment of young. If precipitation levels biased the isotope analyses, I would expect a more uniform response

Reproduced with permission of the copyright owner. Further reproduction prohibited without permission.

across the age classes because the difference between the adult and young rescaling is a fixed linear offset. Instead, I see the highest levels of precipitation associated with the lowest proportions of young in every year (Figure 7) and I see a 1-2 year lagged response to precipitation in adults that is more parsimoniously explained as population turnover: recruitment of young into the adult population combined with the loss of older (>2-3 years old) adults.

CONCLUSIONS

Geographic Recruitment Dynamics of Mountain Plover

The mountain plover population is well-mixed during winter and recruitment may be driven at a coarse level by regional patterns in climate. The species responds favorably to drought conditions, likely because of a combination of reduced predation and increased food availability. Most predators of plover eggs and chicks are olfactory-driven (Knopf and Wunder 2006), and wet conditions enhance this cueing method. Arthropod abundances respond strongly and favorably to drought (White 1976, Mattson and Haack 1987). Sillet et al. (2000) documented this same ENSO-related pattern of increased recruitment in dry years for black throated blue warblers (*Dendroica caerulescens*), and attributed it to increased food availability during dry years. I caution that my data do not include estimates of absolute abundance or direct estimates of recruitment. My inferences are limited to likely relative geographical compositions of recruitment. It is possible that although dry areas and years provide proportionally more recruitment, the overall demographic trajectory is unrelated. There may be as yet undiscovered lower-order influences that override the 2-3 year fluxes I describe here.

Reproduced with permission of the copyright owner. Further reproduction prohibited without permission.

The Hierarchical Model

My modeling approach offers greater accuracy and a more flexible framework than other methods explored so far. By transforming a precipitation-based model into a probability surface, I am no longer locked into outlining the broad ranges that are associated with a 95% prediction interval from a regression used to rescale expected δ^2H_{precip} to $\delta^2H_{feather}$ (e.g. ranges shown in Bowen et al. 2005). Because my model describes the probability of a pixel as the origin, rather than the probability of observing a value of some statistic, I can continuously trade off error rate for geographic precision according to the relative importance of each. Furthermore, the structure of my model is easily expanded to incorporate experimental results as they become available. These modifications would likely manifest via the structure of the rescaling (e.g. it need not be linear), but may also affect my sampling precision, either directly or indirectly. It will probably be necessary to continue requiring the simulated sampling hierarchy I used, but the magnitude of the variances may be reduced by increased knowledge from experimental work. I caution that the efficacy of this approach is directly related to sampling intensity; as it stands, it still requires widespread and exhaustive sampling of known-origin tissue specific to the species and age class of interest. But the potential for reliable results remains high with enough effort.

Reproduced with permission of the copyright owner. Further reproduction prohibited without permission.

LITERATURE CITED

Bowen, G.J., L.I. Wassenaar, and K.A. Hobson. 2005a. Global application of stable hydrogen and oxygen isotopes to wildlife forensics. Oecologia **143**:337-348.

Dansgaard W. 1964. Stable isotopes in precipitation. Tellus **16**:436-468.

Dinsmore, S.J., G.C. White, and F.L. Knopf. 2002. Advanced techniques for modeling avian nest survival. Ecology **83**:3476-3488.

Dinsmore, S.J., G.C. White, and F.L. Knopf. 2003. Annual survival and population estimates of mountain plovers in southern Phillips County, Montana. Ecological Applications **13**:1013-1026.

Finzel, J.E. 1964. Avian populations of four herbaceous communities in southeastern Wyoming. Condor **66**:496-510.

Holmes, R.T., T.W. Sherry, and L. Reitsma. 1989. Population structure, territoriality, and overwinter survival of two migrant warbler species in Jamaica. Condor **91**:545-561.

Gill, J.A., K. Norris, P.M. Potts, T.G. Gunnarsson, P.W. Atkinson, and W.J. Sutherland. 2001. The buffer effect and large-scale population regulation in migratory birds. Nature **412**:436-438.

Graul, W.D. 1975. Breeding biology of the mountain plover. Wilson Bulletin **87**:6-31.

Hobson, K.A. 2005. Stable isotopes and the determination of avian migratory connectivity and seasonal interactions. Auk **122**:1037-1048.

Knopf, F.L. and M.B. Wunder. 2006. Mountain plover (*Charadrius montanus*). In *The Birds of North America Online (A. Poole Ed.)* Ithaca: Cornell Laboratory of Ornithology; Retrieved from The Birds of North America Online database:

Reproduced with permission of the copyright owner. Further reproduction prohibited without permission.

http://bna.birds.cornell.edu/BNA/account/Mountain_Plover. doi:10.2173/bna.211

Knopf, F.L. and J. R. Rupert. 1995. Habits and habitats of mountain plovers in California. Condor **97**:743:751.

Langin, K.M., M.W. Reudink, P.P. Marra, D.R. Norris, T.K. Kyser, and L.M. Ratcliffe. 2007. Hydrogen isotopic variation in migratory bird tissues of known origin: Implications for geographic assignment. Oecologia *In Press*

Mattson, W.J. and R.A. Haack. 1987. The Role of drought in outbreaks of plant-eating insects. Bioscience **37**:110-118.

McKechnie A.E., B.O. Wolf, and C. Martinez del Rio. 2004. Deuterium stable isotope ratios as tracers of water resource use: an experimental test with rock doves. Oecologia **140**:191-200.

Meehan, T.D., R.N. Rosenfield, V.N. Atudorei, J. Bielefeldt, L.J. Rosenfield, A.C. Stewart, W.E. Stout, and M.A. Bozek. 2003. Variation in hydrogen stable-isotope ratios between adult and nestling Cooper's hawks. Condor **105**:567-572.

Norris, D.R., P.P. Marra, T.K. Kyser, T.W. Sherry, and L.M. Ratcliffe. 2004a. Tropical winter habitat limits reproductive success on the temperate breeding grounds in a migratory bird. Proceedings of the Royal Society of London, Series B **271**:59-64.

Norris D.R., P.P. Marra, R. Montgomerie, T.K. Kyser, and L.M. Ratcliffe. 2004b. Reproductive effort, molting latitude, and feather color in a migratory songbird. Science **306**:2249-2250.

Olsen-Edge, S.L. and W.D. Edge. 1987. Density and distribution of the mountain plover on the Charles M. Russell Wildlife Refuge. Prairie Naturalist **19**:223-228.

Reproduced with permission of the copyright owner. Further reproduction prohibited without permission.

Parrish, T.L., S.H. Anderson, and W.F. Oelklaus. 1993. Mountain plover habitat selection in the Powder River Basin, Wyoming. Prairie Naturalist **25**:219-226.

Plumb, R.E., S.H. Anderson, and F.L. Knopf. 2005. Habitat and nesting biology of mountain plovers in Wyoming. Western North American Naturalist **65**:223-228.

Rubenstein, D.R. and K.A. Hobson. 2004. From birds to butterflies: animal movement patterns and stable isotopes. Trends in Ecology and Evolution **19**:256-263.

Sillet, T.S., R.T. Holmes and T.W. Sherry. 2000. Impacts of a global climate cycle on population dynamics of a migratory songbird. Science **288**:2040-2042.

Stenseth, N.C., A. Mysterud, G. Ottersen, J.W. Hurrell, K. Chan, and M. Lima. 2002. Ecological effects of climate fluctuations. Science **297**:1292-1296.

Webster, M.S., P.P. Marra, S.M. Haig, S. Bensch, and R.T. Holmes. 2002. Links between worlds: unraveling migratory connectivity. Trends in Ecology and Evolution **17**:76-83.

White, T.C.R. 1976. Weather, food and plagues of locusts. Oecologia **22**:119-134.

Wunder, M.B. and F.L. Knopf. 2003. Imperial Valley of California is critical to mountain plovers. Journal of Field Ornithology **74**:74-80.

Wunder, M.B., F.L. Knopf and C.A. Pague. 2003. The high elevation population of mountain plovers in Colorado. Condor **105**:654-662.

Wunder M.B., C.L. Kester, F.L. Knopf, and R.O. Rye. 2005. A test of geographic assignment using isotope tracers in feathers of known origin. Oecologia **144**:607-617.

Reproduced with permission of the copyright owner. Further reproduction prohibited without permission.

Figure 1. Map of study area. Breeding range is the spaghetti outline oriented north-south from Canada into Mexico. Wintering range is oriented east-west across northern Mexico into California. Dots within breeding range and stars within wintering range are banding and feather sample locations. Nueva Leon is both breeding and wintering site. Long-term study sites are indicated as Phillips County, Pawnee National Grassland (PNG), South Park, and Lincoln County. Imperial Valley indicates the largest known wintering concentrations.

Figure 2. Distributions of differences between feather δ^2H and predicted precipitation δ^2H (from Bowen et al. 2005) for birds of known origin. Sample sizes were *n=352* for young birds, and *n=110* for adult recaptures.

Figure 3. Relative probability of origin maps for four plovers banded on the breeding grounds and caught during a subsequent winter. Stars indicate true origin; black indicates age and species appropriate rescaling. Red stars indicate generic or mismatched age rescaling. See text for information about the individual birds.

Figure 4. Error rates for encompassing the true origin of known-origin birds as a function of odds. Nominal odds are the odds that the circumscribed area includes the true origin. Diamond markers indicate plover-specific rescaling; open diamonds are inappropriate age rescaling; filled diamonds are age appropriate rescaling. Stars indicate generic rescaling. Dotted lines are pre-fledged young. Solid lines are adult recaptures.

Reproduced with permission of the copyright owner. Further reproduction prohibited without permission.

Figure 5. Offsite color-band relocations. The panel on the left shows site links for plovers that were banded on the breeding grounds and relocated during winter or migration. The panel on the right shows links for plovers banded during winter in Imperial County, CA and relocated during the breeding season or migration.

Figure 6. Annual probability-weighted compositions of plovers wintering in Imperial County, CA in terms of breeding origin. Rows are years (2000-2003). The left column is for wintering adults. The middle column is the weighted distribution for first-winter plovers. The right column is the additive measure of precipitation in the U.S portion of the breeding range for the months of May and June of each year (from PRISM Group, Oregon State University, http://www.prismclimate.org, created 4 Aug 2004).

Figure 7. Probability-weighted proportional composition of wintering young (first winter) plovers compared with precipitation amount for the months of May and June for 2000-2003.

Reproduced with permission of the copyright owner. Further reproduction prohibited without permission.

Figure 1

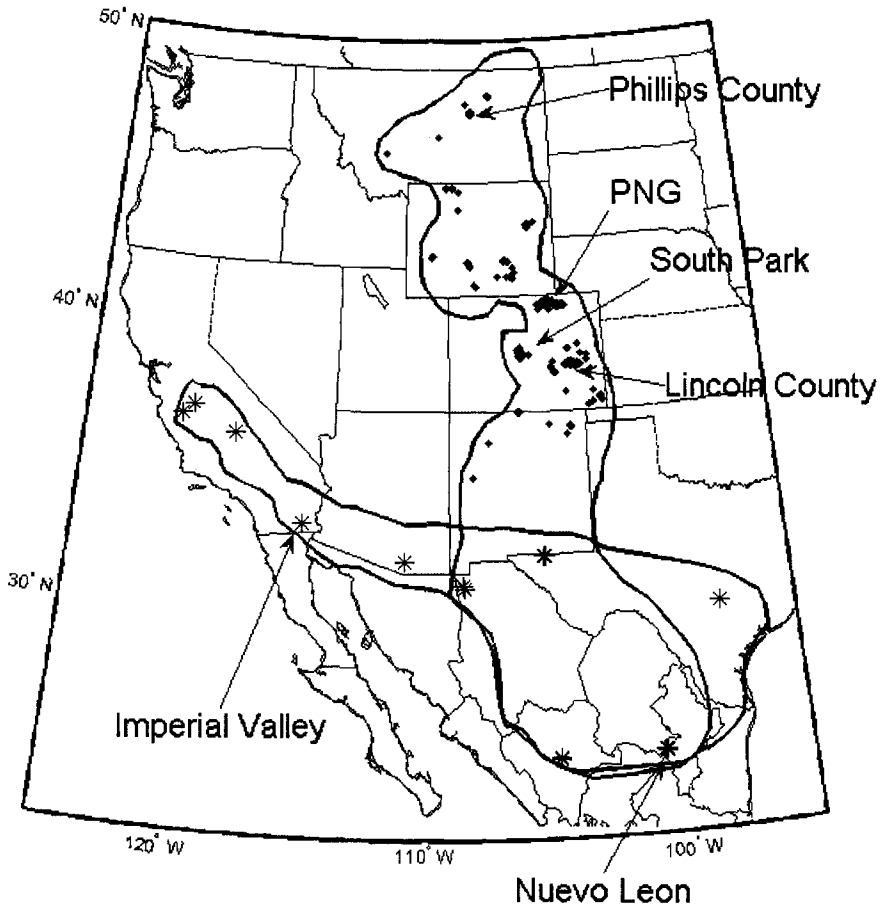

Reproduced with permission of the copyright owner. Further reproduction prohibited without permission.

Figure 2

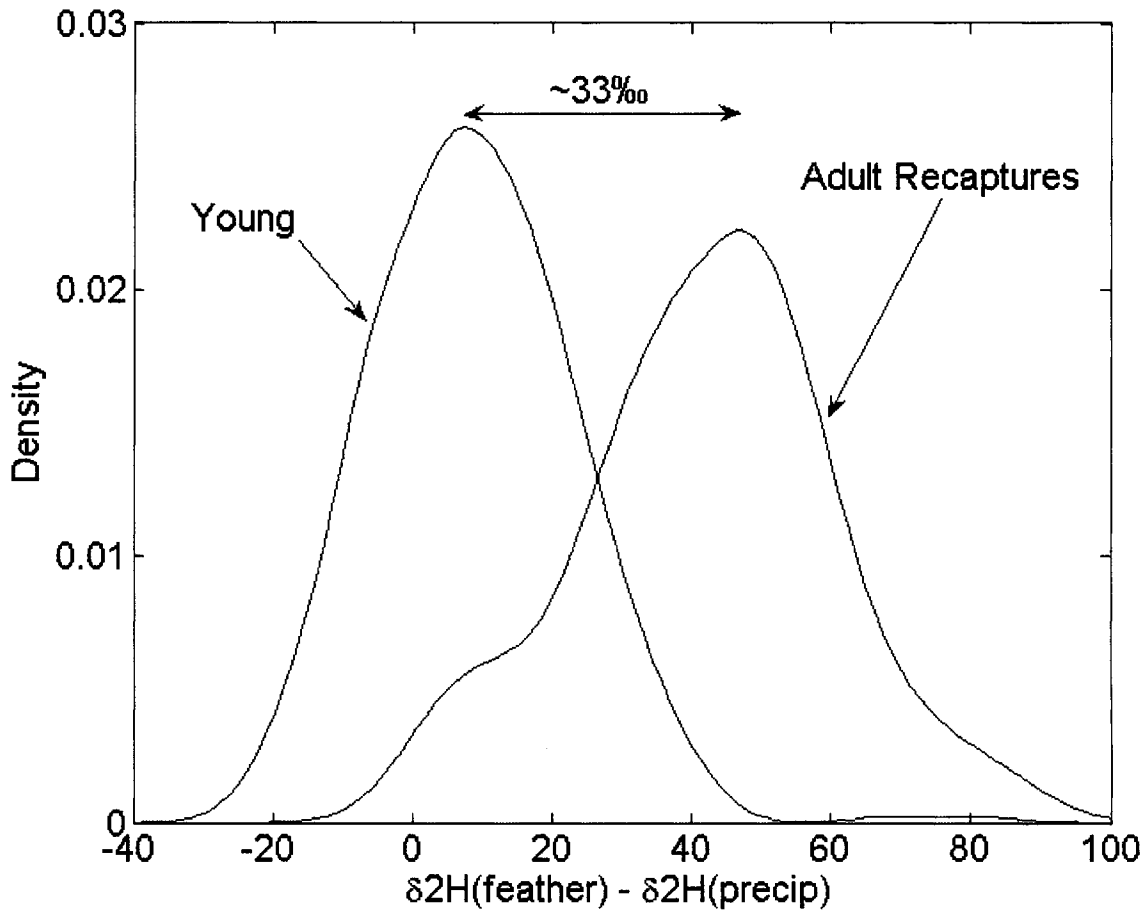

Reproduced with permission of the copyright owner. Further reproduction prohibited without permission.

Figure 3

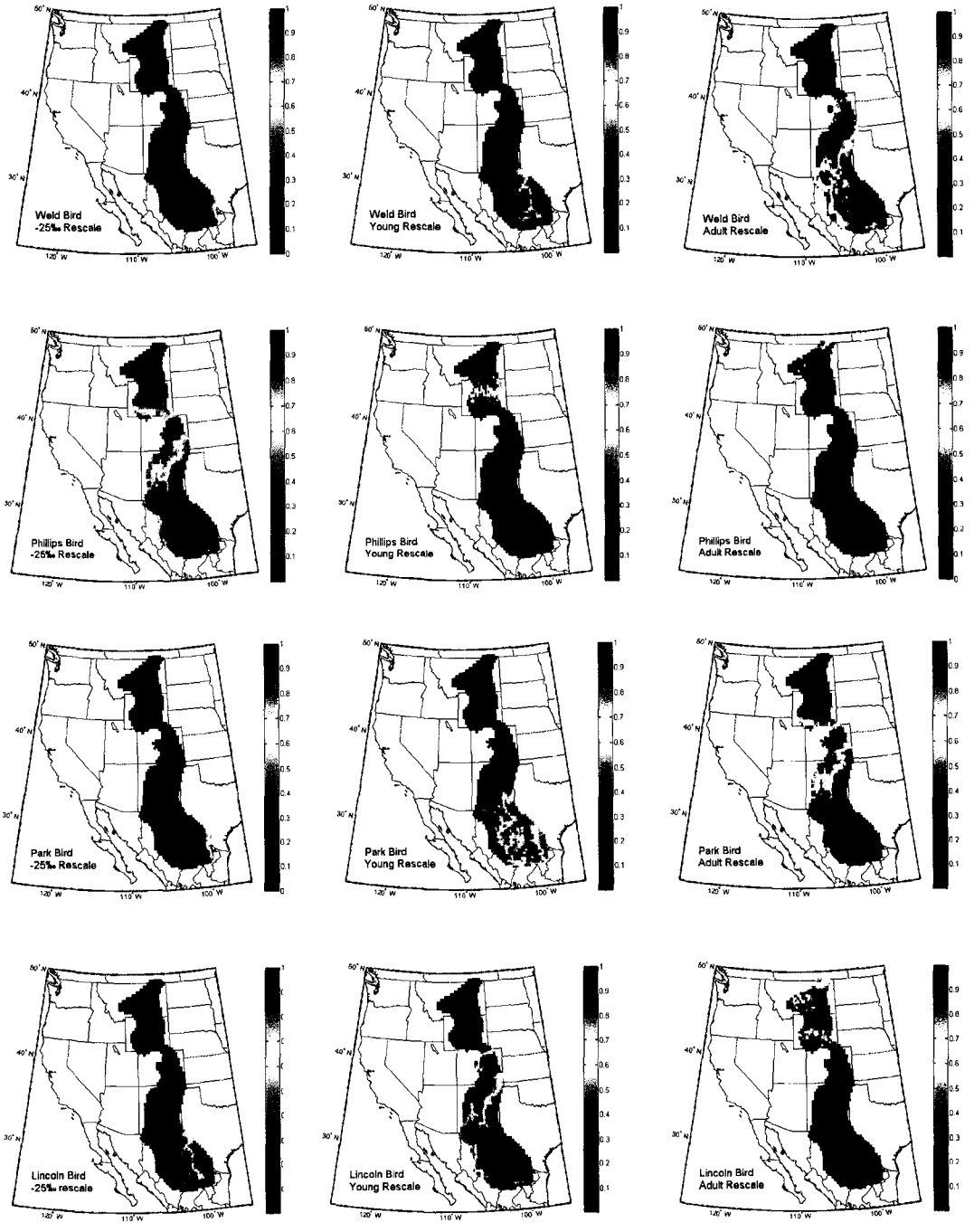

Reproduced with permission of the copyright owner. Further reproduction prohibited without permission.

Figure 4

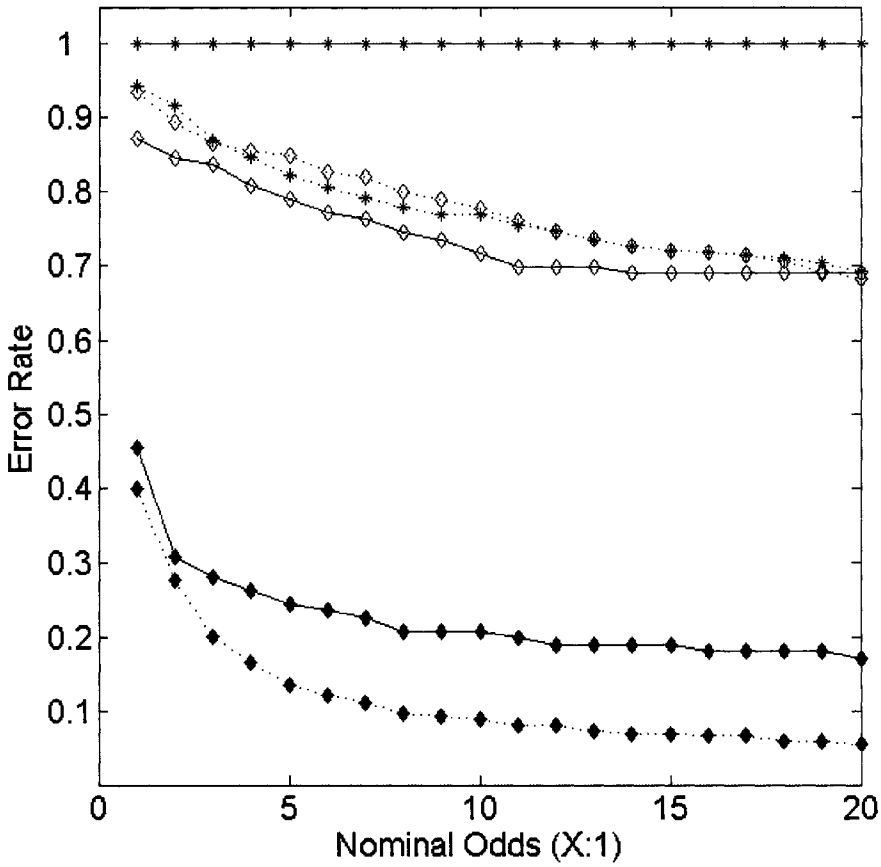

Reproduced with permission of the copyright owner. Further reproduction prohibited without permission.

Figure 5

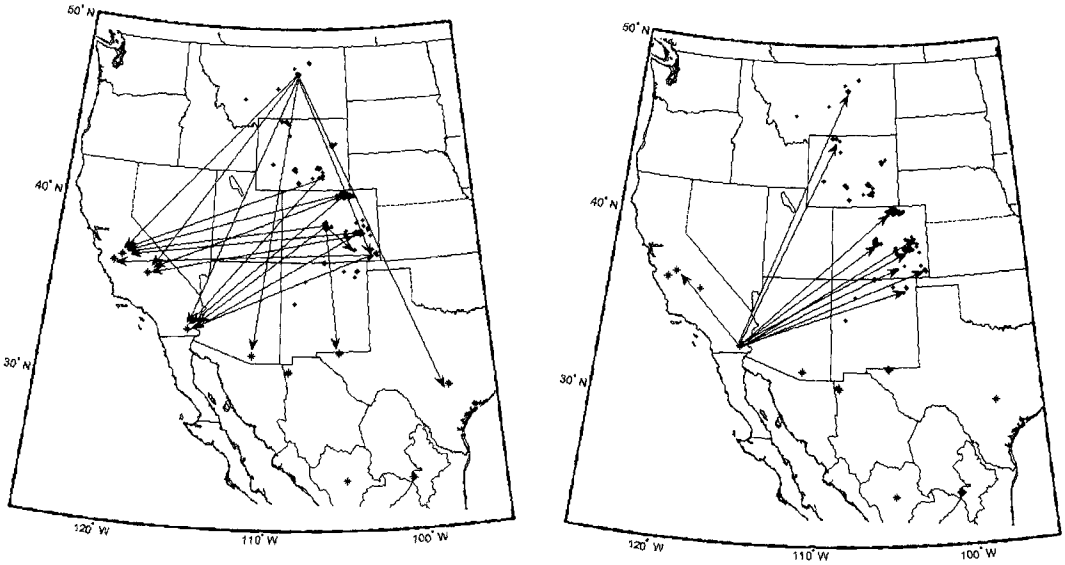

Reproduced with permission of the copyright owner. Further reproduction prohibited without permission.

Figure 6

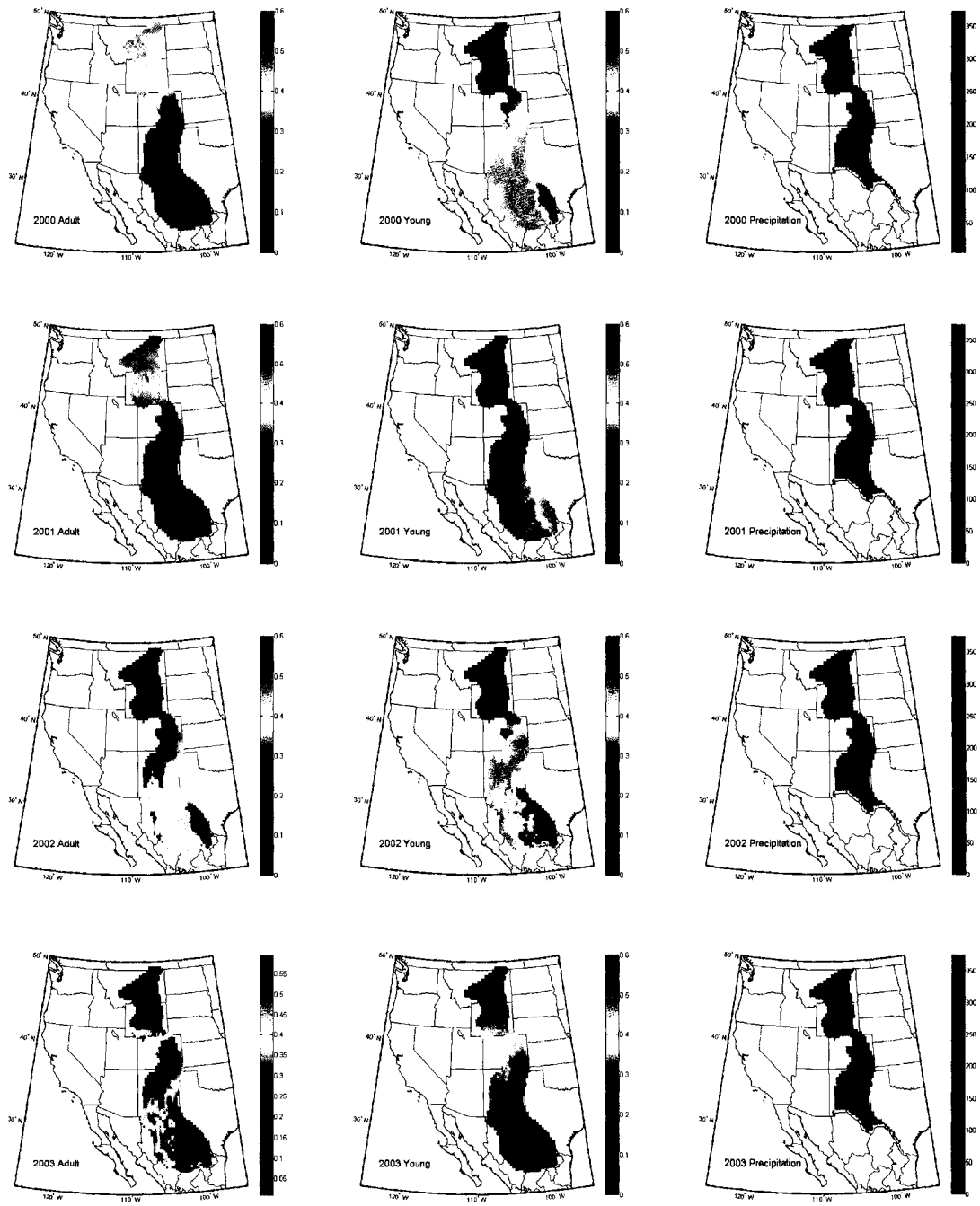

Reproduced with permission of the copyright owner. Further reproduction prohibited without permission.

Figure 7

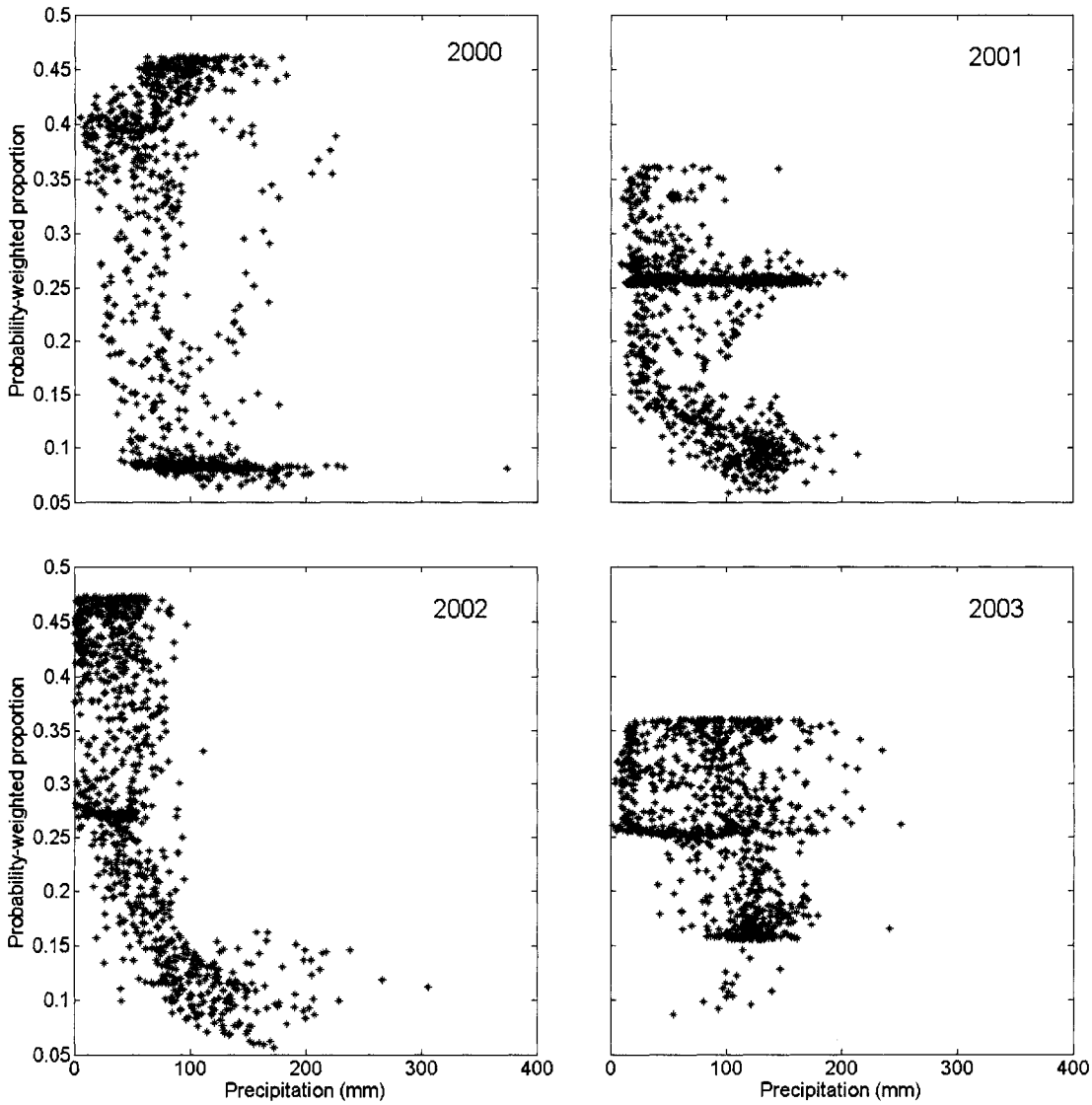

Reproduced with permission of the copyright owner. Further reproduction prohibited without permission.